RNA REGULATION DURING GAMETOGENESIS AND TRIGGERS OF EGG ACTIVATION IN DROSOPHILA MELANOGASTER

A Dissertation

Presented to the Faculty of the Graduate School

of Cornell University

In Partial Fulfillment of the Requirements for the Degree of

Doctor of Philosophy

by

Caroline V. Sartain

August 2013

RNA REGULATION DURING GAMETOGENESIS AND TRIGGERS OF EGG ACTIVATION IN DROSOPHILA MELANOGASTER

Caroline Sartain, Ph.D.

Cornell University 2013

One of the most critical transitory periods during development occurs when an oocyte prepares to undergo embryogenesis, in a process called “egg activation”. In many organisms, the oocyte has been at rest in the ovary, stored in a dormant state for a period ranging from a number of days (as in flies) to several decades (as in humans). Upon egg activation, this dormant egg must suddenly undergo several major cellular and molecular changes that prepare it for embryogenesis, including restructuring of the vitelline membrane, completion of meiosis, and changes to mRNA and protein pools. Where most organisms require a fertilizing sperm to set off these events, fruitflies are unique in that egg activation occurs prior to requirement of fertilization. I have used Drosophila melanogaster as a model system to dissect apart some key events of egg activation that are driven solely by the maternal components of the oocyte.

In most animals, the initial trigger from the sperm sparks a calcium wave that traverses through the oocyte, acting as a message to kick off previously silenced biochemical pathways. For many years, it was unknown whether calcium played a role in egg activation in Drosophila. I have discovered that although Drosophila oocytes do not require a fertilizing sperm, a calcium wave does occur during egg activation. I have characterized the dynamics of this calcium influx using live imaging of Drosophila

oocytes undergoing *in vitro* egg activation. Furthermore, I found that the calcium flux is not dependent upon internal stores but depends on extracellular calcium concentrations. Additionally, I have determined that the extracellular calcium likely enters the oocyte through mechanosensory TRP channels.

Downstream of the calcium signal, there is major turnover of the maternally-stored mRNAs within the oocyte. I have examined the phenotype and transcriptome changes in eggs from mothers carrying the *prage* mutation, an allele previously uncharacterized in egg activation. I have also performed microarray analysis of the global set of transcripts that undergo cytoplasmic polyadenylation by WISPY at egg activation. These data taken together give us a big-picture view of the global changes occurring in the mRNA pool during egg activation.

BIOGRAPHICAL SKETCH

Caroline grew up in a small town called Greers Ferry in northern Arkansas. Frustrated with the town's public school system, she left Greers Ferry to finish high school at the Arkansas School for Math and Science (ASMS) in Hot Springs, Arkansas. During her time at ASMS, she focused on biological sciences and gained an appreciation for molecular biology and laboratory research. As an undergraduate at Rhodes College, she began regular research as a freshman in the labs of Drs. Terry Hill and Darlene Loprete, where she learned cell imaging, molecular biology, and biochemical techniques as they applied to gene mapping and discovery in *Aspergillus nidulans*. During the latter part of her undergraduate career, Caroline worked with Drs. Beatriz Sosa-Pineda and Guillermo Oliver at St. Jude Children's Research Hospital, where she got her first taste of developmental biology studying homeobox transcription factors in mouse pancreatic development. She continued her passion for research and developmental biology at Cornell University in the lab of Dr. Mariana Wolfner, where she studied what she considers the most fascinating and most critical timepoint of organismal development: the egg-to-embryo transition, or those events which occur just prior to and just after fertilization that allow a fully functional multicellular organism to develop from just sperm and egg. After her time at Cornell, Caroline will join the lab of Dr. Patricia Hunt at Washington State University, where she will study the toxicity effects of bisphenol-A (BPA) on mammalian reproductive tracts.

ACKNOWLEDGEMENTS

I have had a wonderful experience at Cornell, and there are many individuals I would like to thank for that. Mariana has been an exceptional mentor, concerned not only with the progress of the science but also with the personal well-being of her lab members. Many times I have walked into her office with some muddled and confusing scientific problem, and through our discussion always have left with a clear picture of what needs to be done next. I also thank her for creating a nurturing atmosphere in which to work. Having seen peers in some terrible lab environments, I do not take this for granted.

I would also like to thank my committee members, Mike Goldberg and Kelly Liu, for so many helpful comments and ideas for new research directions. I enjoy that I can run into Mike in the hallway or in the break room and end up in a 45-minute conversation about the best way to perform a specific experiment. I must acknowledge Kelly for running the developmental biology journal club, which has kept me up to speed in the field when I don't always have time to read the journals.

There are many past and present lab members I must acknowledge. Jun Cui taught me the ropes in the Wolfner lab, and Norene Buehner and Amber Krauchunas have always been there to bounce ideas off of. Although I've never met Vanessa Horner, I must acknowledge her for laying the groundwork for the calcium project, and for keeping such well-organized lab notebooks and a well-written thesis. I've read them all cover-to-cover at least twice.

Finally, I must thank my friends and family for all their trust and support during my graduate career, without which I wouldn't have been nearly as fruitful.

TABLE OF CONTENTS

LIST OF FIGURES

LIST OF TABLES

CHAPTER 1

INTRODUCTION[1]

Through the process of egg activation, a single resting cell – the mature oocyte – suddenly is triggered to undergo several major changes that give it the capacity, once fertilized, to give rise to every type of tissue in the adult. Understanding the intricacies of egg activation is fruitful for understanding how cells can transition between differentiated and totipotent states, and also has relevance to our understanding of fertility and the development of assisted reproductive technologies.

In many organisms, mature oocytes remain stalled in a species-specific stage of meiosis. Release from this arrest point occurs during egg activation. This process initiates a number of changes at the molecular and cellular levels in the oocyte that prepare it to undergo embryogenesis after fertilization (Horner and Wolfner, 2008b; Krauchunas and Wolfner, 2013; Raz and Shalgi, 1998). The molecular changes include modification of vitelline membrane structure, alterations in RNA and protein pools through translation or degradation of stored maternal RNAs, and post-translational modifications made to existing proteins. These molecular events drive major changes at the cell level, including release from meiotic arrest, pronuclear fusion, and finally progression to embryonic mitoses.

Precise regulatory control of RNAs and proteins is critical for developmental processes to occur normally. Sperm and egg development in many organisms relies upon a decoupling of transcription and translation in addition to stage-specific modulation of protein activity;

[1] Part of this chapter has been published as: C.V. Sartain and M.F. Wolfner (2013). *Cell Calcium* 53(1), 10-15. This is reprinted here with permission.

therefore, gametogenesis and the transition from egg to embryo are particularly sensitive to such regulation. During oogenesis in *Drosophila*, the developing oocyte is stocked with many RNAs and proteins produced by the adjoining nurse cells. These materials are stored in a stable yet inactive state during egg development and become active during oocyte maturation and egg activation to facilitate these transitory states. If these mRNAs are prematurely translated, embryonic development could be compromised.

The initiation of egg activation itself must also be tightly regulated to ensure that oocytes do not undergo spontaneous activation before they exit the ovary. In many animals, egg activation is triggered by components introduced to the egg by the sperm during fertilization. In each case, the sperm component initiates a rise in intracellular calcium (Ca^{2+}) levels, which prompts signaling cascades leading to meiotic resumption, changes in RNA and protein pools, and polyspermy block (Saunders et al., 2002; Swann et al., 2006). Interestingly, *Drosophila* egg activation does not require fertilization, though previous studies indicate that increased internal Ca^{2+} is necessary for the process to begin (Horner and Wolfner, 2008a). The first part of this chapter focuses on the requirement of Ca^{2+} during egg activation and the mode of cytosolic Ca^{2+} increase.

Many changes occur in the pool of maternally-produced stored RNAs downstream of the egg activation trigger in *Drosophila*. In contrast to *de novo* transcription, regulation of a large pool of existing RNAs can cause rapid, widespread change in cell state and function. RNA exonucleases and poly(A) polymerases contribute to the fate of stored RNAs through degradation or by promoting translation, respectively (Tadros and Lipshitz, 2005; Vardy and Orr-Weaver, 2007a). The second part of this chapter focuses on the mechanisms by which stored RNAs are degraded or translated.

1.1 Gametogenesis and early embryonic development in *Drosophila*

Drosophila females produce oocytes throughout their lifetime. Here, oogenesis occurs within ovarioles in the ovary (Spradling, 1993). Each ovariole (of which there are 14-16 per ovary) is essentially an assembly line for oogenesis and consists of an asymmetrically dividing germline stem cell (GSC) and germarium with several developing egg chambers, such that each chamber further from the GSC contains an oocyte at a later stage of development. Each egg chamber eventually reaches 16 cells in number through four mitotic divisions: one of the first daughter cells of the initial divisions is determined to be the oocyte through inheritance of a unique germ cell component called the spectrosome, whereas the rest of the cells become nurse cells. The nurse cells within the egg chamber are connected to each other and to the oocyte through ring canals. The purpose of the nurse cells is to produce many nutrients, including mRNAs and proteins, which they deliver to the oocyte in a process called “dumping” or ooplasmic streaming to support early embryogenesis. After dumping, the nurse cells are no longer needed, and they apoptose.

The somatic follicle cells that surround the egg chamber build a complex eggshell made up of a vitelline membrane and a chorion that will protect the developing embryo after egg laying. Built into the chorion on the anterior of the oocyte is a structure called the micropyle (an opening that serves as the single entry point for a fertilizing sperm) as well as dorsal appendages (tubes that serve as “breathing” appendages so that the developing embryo can exchange gases with the environment outside the eggshell). At the end of oogenesis, the oocyte is essentially a prolate spheroid approximately 0.5mm in length and 0.2mm in diameter at its waist (Markow et al., 2009). Thus, the Drosophila oocyte is particularly large among those of model organisms.

Within the mature oocyte, the cell cycle is stalled at metaphase I of meiosis, and many mRNAs and proteins are poised to undergo modification and activation in preparation for fertilization.

Once oogenesis is complete, the oocyte exits the ovary and enters the oviduct for ovulation. Egg activation in Drosophila begins during passage through the oviduct, in contrast to many other species whose eggs activate at fertilization (Doane, 1960; Heifetz et al., 2001). In Drosophila, these events are sequential rather than simultaneous: just after ovulation, the oocyte will pass by the spermathecae (sperm storage organs), where sperm are released (if the female has mated) and a single sperm enters the oocyte through the micropyle. By the time the female deposits the oocyte on her substrate of choice, oftentimes fruit, embryogenesis is already underway, beginning with synchronous and very rapid (only 8 minutes per cycle) nuclear divisions that proceed without G-phases and without cytokinesis until the 14^{th} cell cycle.

In most organisms, transcription from the zygotic genome does not begin right away. Zygotic genome activation (ZGA) begins at the 2-cell stage in mice and at the 4-8 cell stage in humans, whereas in organisms with external development ZGA occurs much later (14th cleavage cycle in frogs, fish, and Drosophila) (Tadros and Lipshitz, 2009). Notably, eggs of this latter group are much larger than those of the former, reflecting the fact that embryogenesis depends on nutrients stored in the oocyte from the mother until ZGA is complete. Thus, there is a great requirement for proper timing of translation of those stored mRNAs and post-translational modifications of proteins prior to ZGA in Drosophila so that embryogenesis can run smoothly until the embryo can produce these essential macromolecules for itself. The activation of maternal RNA and protein stores, which were previously quiescent during oogenesis, occurs during egg activation in the oviduct, and must be maintained until ZGA.

Due to the large size of Drosophila oocytes, ease of genetic manipulation in Drosophila in general, short generation time of the organism, and the fact that egg activation and fertilization are separable events, Drosophila is an excellent model organism for studying egg activation. We and others have already successfully used Drosophila to identify genes and mechanisms involved in this complex cellular transition. Some notable work in this area includes *sarah* (*sra*) and *calcineurin* (*Cn*), involved in calcium signaling upon the trigger for egg activation (Horner et al., 2006; Takeo et al., 2006; Takeo et al., 2010; Takeo et al., 2012); *Young Arrest* (*Ya*), required for maintenance of nuclear organization (Lin and Wolfner, 1991; Sackton et al., 2009); *cortex* (*cort*), a Cdc20 ortholog required for meiosis (Pesin and Orr-Weaver, 2007; Swan and Schupbach, 2007); *wispy* (*wisp*), a poly(A) polymerase required for translational activation of stored transcripts ((Benoit et al., 2008; Brent et al., 2000; Cui et al., 2008) and Chapter 4); the Pan Gu Kinase (PNG) complex [including *giant nuclei* (*gnu*) and *plutonium* (*plu*)], which also regulates translation of stored mRNAs (Tadros et al., 2003); *smaug* (*smg*), which degrades stored mRNAs that will not be needed (Tadros et al., 2007); and *prage* (*prg*), which may be involved in degradation of unneeded mRNAs at egg activation ((Tadros et al., 2003) and Chapter 3).

1.2 Calcium during egg activation

In the vertebrate and invertebrate organisms studied, egg activation requires an increase in intracellular calcium levels within the oocyte (reviewed in (Malcuit et al., 2006; Miyazaki and Ito, 2006; Townley et al., 2006; Whitaker, 2008)). In most cases, the calcium increase is triggered through the fertilizing sperm, commonly through activation of an intracellular calcium signaling pathway. For example, in mice the sperm introduces a specific isoform of phospholipase C, which activates the inositol triphosphate pathway in the fertilized egg,

ultimately causing release of calcium stores from the endoplasmic reticulum (ER) (Rice et al., 2000).

However, the specific trigger for egg activation is different in at least some insects, including fruitflies and hymenoptera such as ants and bees (whose unfertilized eggs develop into males) (King and Rafai, 1970; Mahowald et al., 1983). Egg activation in these insects does not require fertilization (Doane, 1960). Instead, a mature oocyte begins to activate as it travels through the female reproductive tract. Activation is triggered by passage through the ovipositor in wasps (Went and Krause, 1974), or upon the oocyte's release from the ovary into the oviduct in Drosophila (Heifetz et al., 2001).

Calcium signals in many cell types are commonly transmitted through the calcium binding protein calmodulin (CaM), which may then interact with other proteins to activate downstream events. Studies in vertebrates had previously pointed to roles for CaM-mediated pathways in egg activation. In mouse, for example, activity of the calmodulin-dependent kinase CaMKII increases with the multiple calcium spikes in the oocyte, and each wave of CaMKII activity progressively promotes further landmarks of egg activation (Markoulaki et al., 2003). CaMKII and the calcium-dependent phosphatase calcineurin also play a role in activation of Xenopus oocytes, where much of the signaling network downstream of the calcium rise has been identified. In resting Xenopus oocytes, meiosis is held in an arrested state by inhibition of the anaphase promoting complex, APC/C, whose action is required to initiate anaphase. The APC/C acts as an E3 ligase when bound to its coactivator CDC20 to signal the degradation of cell cycle regulators at the spindle assembly checkpoint, thus promoting progression from metaphase to anaphase (reviewed in (Peters, 2006)). In the resting cell, anaphase progression is blocked by inhibitory phosphorylation of CDC20 and by active Emi2, a spindle checkpoint regulator

(Hansen et al., 2006). Upon fertilization (and thus egg activation), the resulting rise in cytosolic Ca^{2+} activates (1) CaMKII, which places an inhibitory phosphorylation on Emi2; and (2) the calcium-dependent phosphatase calcineurin, which removes CDC20 phosphorylation. These post-fertilization events release inhibition of APC/C and allow progression through anaphase (Hansen et al., 2006; Mochida and Hunt, 2007; Nishiyama et al., 2007).

The first indication that calcium may play an important role in Drosophila egg activation came from genetic analysis: the gene for the calcineurin regulator *sarah* (Sra, calcipressin) was identified in a screen for mutations affecting early post-fertilization embryonic development. Embryos from *sra* mutant mothers arrest normally at metaphase I, but upon meiotic resumption at egg activation they are unable to proceed past anaphase I (Horner et al., 2006; Takeo et al., 2006). Calcipressins typically regulate the activity of the Ca^{2+}/CaM-dependent phosphatase calcineurin (CaN) through direct binding (Fuentes et al., 2000; Gorlach et al., 2000; Kingsbury and Cunningham, 2000). Recent evidence establishes that during egg activation in flies, the calcipressin Sra activates calcineurin. First, the phenotype of embryos derived from germline clones of a null allele of the CnB subunit gene of calcineurin is remarkably similar to that of *sra* mutants: meiosis arrests properly at metaphase I but is unable to continue past anaphase I upon release from meiotic arrest (Takeo et al., 2010). Second, a recent study confirms that Sra associates with calcineurin *in vivo* and further shows that phosphorylation of Sra at Ser215 is necessary for calcineurin activity (Takeo et al., 2012). This residue is phosphorylated only in activated eggs and not in mature oocytes, and this phosphorylation event is dependent upon activity of glycogen synthase kinase (GSK-3, *shaggy*) (Takeo et al., 2012); however, it is not known how GSK-3 activity is turned on specifically at egg activation. Taken together, these

results indicate the following scenario: upon egg activation, Sra becomes phosphorylated at a specific residue, which allows Sra to activate calcineurin.

Interestingly, Sra is bound to calcineurin both in ovaries, where calciuneurin is not active, and in early embryos, where calcineurin is active (Takeo et al., 2012). In other organisms, calcipressin has been shown to bind groups of different targets for activating or repressive regulation depending on its phosphorylation status, and this association can be either repressive or activating (Takeo et al., 2012). The same may be true in Drosophila, where the association of Sra and calcineurin in the ovary may be inhibitory until Sra's phosphorylation at egg activation.

Roles for CaM and CaMKII in Drosophila egg activation have not yet been directly determined through genetics. We suspect that both proteins are important for signal transduction upon Ca^{2+} influx during egg activation. For example, the results just described indirectly point to at least one role for CaM through the calmodulin-dependent phosphatase calcineurin. In fact, CaM was identified in calcineurin-containing immunoprecipitates of Sra (Takeo et al., 2012), further suggesting that CaM is required to convey the calcium signal to effector proteins.

Exogenous calcium is needed for Drosophila egg activation

Early observations of Drosophila oocytes noted that laid eggs were already activated, even if they had not been fertilized (Doane, 1960; Mahowald et al., 1983). Oocytes in the ovaries were never activated, indicating that activation had to occur sometime between the release of eggs from the ovary and their being laid by the female. Subsequent detailed physiological studies indeed indicated that oocytes become activated as they pass into the oviduct (Heifetz et al., 2001). Figure 1 demonstrates that transit through the oviducts promote activation: among oocytes that had just begun to exit the ovary, only a small percentage had undergone activation.

However, the percentage of activated oocytes increased progressively at positions further along the oviduct.

The specific egg activation trigger that occurs in the Drosophila oviduct is still unknown, though the available evidence points toward a mechanical stimulus independent of sperm (Heifetz et al., 2001; Horner and Wolfner, 2008a). Mature oocytes in the ovary have a limp, deflated appearance; however, activated, laid eggs appear turgid and taut. Examination of the oviduct before and after egg laying indicates that fluid (possibly with any ions it contains) may be transferred from the oviduct epithelium to the egg during ovulation: the walls of the oviduct are swollen with fluid in female flies that have not yet ovulated an egg; after ovulation, the oviduct walls appear to have lost fluid (measured by the decrease in matrix space between the intima and the oviduct epithelium) and the laid egg to have gained fluid (Mahowald et al., 1983). Therefore, one model for egg activation in Drosophila posits that this passage of fluid from the walls of the oviduct into the oocyte is sufficient to activate the egg (Heifetz et al., 2001). Given the fact that females produce many eggs, this hypothesis would require a continual, net production of new fluid to flow into each subsequent oocyte. This transferred oviductal fluid could contain ions such as calcium that potentially could participate in egg activation. While Drosophila ovaries express RNAs for aquaporin water channels and, at low levels, for some other transporters such as the orthologs of NBC, NKCC1, and some potassium channels (Chintapalli et al., 2007; McQuilton et al., 2012), involvement of these molecules in egg activation has not been tested. Moreover, expression of aquaporins and ion transporters in the oviductal epithelium has not yet been examined.

A second model suggests that exit from the ovary and passage through the oviduct exerts pressure on the oocyte, activating mechanosensitive ion channels that ultimately trigger egg

Figure 1.1. Model of egg activation in Drosophila. The current model for egg activation posits that a mechanical tension force (F_T) on the oocyte during its transit through the oviduct activates mechanosensitive Ca^{2+} channels. Ca^{2+} enters the cytoplasm where it binds and activates calmodulin (CaM; (transition from inactive CaM_i to active CaM_a), which can then act on downstream effectors like CaMKII and calcineurin (CaN) (dashed lines indicate that evidence has not yet been provided; subscripts "i" and "a" indicate inactive and active forms, respectively). Separately, calcipressin (Sra) is phosphorylated by GSK-3 upon egg activation, which allows Sra to positively regulate CaN. These phospho-modulatory proteins, as well as as-yet unidentified kinases and phosphatases, are proposed to modulated the phosphorylation state, and thus activity, of over 300 proteins (Krauchunas et al., 2012), leading to the cellular changes of egg activation.

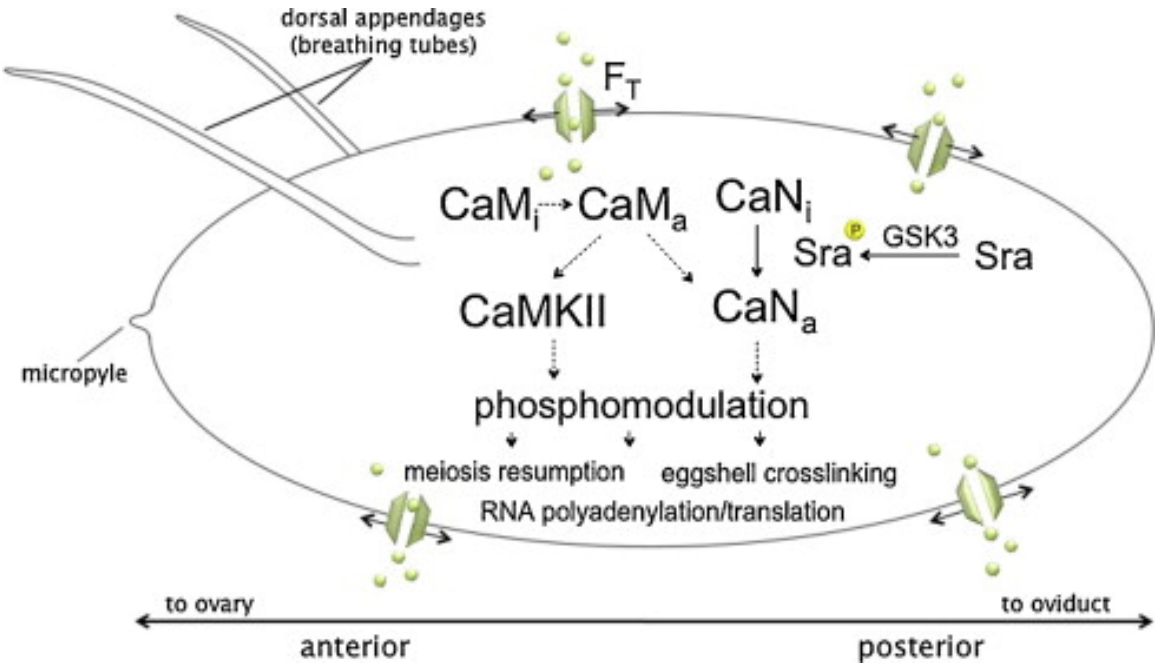
dorsal appendages
(breathing tubes)
micropyle
F_T
CaM_i
CaM_a
CaN_i
Sra
GSK3
Sra
CaMKII
CaN_a
phosphomodulation
meiosis resumption
eggshell crosslinking
RNA polyadenylation/translation
to ovary
to oviduct
anterior
posterior

activation (Heifetz et al., 2001; Horner and Wolfner, 2008a). In accordance with this model, simply pulling on the dorsal appendages attached to the eggshell of a dissected Drosophila oocyte can induce egg activation (Endow and Komma, 1997), and external pressure on the oocyte can accelerate its activation in a buffer that contains calcium (Horner and Wolfner, 2008a) (see below). These two models (fluid transfer, and mechanosensitive triggers) are not mutually exclusive. One can imagine, for example, that swelling of the egg due to hydration from oviductal fluid would cause mechanical stress in the oocyte membrane, which could activate mechanosensitive ion channels and initiate egg activation.

It has been possible to analyze the trigger for egg activation by using an *in vitro* system. Oocytes dissected from the ovary are incubated in an "activation buffer" that is hypotonic to the egg and contains the appropriate ionic makeup (see below) (Mahowald et al., 1983; Page and Orr-Weaver, 1997). This method of hypoosmotic egg activation causes the oocyte to take up fluid and to become turgid, perhaps mimicking the hydration that occurs in the oviduct. These *in vitro* activated oocytes show all the signs of normal *in vivo* egg activation, including normal progression through meiotic stages (Page and Orr-Weaver, 1997), translation of stored mRNAs (Horner and Wolfner, 2008a), and vitelline membrane crosslinking (Page and Orr-Weaver, 1997).

In vitro experiments indicate that calcium plays a major role in Drosophila egg activation. The presence of calcium in the activation buffer is essential for hypoosmotic activation of Drosophila oocytes *in vitro*: oocytes dissected from the ovary cannot activate if incubated in calcium-depleted activation buffer (Horner and Wolfner, 2008a). Furthermore, *in vitro* activation of dissected Drosophila oocytes can be inhibited by treatment with gadolinium, which blocks some ion channels including mechanosensitive stretch-activated channels. The effects of

gadolinium and the buffer constitution suggest that calcium ions enter the oocyte from the external environment to trigger activation (Horner and Wolfner, 2008a). Taken together, the available data are most consistent with a model in which calcium from the oviductal fluid enters the oocyte from the outside due to a mechanical stimulus experienced by the oocyte as it passes through the oviduct, and this influx of calcium ultimately triggers egg activation.

RNA regulation at egg activation

Once activation is triggered in the oviduct and if fertilization occurs during passage through the lower reproductive tract, the egg will begin to undergo embryogenesis. Early embryogenesis in Drosophila is unique from that of some other model organisms in that ZGA does not begin to occur until the 11th cell cycle, and maternal-zygotic transition (MZT) is not completed until the 14th cell cycle. Therefore, the Drosophila embryo must drive early embryogenesis solely from the activity of maternally provided mRNAs and proteins. These first cell cycles prior to MZT occur extremely rapidly, with S phase moving directly into M phase without any interruption for G phases.

After the initial trigger for egg activation during ovulation, the existing maternally-deposited RNA and protein pools undergo major turnover. Many RNAs must either be translated or degraded, and a significant portion of the protein pool will experience post-translational modifications such as phosphomodulation, which can influence their activity and binding partners (Krauchunas et al., 2012). Altogether, these sweeping changes made to the oocyte RNA and protein populations are a major driving force for many events of egg activation.

RNA degradation

Perhaps the largest turnover in mRNA populations within the early embryo occurs at egg activation, with another significant wave of degradation occurring at MZT. The mature oocyte

contains an enormous pool of transcripts representing 55% of the entire genome (Tadros et al., 2007). Approximately 20% (1600 of 7745) of these maternally deposited mRNAs are destabilized upon egg activation, and another 15% are degraded at MZT (Tadros et al., 2007). In some cases, these mRNAs exist throughout the cytoplasm of the oocyte; global degradation of such transcripts combined with regional protection results in specific localization, which can be critical for setting up the early embryonic axes and for embryonic patterning. Examples of mRNAs that are regulated in this way are *Pgc*, *nanos*, and *Hsp83* (Bashirullah et al., 1999). Many other mRNAs that require posttranscriptional regulation at egg activation encode cell cycle components, such as *cyclin B*, which is important for proper timing of nuclear divisions [(Vardy and Orr-Weaver) and Chapter 4).

Some of the mechanisms of transcript destabilization are known. Approximately two-thirds of the transcripts that are destabilized at egg activation are dependent upon the activity of the posttranscriptional regulator SMAUG (SMG) (Tadros et al., 2007). SMG-regulated transcripts contain a SMG regulatory element (SRE) in the 3' end of the transcript. Upon SMG binding, the CCR4/NOT deadenylation complex is recruited to the transcript, keeping the poly(A) tail short and inhibiting translation. Different regulatory mechanisms may be in place for transcripts not regulated by SMG, such as repression by PUMILIO (PUM), which also recruits the deadenylation machinery (Vardy and Orr-Weaver, 2007a). In addition, not all destabilized transcripts containing the SRE are necessarily regulated by SMG, indicating that other regulatory factors may be at play and may in fact bind the same element. The mechanism by which the transcript is actually degraded is unknown, but it is likely ultimately due to a short poly(A) tail on the transcript.

Cytoplasmic RNA polyadenylation

Many maternally-deposited RNAs that exist within the cytoplasm are poised for translation. Here, the mRNA is bound within a regulatory complex that suppresses translation until the appropriate signal is received. Upon a signal to translate, phosphomodulation and other changes to proteins within the regulatory complex relieves translational suppression, and ribosomal subunits can then act on the transcript (Kim and Richter).

There are several modes by which translational suppression can occur (Vardy and Orr-Weaver, 2007a). In several cases, translation is regulated through controlling the length of the poly(A) tail. During RNA synthesis in the nucleus, a pre-mRNA undergoes processing before its exit into the cytoplasm. Processing includes removal of introns and splicing of exons, addition of a 7-methylguanosine cap to the 5' end of the transcript, and addition of a poly(A) tail containing 30-200 adenosine residues. The poly(A) tail serves two major purposes: 1) it protects the transcript from enzymes in the cytoplasm that may degrade the transcript, and 2) it recruits binding proteins and other factors that promote ribosome binding and translation. Thus, a transcript with a short poly(A) tail is more likely to be degraded and less likely to be translated, whereas a transcript with a long poly(A) tail will be more stable and more likely to be translated (reviewed in (Mendez and Richter).

There are several different ways to achieve translational control through the poly(A) tail, depending on the specific sequence elements present in the 3'UTR of the transcript. Repressive elements have been identified as binding sites for SMAUG (SMG) and PUMILIO (PUM), which promote deadenylation, as well as BICOID (BCD), which prevents translation initiation factors from binding to the 5' cap, and BRUNO (BRU), which represses translation in a poly(A)-independent manner (Vardy and Orr-Weaver, 2007a).

Thus, translation of these repressed transcripts often necessitates polyadenylation not only in the nucleus, but again in the cytoplasm to act against the repressive deadenylation. Studies from Xenopus models have demonstrated that specific RNAs preferentially undergo poly(A) tail lengthening upon egg activation, and that this lengthening correlates with their translation. The mechanism by which this occurs has been well studied in this organism. Here, an mRNA that is destined for cytoplasmic poly(A) tail adjustment contains specific sequences in the 3' UTR: The CPE (cytoplasmic polyadenylation element) and hexamer sequence AAUAAA recruit binding factors that keep the mRNA in a stable, quiescent state. Included in this complex are a deadenylase as well as a cytoplasmic poly(A) polymerase (PAP). Upon a signal to translate the mRNA, phosphorylation of CPEB triggers the release of the deadenylase, and the poly(A) polymerase is free to lengthen the poly(A) tail of the transcript (Kim and Richter, 2006; Mendez et al., 2000). The long poly(A) tail recruits poly(A) binding factors, which ultimately recruit translation initiation factors and the ribosomal subunits.

The particular family of poly(A) polymerase on which I focused on in my studies is the GLD2 (germline development) family of cytoplasmic PAPs. Members of this family have been identified in the oocytes of all species examined so far (Barnard et al., 2004; Benoit et al., 2008; Cui et al., 2008; Kadyk and Kimble, 1998; Wang et al., 2002).

Poly(A) polymerases that act in the cytoplasm are different from those that act in the nucleus. Nuclear PAPs [such as hiiragi in Drosophila (Juge et al., 2002)] contain both an enzymatic domain as well as an RNA binding domain (Wang et al., 2002). GLD2 cytoplasmic PAPs, on the other hand, have an enzymatic domain but lack the RNA binding domain. Thus, in order to act on a particular transcript, a GLD2 protein must form a heterodimer with an RNA binding protein (Wang et al., 2002). In Drosophila, two GLD2 proteins exist, encoded by the

wispy and *gld2* genes. At least one GLD2 binding protein has been also been identified in fruitflies, encoded by the GLD3 homolog *BicC* (Benoit et al., 2008; Cui et al., 2008). Other binding partners may exist for the Drosophila GLD2 proteins, but as of yet no others have been identified. Because the binding partner in the heterodimer contains the RNA binding domain, a GLD2 protein may have a different set of target transcripts depending on which RNA binding protein it is partnered with. In *C. elegans*, for example, the GLD2 homolog can pair either with GLD3 or with RNP8; binding to the former can induce a spermatogenesis developmental program, whereas GLD2 binding with the latter promotes oogenesis (Kim et al., 2009). Similar mechanisms may occur in Drosophila, but our data so far show an identical binding partner for both male and female gametogenic programs (Cui et al., 2008; Sartain et al., 2011).

Drosophila has – unusually – two Gld-2 genes: the Drosophila genus has independently developed a duplication of the original *gld2* locus. Though the binding partner may be identical, the GLD2 homologs active in the male and female germlines in Drosophila are not. The two genes now present in the genome may have undergone subfunctionalization to carry out male and female developmental programs independently. This hypothesis will be explored further in Chapter 5.

1.4 Dissertation Outline

In this dissertation I present studies pertaining to several molecular and physiological aspects of egg activation and gametogenesis in *Drosophila melanogaster*. My studies confirm the requirement of calcium during egg activation in this organism and further explore the source thereof. Furthermore, I show the extent to which the maternally stored mRNA pool is affected at egg activation, and investigate which gene classes are most affected during this time. Taken together, this work provides a comprehensive view of some of the large-scale changes that occur

within the egg on the physiological, cellular, and molecular levels, and demonstrates the power of Drosophila as an important emerging model organism for the study of egg activation.

In Chapter 2, I examine the dynamics of intracellular calcium concentrations within the oocyte during egg activation. Previous studies had suggested that cytosolic calcium levels likely increase within the egg during activation, but imaging studies had not been able to detect such an increase. I used a fluorescent calcium sensor to definitively detect an increase in intracellular calcium levels within the activating egg. Furthermore, I used pharmacological agents to test the requirement of particular calcium channels or pathway components. My results indicate that calcium enters the oocyte from the extracellular environment during egg activation through TRP ion channels.

In Chapter 3, I present mapping and classification of the *prage* gene and mutation. Although this gene encodes a predicted exonuclease and has previously been described as having roles in egg activation, my RNA-seq data and phenotypic analyses indicate that *prage* may play roles primarily in oogenesis, with little direct effects on the process of egg activation.

In Chapter 4, I present analysis of the cytoplasmic Gld-2 family PAP *wispy* in a large-scale transcriptomics study initiated by Jun Cui (2008). Our microarray data indicate that cytoplasmic polyadenylation through WISP activates a very large portion of the extant maternally stored mRNAs both at egg maturation and at egg activation.

In Chapter 5, I examine the role of a second Gld-2 family PAP, *Gld2*. Interestingly, this is the only Gld-2 family member identified to date with roles exclusively in the male germline. I discovered that instead of having roles in oogenesis or egg activation, *Gld2* is expressed in the testes and is required for post-meiotic spermatogenesis. Investigation into the evolutionary history of these genes revealed that *Gld2* arose from a duplication of the *wispy* locus.

Chapter 6 is a brief discussion of my thesis work with suggestions for future directions.

Appendix A contains a comprehensive list of all pharmacological reagents used in our lab to test the requirement of calcium during egg activation. This list summarizes the experiments and results spanning approximately 10 years of the project described in Chapter 2.

Appendix B contains all supplemental tables of gene ontology analysis from the microarray data described in Chapter 4.

CHAPTER 2

A CONVERGENT CALCIUM RISE TRAVERSES THE DROSOPHILA OOCYTE DURING EGG ACTIVATION[2]

2.1 Introduction

The oocyte is, in many ways, unlike any cell type in the body. This highly specialized cell, once fertilized, will become totipotent, yet in many organisms the oocyte must remain quiescent for many years. The resting oocyte within the ovary is filled with maternally-provided stores of mRNAs and proteins that will drive embryogenesis and cell divisions prior to zygotic genome activation; its cell cycle is stalled in a species-specific stage of meiosis (typically metaphase I or II); its vitelline membrane is amenable to penetration by sperm and small molecules (Horner and Wolfner, 2008a; Raz and Shalgi, 1998). The mature oocyte remains in such a state until it is ready to be ovulated and fertilized; this quiescence period ranges from days in fruitflies to decades in humans.

The series of events that leads to actualization of the oocyte's developmental potential is collectively termed "egg activation". In the vertebrates and marine invertebrates in which it has been studied activation is sparked by a rise in cytosolic Ca^{2+} levels that is triggered by the fertilizing sperm (Miao et al., 2012; Roux et al., 2006; Xu et al., 1994). Depending on the organism, this Ca^{2+} rise sweeps through the egg in a single wave or in multiple oscillations, but in all cases the results are the same: meiosis resumes, changes occur to the vitelline envelope, and mRNA and protein pools undergo modifications and turnover (Stricker, 1999; Whitaker,

[2] I acknowledge Professor Toshiro Aigaki, Taro Kaneuchi, and Misato Okajima (Tokyo Metropolitan University) for helpful collaborations on this project. GCaMP fly stocks used in these experiments were created by Taro Kaneuchi.

2006). Evidence from other organisms such as mice and frogs indicates that the rise in Ca^{2+} likely starts a signaling cascade through calcium-dependent kinases and phosphatases such as CamKII and calcineurin, which may have myriad effects on downstream events to produce all of the hallmarks of egg activation (Ducibella et al., 2006; Markoulaki et al., 2003).

In nearly every organism studied, egg activation occurs at fertilization and requires a fertilizing sperm. In these cases, the sperm either introduces a specific isoform of phospholipase C (PLC) (as in mice (Saunders et al., 2002)), or sperm binding activates a Src-family kinase and in turn activates PLC (as in echinoderms (Giusti et al., 1999)); active PLC induces phosphoinositide signaling and ultimately results in release of Ca^{2+} from stores in the egg's endoplasmic reticulum (ER) (Saunders et al., 2002; Swann et al., 2006). However, there are several examples of organisms whose eggs undergo activation in the absence of sperm: eggs of some insect species such as fruitflies activate during passage through the female reproductive tract, before the sperm is introduced (Heifetz et al., 2001). In addition, parthenogenetically-reproducing organisms do not require sperm for egg activation to occur. I am interested to discover the requirement of Ca^{2+} during egg activation in such cases.

Drosophila is a very useful and unique model for this egg activation since its egg activation is separable from fertilization (Doane, 1960). This allows a view of egg activation events driven solely by maternal processes, which will be of interest to the larger scientific community studying oocyte quality as well as fertility and infertility. Aside from this difference, we know that Drosophila egg activation is signaled through many of the same pathways and components as in other organisms: the requirement for calcineurin (Horner et al., 2006; Takeo et al., 2010; Takeo et al., 2006), likely involved in the initial transmission of the calcium signal, is conserved, as are the activities of CDC20 (Drosophila *cortex*) in meiotic resumption (Swan and

Schupbach, 2007), GLD-2 (Drosophila *wispy*) in cytoplasmic polyadenylation (Barnard et al.; Benoit et al., 2008; Cui et al., 2008; Kadyk and Kimble), and MAPK in signal transduction (Choi et al. 1996; Sackton et al., 2007). Furthermore, approximately 80% of proteins that undergo phosphomodulation at egg activation in Drosophila are conserved across species and may indicate a conserved function at egg activation (Krauchunas et al., 2012). Together with the sophistication of genetic tools and ease of manipulation of this organism, Drosophila is an excellent model system for the study of egg activation.

Our lab has previously shown that activation of Drosophila oocytes occurs in the oviduct (Heifetz et al., 2001), likely involves some mechanosensitive component, and requires Ca^{2+} in the extracellular environment (Horner and Wolfner, 2008a). In this study, I further explore the dynamics of Ca^{2+} flux within the activating egg. Our lab has made previous attempts to image this phenomenon using a variety of fluorescent sensors, but those attempts were unsuccessful because the high autofluorescence of Drosophila oocytes resulted in a signal-to-noise ratio too low to reliably detect a true calcium flux (V.L. Horner thesis, 2008). Studies of calcium flux during egg activation in many other organisms use fluorescent sensors injected directly into the cytosol of the egg; however, injection poses a problem for Drosophila oocytes, since the pressure of a needle puncturing the egg or the liquid introduced during injection could itself induce activation. Therefore, monitoring Ca^{2+} at egg activation in Drosophila requires a diffusible or genetically encoded calcium sensor. Several lab members including myself have attempted use of diffusible sensors including Rhod-2, Fluo-4, and Calcium Orange (Invitrogen) (Vanessa Horner, Amber Krauchunas, unpublished data). However, in these studies we noticed that the fluorescent compounds were unable to diffuse into the egg, possibly because of Drosophila's complex eggshell. Therefore, we explored genetically encoded sensors. Many fluorescent

calcium sensors are engineered from the calcium binding protein calmodulin, which undergoes conformational change when bound to calcium. Calmodulin-based calcium sensing tools typically encode a calmodulin protein linked to GFP or other fluorophore (Whitaker 2010). When calcium is not present, the fluorophore is weakly fluorescent. When calcium binds this chimera, the conformational change in calmodulin shifts the shape of the fluorophore such that fluorescent intensity increases. Vanessa Horner had previously attempted imaging using two such chimeras, GCaMP (Tian et al. 2009) and Cameleon (Miyawaki et al. 1997) (expressible in the GAL4-pUAS system), to visualize calcium dynamics in the activating egg. However, the UAS constructs that allow expression in the Drosophila soma work poorly in the female germline (Duffy, 2002; Rorth, 1998). The genetically encoded constructs we were working with were poorly expressible in the female germline. I later tried combining the same pUAST-GCaMP with a stronger maternal germline GAL4 driver. Though I could sometimes see an increase in fluorescence upon egg activation, the signal was very low and difficult to reproduce.

To overcome these issues, we collaborated with Toshiro Aigaki's lab at Tokyo Metropolitan University. They created two GCaMP lines expressible at high levels in the female germline: pUASP-GCaMP and GCaMP driven directly behind the *nanos* promoter. Using these lines for live imaging of oocytes undergoing *in vitro* activation, my collaborators and I discovered two converging waves of Ca^{2+} increase that occur during egg activation. Incubation of activating oocytes *in vitro* in the absence of Ca^{2+} or with inhibitors of specific parts of the calcium release or uptake machinery indicate that this wave is not dependent upon release of internal Ca^{2+} stores, but instead requires external calcium, and the activity of channels in the egg's plasma membrane. My data suggest that these channels are likely mechanosensitive channels of the TRP family.

2.2 Materials and Methods

Live imaging of oocytes. Oocytes were imaged using a Zeiss 710 LSM in Cornell's Core facility. The Zeiss 710 LSM is an inverted confocal microscope capable of holding a petri dish. Oocytes were dissected from females carrying two copies of GCaMP driven by the *nanos* promoter (developed by Toshiro Aigaki and Taro Kaneuchi) and induced to activate *in vitro* following methods similar to those previously described (Horner and Wolfner, 2008a; Page and Orr-Weaver, 1997). For imaging, a single oocyte was placed in a drop of isolation buffer (IB) (Page and Orr-Weaver, 1997) in a glass-bottomed dish (MAT-TEK). Imaging parameters were then set on the scope using ZEN software. The gain on the 488 channel was set to 700, the pinhole was fully opened, and the laser power was set to 10% (laser power will need to be adjusted depending on the age of the laser). The experiment was programmed as a time series, obtaining one image every 20 seconds for approximately 100 cycles. Line averaging for each image was set to 4. Zoom was set to 0.6 so that an entire egg could fit within the imaging field. All imaging was done with a 25x objective. Once parameters were set and the egg was in focus, I flooded the dish with approximately 1mL of PIPES-based activation buffer (AB) (Horner and Wolfner, 2008a) and began imaging. Occasionally, if I was unable to see any increase in calcium signal in the egg with the controls, I added a few drops of ddH_2O (thus increasing the osmotic pressure inside the egg).

Drug and inhibitor treatment

Removal of external Ca^{2+}: BAPTA [1,2-bis(2-aminophenoxy)ethane-N,N,N',N'-tetraacetic acid tetrapotassium salt] (Sigma-Aldrich) was used to chelate trace amounts of calcium from IB and AB. IB and AB were prepared without the addition of $CaCl_2$, and sucrose was instead added to these buffers to match the osmolarity of control buffers, which were prepared normally. BAPTA

was added to IB and AB as previously described (Horner and Wolfner, 2008a) to buffer Ca^{2+} to levels below 50nM.

Inhibitors of Ca^{2+} entry or release: Stock solutions of wortmannin (PI3K inhibitor), U73122 (PLC inhibitor), *N*-(p-Amylcinnamoyl)anthranilic Acid (ACA) (broad TRP channel inhibitor), $GdCl_3$ (stretch-activated channel inhibitor), and ruthenium red (ryanodine receptor and selective TRP blocker) were prepared and added to IB and AB on the day of the experiment. Oocytes were dissected and incubated in drug-treated IB or control IB for 30 minutes before beginning the experiment. Inhibitor-treated oocytes were then activated in AB also containing the inhibitor, and oocytes incubated in control IB were activated in control AB lacking the inhibitor. Final concentrations of inhibitors used are as follows: wortmannin, 1µM or 5µM (De Nadai et al., 1998); U73122, 10µM or 20µM (Lee et al., 1998; Sato et al., 2000); ACA, 10µM or 20µM (Harteneck et al., 2007); $GdCl_3$, 10µM, 100µM, 200µM, or 400µM (Hardie, 2007; Horner and Wolfner, 2008a); Ruthenium red, 10µM. Control solutions made in parallel were prepared normally.

2.3 Results

Ca^{2+} waves traverse the Drosophila oocyte during egg activation

Using GCaMP as a fluorescent indicator of Ca^{2+} concentration, we observed an increase in cytosolic Ca^{2+} levels during egg activation *in vitro* in Drosophila oocytes. Oocytes were dissected in isolation buffer (IB), a solution hypertonic to the egg that maintains the egg in a dehydrated, inactivated state. For imaging, the dish was flooded with AB, a solution hypotonic to the egg, which causes egg hydration, swelling, and activation. We observed two converging waves of increased cytosolic Ca^{2+} concentrations after addition of AB, after the egg began to swell. In most cases, a wave initiated first from the anterior, followed shortly afterwards by a

secondary increase initiating from the posterior. Ca^{2+} increased in a wave moving toward the middle of the oocyte from either pole, creating a bidirectional wave of calcium flux through the cytosol. Fluorescence peaked, maintained a brief plateau, and then decreased in the same bidirectional manner (Figure 2.1). Total time from wave initiation to peak fluorescence was approximately 15 minutes, and waves typically began within 10 minutes of adding AB, though they occasionally took longer to begin. If I did not see a wave beginning within 30 minutes, I was usually able to initiate a wave by adding 1-5 drops of deionized H_2O. I hypothesize that the addition of water to the activating solution causes greater hypotonicity of the solution to the egg, resulting in further egg swelling, which may be critical for egg activation as further discussed below (Horner and Wolfner, 2008a).

The Ca^{2+} wave is not dependent upon release from internal stores

In most organisms studied to date, the first calcium wave that occurs at egg activation occurs through release of Ca^{2+} from ER stores within the egg through phosphoinositide signaling. To test whether this was also the case in Drosophila oocytes, I performed imaging of *in vitro* activation in oocytes treated with inhibitors of PI3K (wortmannin) (Figure 2.2) and PLC (U73122) (Figure 2.3), which diminishes the calcium wave at egg activation in mice and sea urchin (De Nadai et al., 1998; Deng et al., 1998) (for a review see (Whitaker, 2006)). Using either treatment, I did not observe an increase in cytosolic Ca^{2+} following the same dynamics as that observed in untreated control oocytes observed in parallel. Because the wave dynamics remain intact when phosphoinositide signaling is compromised, I conclude that the mode of cytosolic Ca^{2+} influx in Drosophila oocytes differs from that of other organisms during egg activation and is not sourced from internal ER Ca^{2+} stores.

Figure 2.1. Calcium dynamics during egg activation in *Drosophila melanogaster*. Eggs of *Drosophila melanogaster* show a rise in cytosolic Ca^{2+} during *in vitro* activation, as indicated by GCaMP fluorescence. In control samples, the rise initiates at either pole and travels toward the center of the egg. Time is measured in minutes:seconds.

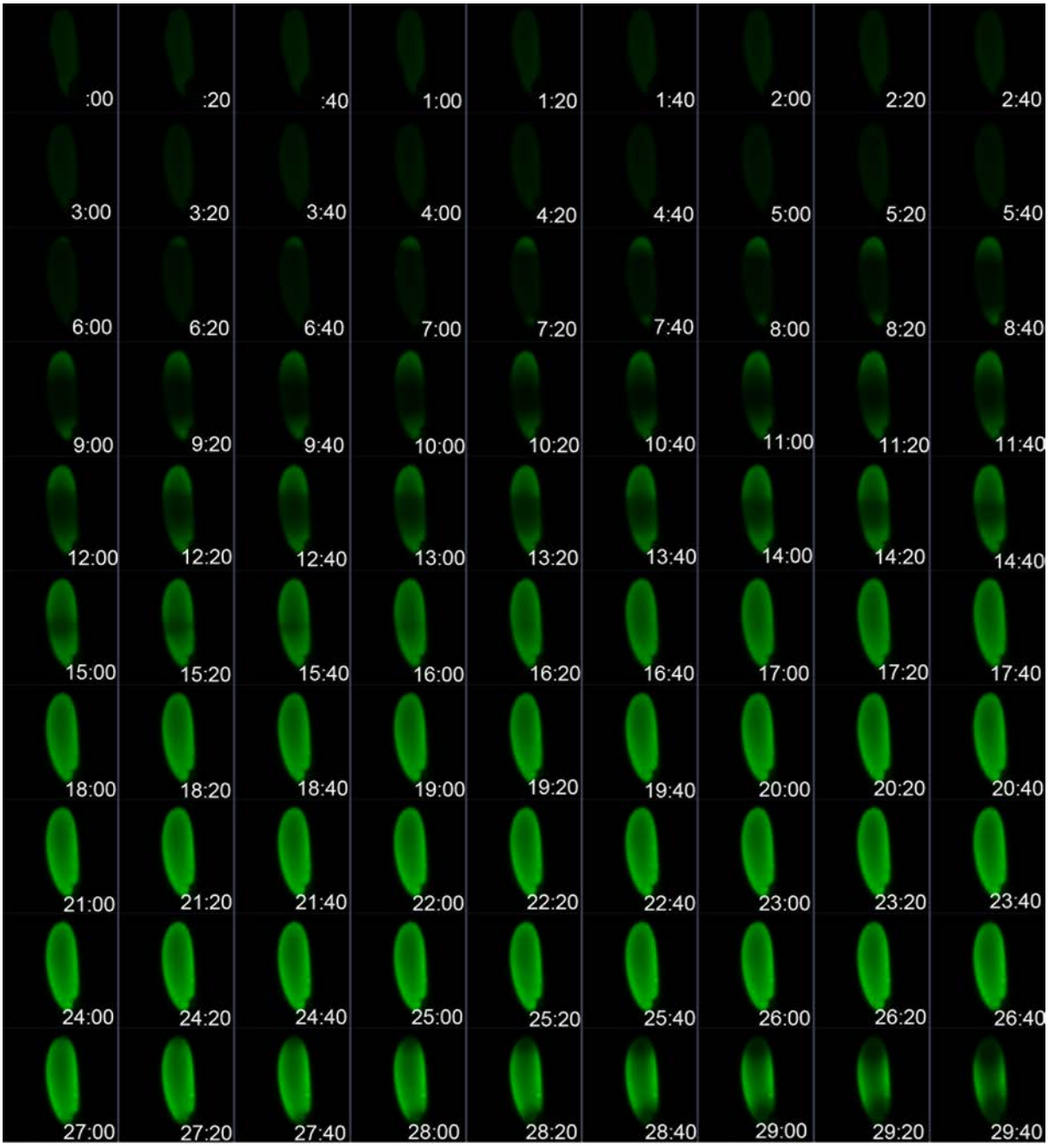
:00
:20
:40
1:00
1:20
1:40
2:00
2:20
2:40
3:00
3:20
3:40
4:00
4:20
4:40
5:00
5:20
5:40
6:00
6:20
6:40
7:00
7:20
7:40
8:00
8:20
8:40
9:00
9:20
9:40
10:00
10:20
10:40
11:00
11:20
11:40
12:00
12:20
12:40
13:00
13:20
13:40
14:00
14:20
14:40
15:00
15:20
15:40
16:00
16:20
16:40
17:00
17:20
17:40
18:00
18:20
18:40
19:00
19:20
19:40
20:00
20:20
20:40
21:00
21:20
21:40
22:00
22:20
22:40
23:00
23:20
23:40
24:00
24:20
24:40
25:00
25:20
25:40
26:00
26:20
26:40
27:00
27:20
27:40
28:00
28:20
28:40
29:00
29:20
29:40

Figure 2.2. Wortmannin does not affect the Ca^{2+} wave at egg activation. Oocytes treated with 1-5μM wortmannin show an intracellular Ca^{2+} flux similar to that seen in control oocytes during egg activation. Time is measured in minutes:seconds.

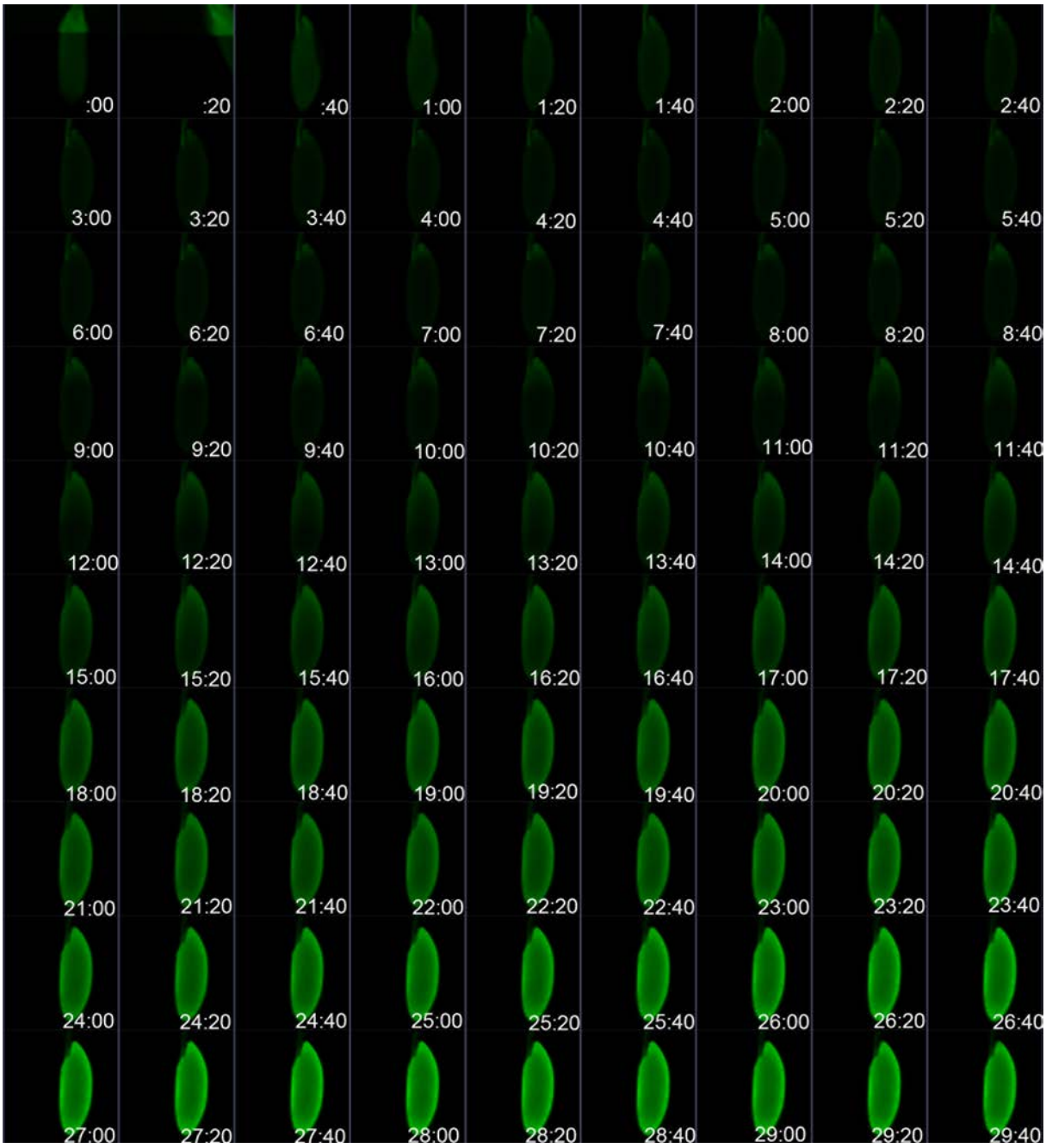
:00
:20
:40
1:00
1:20
1:40
2:00
2:20
2:40
3:00
3:20
3:40
4:00
4:20
4:40
5:00
5:20
5:40
6:00
6:20
6:40
7:00
7:20
7:40
8:00
8:20
8:40
9:00
9:20
9:40
10:00
10:20
10:40
11:00
11:20
11:40
12:00
12:20
12:40
13:00
13:20
13:40
14:00
14:20
14:40
15:00
15:20
15:40
16:00
16:20
16:40
17:00
17:20
17:40
18:00
18:20
18:40
19:00
19:20
19:40
20:00
20:20
20:40
21:00
21:20
21:40
22:00
22:20
22:40
23:00
23:20
23:40
24:00
24:20
24:40
25:00
25:20
25:40
26:00
26:20
26:40
27:00
27:20
27:40
28:00
28:20
28:40
29:00
29:20
29:40

Figure 2.3. U-73122 does not affect the Ca^{2+} wave at egg activation. Oocytes treated with 10-20 μM concentrations of the PLC inhibitor U-73122 show an intracellular Ca^{2+} flux similar to that seen in control oocytes during egg activation. Time is measured in minutes:seconds.

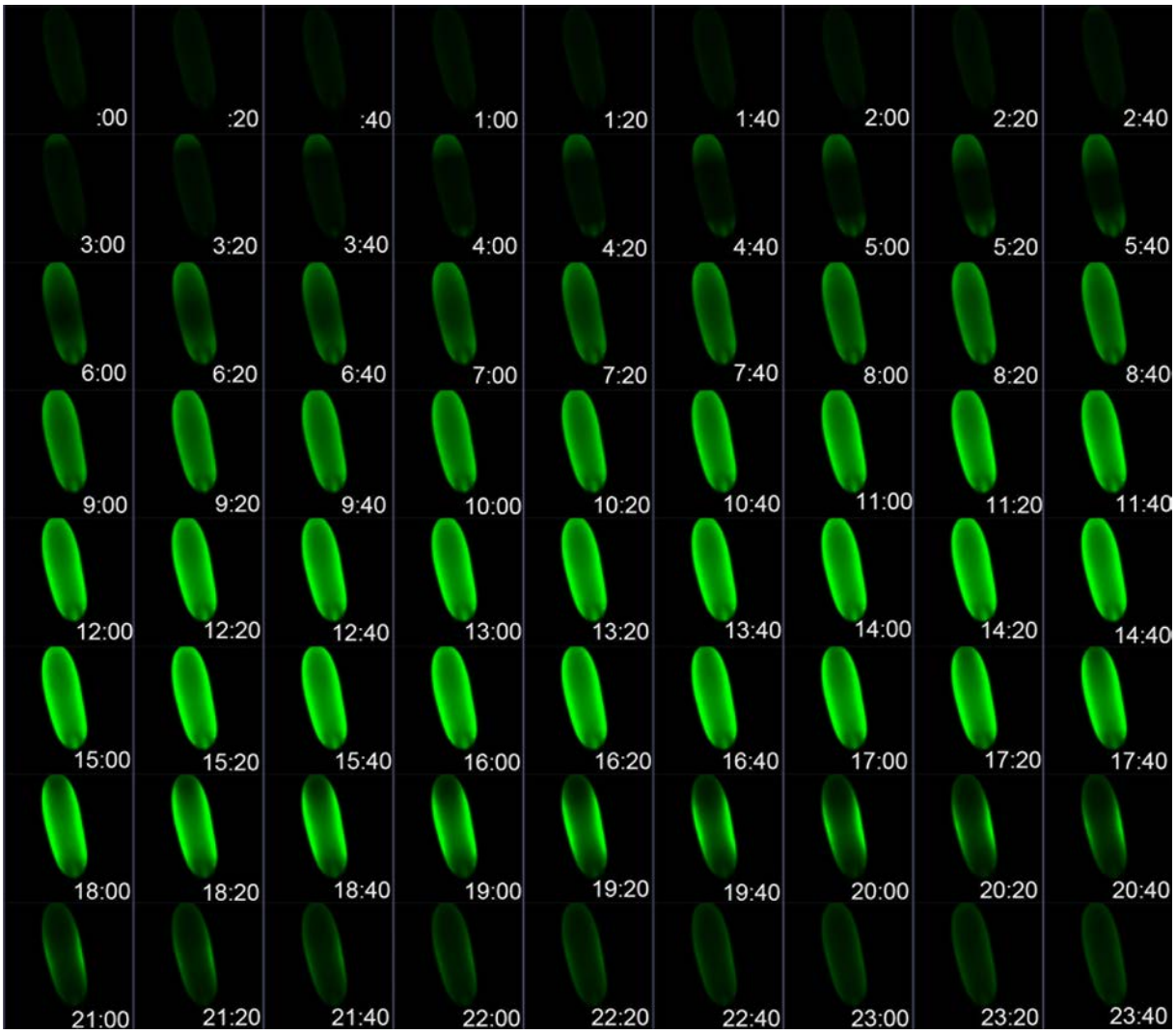
:00
:20
:40
1:00
1:20
1:40
2:00
2:20
2:40
3:00
3:20
3:40
4:00
4:20
4:40
5:00
5:20
5:40
6:00
6:20
6:40
7:00
7:20
7:40
8:00
8:20
8:40
9:00
9:20
9:40
10:00
10:20
10:40
11:00
11:20
11:40
12:00
12:20
12:40
13:00
13:20
13:40
14:00
14:20
14:40
15:00
15:20
15:40
16:00
16:20
16:40
17:00
17:20
17:40
18:00
18:20
18:40
19:00
19:20
19:40
20:00
20:20
20:40
21:00
21:20
21:40
22:00
22:20
22:40
23:00
23:20
23:40

Figure 2.4. Ruthenium red does not affect the Ca^{2+} wave at egg activation. Oocytes treated with 10 μM concentrations of the ryanodine receptor inhibitor ruthenium red show an intracellular Ca^{2+} flux similar to that seen in control oocytes during egg activation. Time is measured in minutes:seconds.

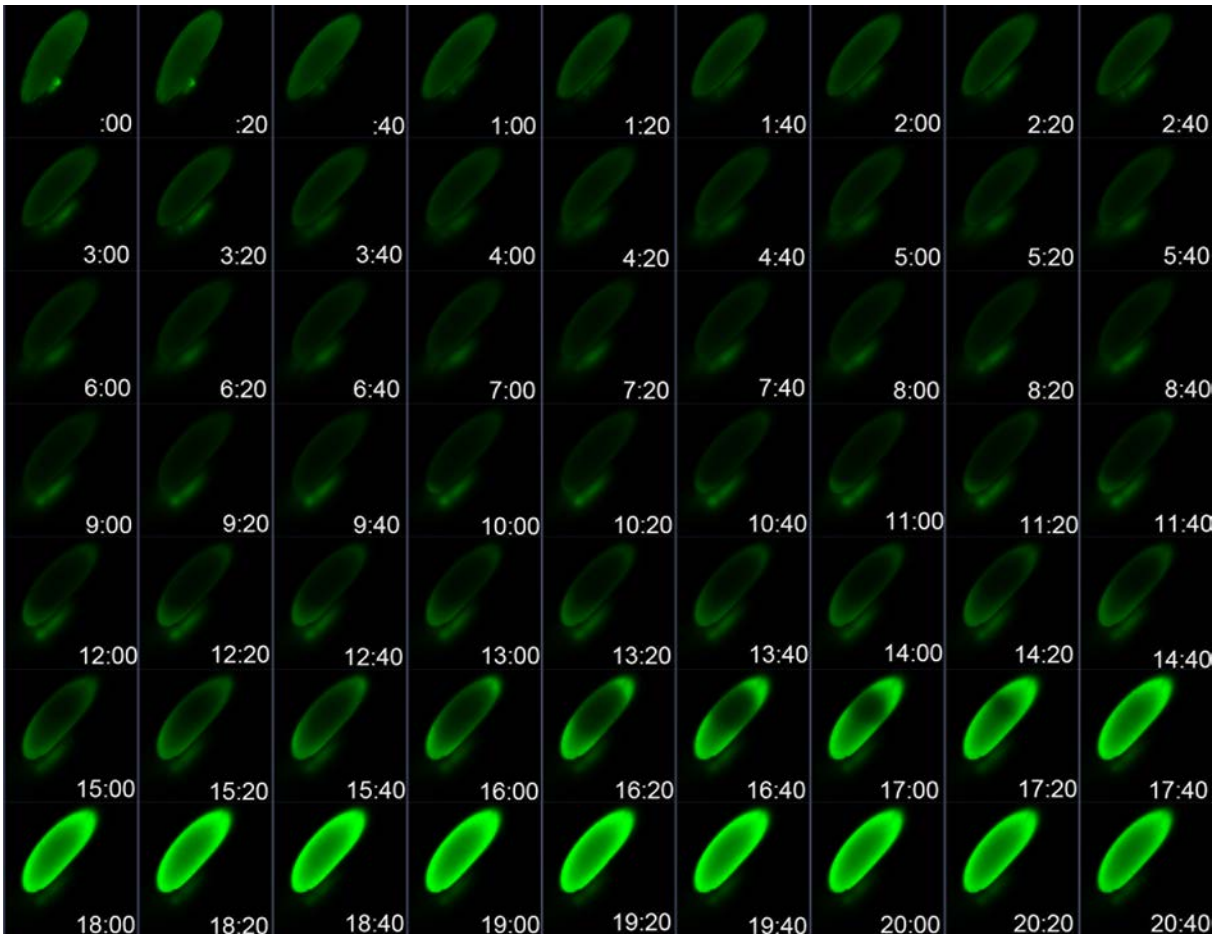
:00
:20
:40
1:00
1:20
1:40
2:00
2:20
2:40
3:00
3:20
3:40
4:00
4:20
4:40
5:00
5:20
5:40
6:00
6:20
6:40
7:00
7:20
7:40
8:00
8:20
8:40
9:00
9:20
9:40
10:00
10:20
10:40
11:00
11:20
11:40
12:00
12:20
12:40
13:00
13:20
13:40
14:00
14:20
14:40
15:00
15:20
15:40
16:00
16:20
16:40
17:00
17:20
17:40
18:00
18:20
18:40
19:00
19:20
19:40
20:00
20:20
20:40

Ca^{2+} can also be released from ER stores through activation of the ryanodine receptor on the ER plasma membrane. To test the possibility of this receptor in Drosophila egg activation, I performed *in vitro* egg activation with eggs treated with ruthenium red, an inhibitor of the ryanodine receptor. The Ca^{2+} flux was also unchanged when eggs were treated with ruthenium red, indicating that ryanodine receptor activity is not required for egg activation (Figure 2.4).

Ca^{2+} influx requires extracellular calcium

Since the Ca^{2+} rise is not dependent on internal calcium stores, I examined the possibility that calcium enters the oocyte from the external environment. Previous studies indicated that Drosophila oocytes cannot undergo *in vitro* activation in buffers depleted of Ca^{2+} (Horner and Wolfner, 2008a), suggesting that calcium from external sources was necessary to activate the eggs. This suggested that the source of calcium for the wave might be external. To test the requirement of extracellular calcium, I performed *in vitro* activation in buffers depleted of Ca^{2+} using the Ca^{2+} chelator BAPTA. Cytosolic Ca^{2+} levels did not increase in oocytes incubated in BAPTA-treated buffers, though egg swelling did occur (Figure 2.5). Control buffers prepared in parallel were able to elicit the Ca^{2+} rise. This result indicates that the Ca^{2+} rise requires calcium in the extracellular medium.

Extracellular Ca^{2+} enters the oocyte through mechanosensitive channels

Previous studies indicated that mechanical stress may be a trigger for egg activation in Drosophila and some other insects. For example, pressure and squeezing applied to Drosophila or wasp eggs can be sufficient for egg activation (Horner and Wolfner, 2008a; Went and Krause, 1974). Horner et al. (2008) previously showed that the stretch-activated ion channel blocker and heavy metal gadolinium inhibits egg activation in Drosophila. To test whether this also interferes with the Ca^{2+} rise, I incubated dissected oocytes in concentrations of $GdCl_3$ ranging from 10µM

Figure 2.5. Chelation of ions using BAPTA inhibits the Ca^{2+} wave at egg activation.

Oocytes activated in Ca^{2+}-depleted buffers containing BAPTA do not show an intracellular Ca^{2+} flux, though egg swelling does occur. Time is measured in minutes:seconds.

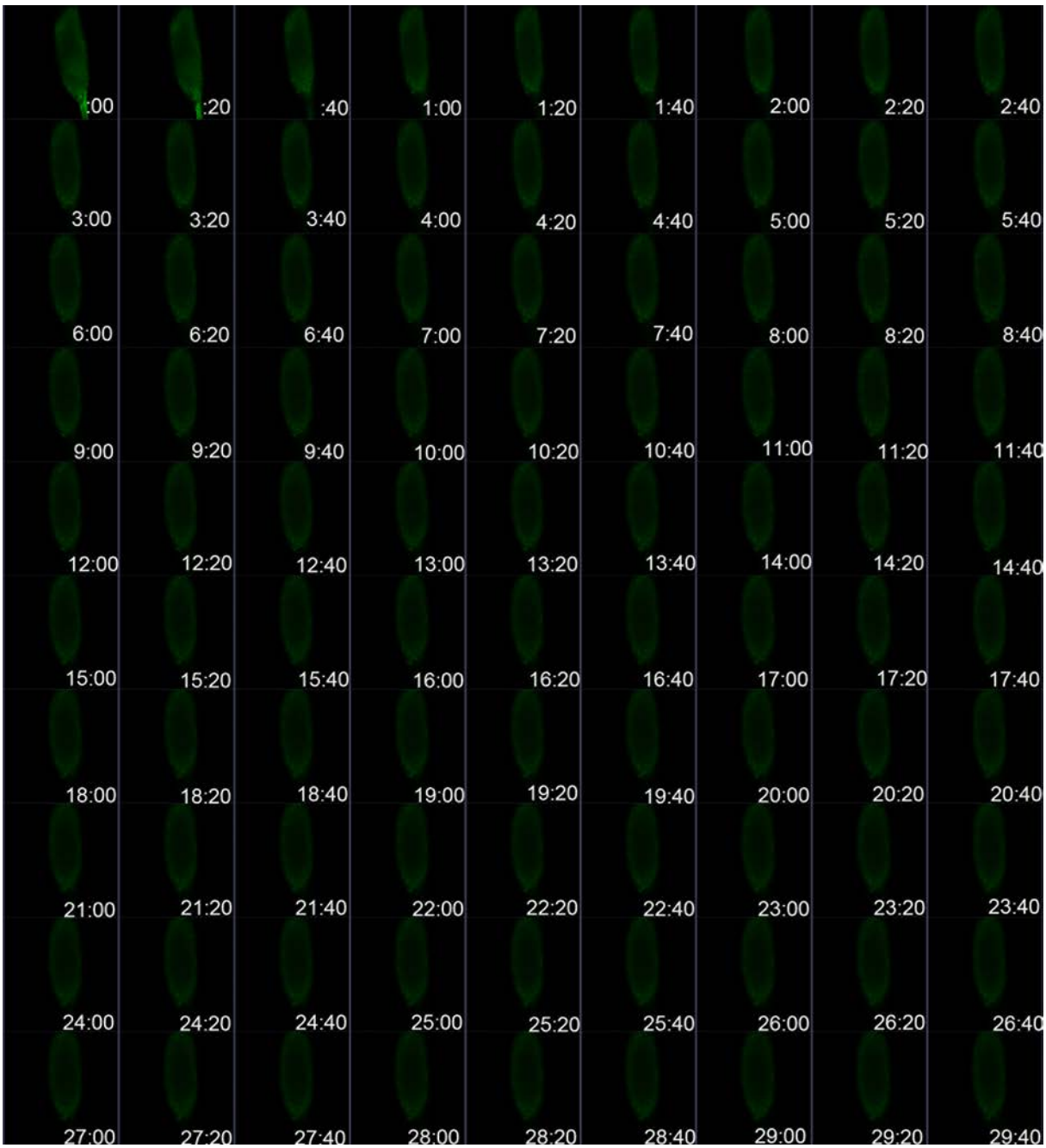
:00
:20
:40
1:00
1:20
1:40
2:00
2:20
2:40
3:00
3:20
3:40
4:00
4:20
4:40
5:00
5:20
5:40
6:00
6:20
6:40
7:00
7:20
7:40
8:00
8:20
8:40
9:00
9:20
9:40
10:00
10:20
10:40
11:00
11:20
11:40
12:00
12:20
12:40
13:00
13:20
13:40
14:00
14:20
14:40
15:00
15:20
15:40
16:00
16:20
16:40
17:00
17:20
17:40
18:00
18:20
18:40
19:00
19:20
19:40
20:00
20:20
20:40
21:00
21:20
21:40
22:00
22:20
22:40
23:00
23:20
23:40
24:00
24:20
24:40
25:00
25:20
25:40
26:00
26:20
26:40
27:00
27:20
27:40
28:00
28:20
28:40
29:00
29:20
29:40

Figure 2.6. Moderate to high concentrations of gadolinium inhibit the Ca^{2+} wave at egg activation. Oocytes treated with 100-400 μM concentrations of gadolinium do not show an intracellular Ca^{2+} flux, though egg swelling does occur. Time is measured in minutes:seconds.

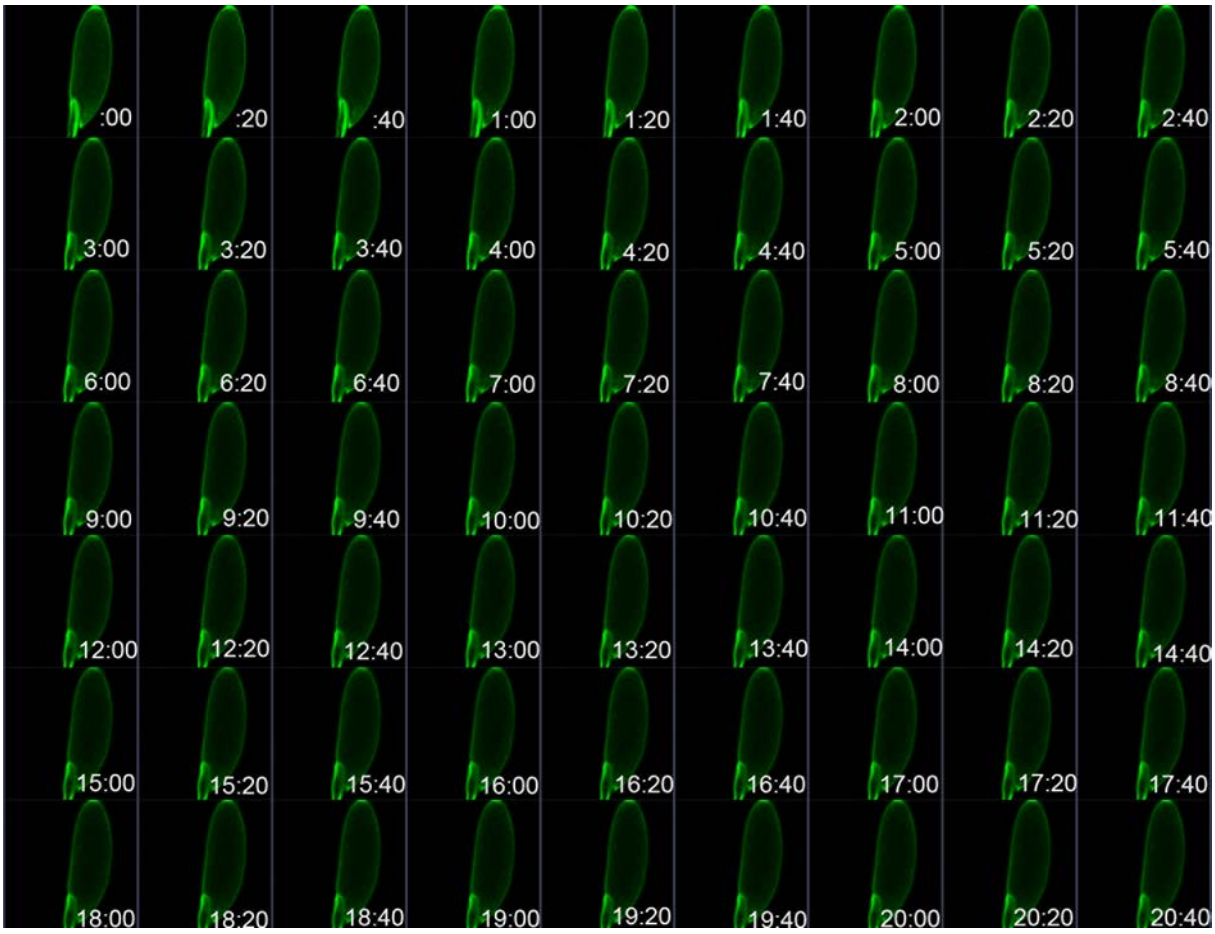
:00
:20
:40
1:00
1:20
1:40
2:00
2:20
2:40
3:00
3:20
3:40
4:00
4:20
4:40
5:00
5:20
5:40
6:00
6:20
6:40
7:00
7:20
7:40
8:00
8:20
8:40
9:00
9:20
9:40
10:00
10:20
10:40
11:00
11:20
11:40
12:00
12:20
12:40
13:00
13:20
13:40
14:00
14:20
14:40
15:00
15:20
15:40
16:00
16:20
16:40
17:00
17:20
17:40
18:00
18:20
18:40
19:00
19:20
19:40
20:00
20:20
20:40

Figure 2.7. The TRP channel inhibitor ACA inhibits the Ca^{2+} wave at egg activation.

Oocytes treated with 10-20 μM concentrations of ACA do not show an intracellular Ca^{2+} flux, though egg swelling does occur. Time is measured in minutes:seconds.


:00
:20
:40
1:00
1:20
1:40
2:00
2:20
2:40
3:00
3:20
3:40
4:00
4:20
4:40
5:00
5:20
5:40
6:00
6:20
6:40
7:00
7:20
7:40
8:00
8:20
8:40
9:00
9:20
9:40
10:00
10:20
10:40
11:00
11:20
11:40
12:00
12:20
12:40
13:00
13:20
13:40
14:00
14:20
14:40
15:00
15:20
15:40
16:00
16:20
16:40
17:00
17:20
17:40
18:00
18:20
18:40
19:00
19:20
19:40
20:00
20:20
20:40

Figure 2.8. Low concentrations of gadolinium do not inhibit the Ca^{2+} wave at egg activation. Oocytes treated with 10 μM concentrations of ACA show an intracellular Ca^{2+} flux similar to that of controls. Time is measured in minutes:seconds.

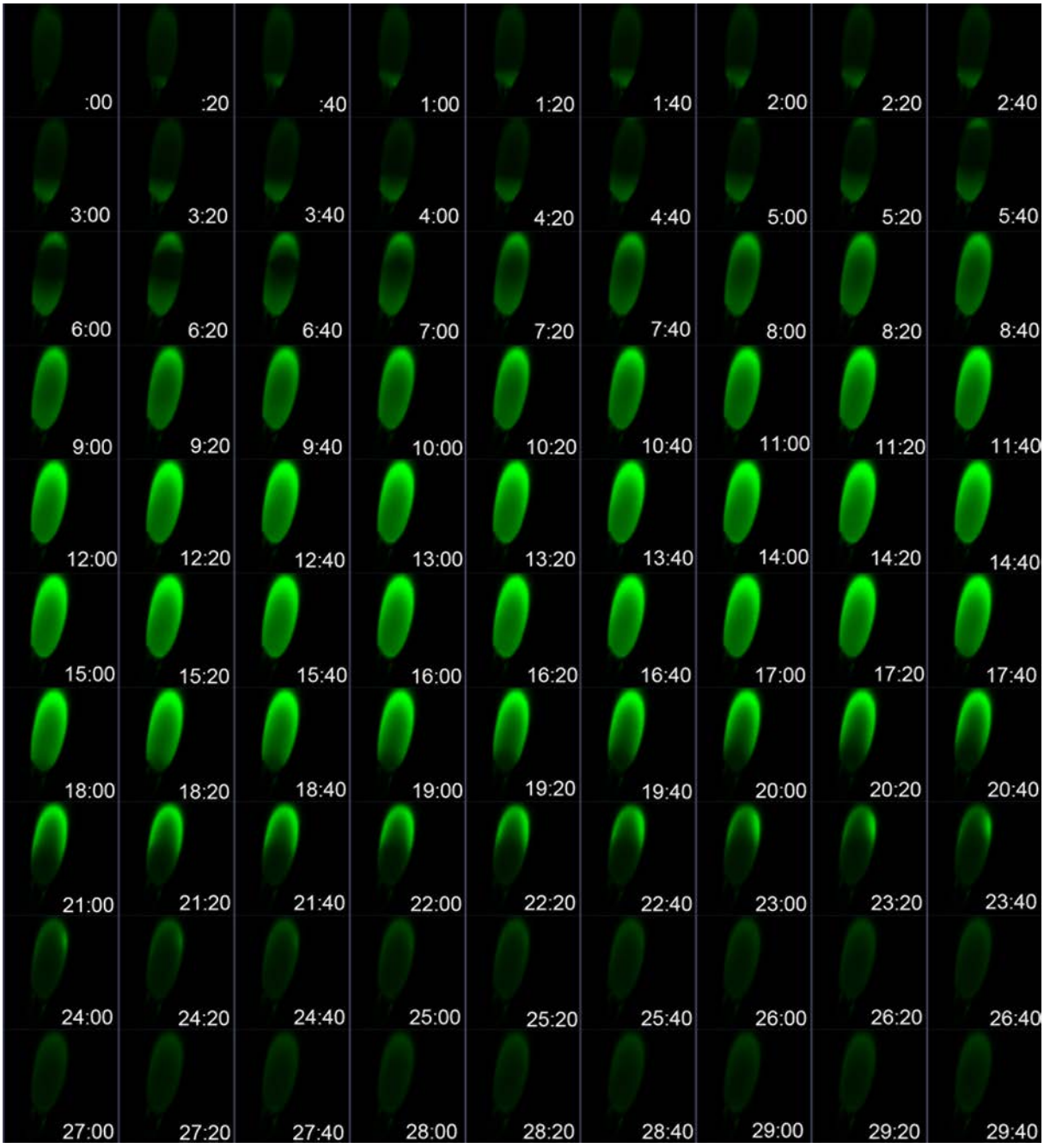
:00
:20
:40
1:00
1:20
1:40
2:00
2:20
2:40
3:00
3:20
3:40
4:00
4:20
4:40
5:00
5:20
5:40
6:00
6:20
6:40
7:00
7:20
7:40
8:00
8:20
8:40
9:00
9:20
9:40
10:00
10:20
10:40
11:00
11:20
11:40
12:00
12:20
12:40
13:00
13:20
13:40
14:00
14:20
14:40
15:00
15:20
15:40
16:00
16:20
16:40
17:00
17:20
17:40
18:00
18:20
18:40
19:00
19:20
19:40
20:00
20:20
20:40
21:00
21:20
21:40
22:00
22:20
22:40
23:00
23:20
23:40
24:00
24:20
24:40
25:00
25:20
25:40
26:00
26:20
26:40
27:00
27:20
27:40
28:00
28:20
28:40
29:00
29:20
29:40

to 400µM in IB before imaging in AB also containing $GdCl_3$. Oocytes treated with 100-400µM $GdCl_3$ did not show an increase in cytosolic Ca^{2+} during egg activation (Figure 2.6), whereas control samples tested in parallel showed the stereotypical bidirectional Ca^{2+} flux. This result indicates that Ca^{2+} likely enters the oocyte through mechanosensitive ion channels. Interestingly, treatment of oocytes with 10µM $GdCl_3$ was unable to inhibit the Ca^{2+} flux during egg activation (Figure 2.8). Some Ca^{2+} channels are more sensitive to gadolinium than others; for example, TRP-L channels are known to be insensitive to low concentrations (10µM) of gadolinium but sensitive to higher concentrations (100µM).

Several mechanosensitive channels may be present in the Drosophila oocyte plasma membrane (for a review see (Sartain and Wolfner, 2013)). Some genes of the transient receptor potential (TRP) family encoding mechanosensitive ion channels are expressed in the ovary, but their role has not been assessed during Drosophila egg activation. I used a broad-spectrum blocker of TRP-type channels, ACA, to see if inhibition of TRP channels would affect the dynamics of the calcium wave during egg activation. I incubated oocytes with 10µM ACA in IB for 30 minutes before activating in AB containing ACA. ACA-treated oocytes could not produce the Ca^{2+} flux during *in vitro* egg activation, though egg swelling did occur (Figure 2.7), whereas untreated controls were able to produce the wave as previously observed. This strongly suggests that calcium enters the oocyte through mechanosensitive TRP channels during egg activation.

2.4 Discussion

Egg activation is a conserved set of events among animal species. This transition prepares an oocyte for successful embryogenesis through completion of meiosis, restructuring of the vitelline membrane, and changes to the existing protein and mRNA pools within the oocyte. Drosophila egg activation is different from the more commonly studied cases of vertebrate and

marine invertebrate egg activation in that it is decoupled from fertilization. Yet despite this critical difference, we have found that calcium remains a constant requirement, even in this species. Together with previous data (Horner and Wolfner, 2008a), we have demonstrated in this study that even though the mechanism of calcium rise differs, it is still a requirement for egg activation and a wave still occurs. Additionally, since many signaling pathways and events downstream of the calcium signal appear to be conserved between Drosophila and other species, we propose that Drosophila is an important model system for studying this process. Drosophila offers the unique perspective allowed by the ability to perform activation without fertilization as well as ease of genetic manipulation and larger-scale "omics" studies.

This study has confirmed that a rise in cytosolic Ca^{2+} occurs during egg activation in Drosophila. In agreement with previous studies (Horner and Wolfner, 2008a), we found that calcium is required in the extracellular environment for the rise to occur, and that blocking or inhibiting mechanosensitive channels also blocks the calcium influx. Additionally, we and others have observed that eggs tend to swell during activation. The conditions *in vivo* may be such that the oocyte takes up fluid during its passage through the oviduct: mature oocytes in the ovary have a somewhat shriveled appearance, but laid eggs appear swollen and taut. In our *in vitro* experiments, we noticed that the calcium wave does not initiate until after the egg has begun to swell. Additionally, we were able to increase the speed of initiation by adding a few drops of water to the activating medium during imaging, thus increasing hypotonicity and causing faster egg swelling. We believe that swelling exerts a stretch tension force on the membrane, which triggers the opening of mechanosensitive Ca^{2+} channels. Our experiments indicate that this is likely a TRP family calcium channel, evidenced by inhibition of the calcium flux by ACA and gadolinium. Further experiments will be needed to determine the particular type of channel and

Table 2.1. Expression of mechanosensitive channels in the adult ovary.

	Expressed (high, moderate, low	**Not expressed**
TRP	*trpm*, *trpml*, *pain*	*trp, trpg, trpl, nompc, nan, iav, trpa1, pkd2, trpml*
DEG/ENaC	*rpk*, *ppk28*	*ppk, ppk4, ppk6, ppk7, ppk10, ppk11, ppk12, ppk13, ppk14, ppk16, ppk19, ppk20, ppk21, ppk23, ppk28*

its localization on the egg cell surface, though we do know that at least three TRP family channels are expressed in the ovary [*painless* (TRPA1), *trpm* (TRPM3), and *trpml* (TRPP1/Pdk2)] (Table 2.1) . It is possible that the channels are localized only to the poles of the egg; this would allow the type of converging wave we observed in this study.

Alternatively, it is possible that the egg cytoskeleton is less rigid on the poles of the egg, which might allow greater tension forces to be experienced there during egg swelling, thus opening those calcium channels first. During egg swelling, pressure on the egg membrane due to uptake of fluid would be experienced uniformly throughout the oocyte. However, because the egg is essentially a prolate spheroid, greater stretch tension would be experienced in the middle of the egg rather than at the ends of the egg, so if channels are uniformly localized in the plasma membrane we might expect stretch activated channels in the middle of the oocyte to open before those at the poles (Regen). However, different cytoskeletal makeup at the poles may cause tension to be experienced differently there, and in this way channels spread uniformly throughout the plasma membrane may open first at the poles. Further experiments will be required to determine why the wave initiates at the poles.

Recent evidence from mice indicates that a requirement for external Ca^{2+} is not unique to insects like Drosophila. In fact, after the initial Ca^{2+} rise induced by sperm PLC in mice, further calcium oscillations require Ca^{2+} uptake from the extracellular environment through a store-operated Ca^{2+} entry mechanism (Miao et al., 2012). Here, when intracellular ER Ca^{2+} stores are depleted, plasma membrane channels open to allow Ca^{2+} back into the cell. Though Drosophila egg activation does not appear to utilize intracellular Ca^{2+} stores, a similar Ca^{2+} entry mechanism may be at play.

In other organisms in which the signaling pathway has been studied downstream of the Ca^{2+} influx, an increase in intracellular Ca^{2+} ultimately causes meiotic resumption and, if the egg has been fertilized, embryonic mitoses. Interestingly, the early embryonic mitoses in Drosophila occur in a convergent wave that initiates at either pole and moves inward (Parry et al., 2005), much like the Ca^{2+} flux demonstrated in this chapter. Although the downstream signaling pathway has yet to be completely understood in Drosophila, this supports the hypothesis that the Ca^{2+} influx triggers the events of egg activation including cell cycle resumption. Future work should aim to link the Ca^{2+} flux to downstream egg activation events.

CHAPTER 3

PHENOTYPIC AND TRANSCRIPTOMIC ANLAYSIS OF EGGS FROM PRAGE MUTANT MOTHERS DURING EGG ACTIVATION[3]

3.1 Introduction

Mature oocytes undergo major cellular changes at fertilization. Oocytes within the ovary are stalled at a species-specific stage of meiosis and are stocked with many maternally-contributed nutrients, RNAs, and proteins. At the egg-to-embryo transition (upon fertilization in most animals), the mature oocyte undergoes a series of changes collectively known as "egg activation", including changes to vitelline membrane, meiotic resumption/completion, and modifications to the existing RNA and protein pools. These changes are critical for blocking polyspermy, for pronuclear formation, and for appropriate embryonic patterning and morphogenesis.

Drosophila melanogaster affords a unique perspective on egg activation, notably because in this model, fertilization is not required for egg activation to occur. Instead, egg activation occurs during passage through the oviduct, prior to fertilization (Heifetz et al., 2001). Thus, we are able to study the events of egg activation decoupled from fertilization and embryogenesis. This has allowed for the identification of many genes required for regulation of this major cellular transition. Of importance to this study, several X-linked loci were identified in a screen for mutants that could not complete egg activation properly, using maternal transcript stability as a marker of proper activation (Tadros et al., 2003). From this screen, several conserved genes essential for egg activation were identified and have gone on for further study, including *wispy*

[3] This project was a collaboration between several members of the lab: Jun Cui mapped the *prg* mutations and Yun-Wei Lai performed expression studies.

(*wisp*), a poly(A) polymerase required for translational activation of stored transcripts ((Benoit et al., 2008; Brent et al., 2000; Cui et al., 2008) and Chapter 4), and the Pan Gu Kinase (PNG) complex (Tadros et al., 2007; Vardy and Orr-Weaver, 2007) [including *giant nuclei* (*gnu*) and *plutonium* (*plu*)], which also regulates translation of stored mRNAs.

Regulation, and specifically degradation, of maternally stored mRNAs is critical for several aspects of embryogenesis (reviewed in (Tadros and Lipshitz, 2005)). At egg activation, some cell cycle regulators must be eliminated in order for meiosis to resume and complete in preparation for pronuclear fusion and embryonic mitoses. In fact, many maternally-stored mRNAs that are degraded at egg activation have roles in cell cycle regulation, such as meiotic cyclins (Tadros et al., 2007). Without mechanisms to signal degradation of these cell cycle regulators, meiotic resumption at egg activation would not be possible.

Regional degradation of transcripts within the mature oocyte or activating egg may be important for establishing patterning within the developing embryo. Precise localization of maternally-provided mRNAs is crucial for specifying embryonic axes. mRNA localization within the Drosophila oocyte can be accomplished in a number of ways. Some mRNAs, such as the transcript of the anterior determinant *bicoid*, are localized through tethering (Weil et al., 2008). However, several transcripts that exhibit specific localization are initially present throughout the oocyte, and undergo massive destabilization during egg activation except in protected local areas. Transcripts that fall into this latter category include *Hsp83*, *nanos*, and *Pgc* (Bashirullah et al., 1999).

A screen for X-linked female sterile mutations identified several loci that are required for maternal transcript destabilization in the early embryo (Tadros et al., 2003). We have characterized a new gene identified in this screen, *prage* (*prg*), whose mutant was reported to fail

to degrade *Hsp83* transcripts. We discovered that the *prg* gene encodes a protein with a predicted exonuclease domain. We performed RNA-seq to determine the extent of transcript destabilization in the absence of PRG function. However, this yielded only a modest number of hits. Further phenotypic analysis of egg activation events in eggs from *prg* mutant mothers indicate that PRG protein likely plays an important role in oogenesis rather than egg activation.

3.2 Materials and Methods

Fly stocks: Oregon-R P2 and *w1118* were used as wild type stocks. prg^{16A}/FM6 and prg^{32}/FM6 (Tadros et al., 2003) were kind gifts from W. Tadros and H. Lipshitz (Hospital for Sick Children, University of Toronto, Canada). Deficiency strains *Df(1)BSC719/Binsinscy* and three P-element insertion lines, P{Mae- UAS.6.11}CG42666^{GG01337}, P{EPgy2}CG42666^{EY21466} and P{XP}CG42666^{d10828} (Bloomington Stock number CG14630, CG19337 and CG22483, respectively) were ordered from the Bloomington Stock Center (Indiana University). *Df(1)BSC719/*Binsinscy virgin females were crossed with FM7c males to get *Df(1)BSC719/*FM7c flies for maintaining the stock. Stocks were maintained on standard yeast/glucose medium at 25°C.

Complementation test: Virgin females from each P-element insertion strain were crossed with *prg* males. Fertility of female progeny carrying P{Mae- UAS.6.11}CG42666^{GG01337}/*prg*, P{EPgy2}CG42666^{EY21466}/*prg* and P{XP}CG42666^{d10828}/*prg* were scored for complementation.

RNA extraction and RT-PCR: Total RNA was extracted from 3-5 day old adult males, adult females, and embryos collected 0-2, 2-4, or 4-6 hours after egg laying. cDNA was synthesized as described previously (Sartain et al., 2011). RT-PCR was performed to determine the expression patterns of *prg* transcripts. The primer sets for the PCR were: *prg* forward 5'-ATGGAGCAAATAACGAACTACTTCG -3'; *prg* reverse 5'-TCAGTCCGTCGTGGTAGTTG

-3’; *19337* forward 5’- GGGCGGGTAGTGGAGATA -3’; *19337* reverse upper 5’- TCGGCTGTAAACGATGCT -3’; *19337* reverse lower 5’- AGCGAATGCTCTGCGTGT -3’; *rp49* forward 5’- AGTATCTGATGCCCAACATCG -3’; *rp49* reverse 5’- TTCCGACCAGGTTACAAGAAC -3’.

RNA-sequencing.

Egg collection. Laid eggs were collected on grape plates as previously described. Briefly, approximately 100 control (prg^{32}/FM6) or mutant (prg^{32}/prg16A) females were placed in a bottle with 100 spermless males (sons of bw sp tud females (Boswell and Mahowald)) or normal fertile males (ORP2) in a reverse-cycle incubator overnight for mating. The following morning, females were allowed to lay eggs on grape plates for 1 hour, and then subsequent egg-lays were collected every 30 minutes. Eggs were placed in eppendorf tubes and frozen in liquid nitrogen at 0-30 minutes or 2-2.5 hours after egg laying.

RNA isolation. RNA from laid eggs was isolated using Trizol reagent (Invitrogen) as previously described (Sartain et al., 2011) and purified using RNeasy clean up kit according to the manufacturer's instructions.

RNA-sequencing. RNA samples were sent to the Weill Cornell Medical College Epigenomics Core facility for library preparation and sequencing. Six samples (WT and mutant, three conditions each) were run in a single lane for HiSeq SR50 single read clustering.

RNA-seq analysis. Sequencing data were aligned by WCMC Epigenomics Core using TOPHAT 2.0. I ran the aligned reads through CuffDiff to get differential expression data using the default parameters (FDR=0.5). The command used was:

cuffdiff -o ./output -p 8 -L FM61,FM62,FM6fert,prg1,prg2,prgfert genes.gtf FM6_0-30.bam FM6_2-230.bam FM6_FERT.bam PRG_0-30.bam PRG_2-230.bam PRG_FERT.bam

3.3 Results

The prage alleles carry nonsense mutations in CG42666

Previously, two allelic mutations causing egg activation failure had been mapped to a relatively large region (1B4-1E2) of the X chromosome by Tadros and colleagues (Tadros et al., 2003). We conducted deficiency mapping to determine the chromosomal locus of two mutation alleles, and sequenced these alleles to identify the molecular nature of the *prg* mutation.

We first tested for complementation between the two *prg* mutant alleles, prg^{16A} and prg^{32}, and six deficiency lines in the 1B4-1E2 region available from the Bloomington Drosophila Stock Center. One line, *Df(1)BSC719*/Binsinscy, fails to complement both *prg* alleles, while another line, *Df(1)A94*/FM6, carrying a partially overlapping deficiency, complements both alleles. These results suggest that the *prg* mutation is in chromosome region 2B12-13. The ten genes that lie in this region were sequenced in both *prg* alleles. We found that both *prg* mutants have molecular lesions in the predicted ORF of CG42666, according to the latest annotation of the Drosophila genome (http://www.flybase.org). Both *prg* alleles have single base pair changes in the 3' end of the transcript, shared by all six isoforms that exist in Drosophila. Interpro sequence analysis and classification identified a single conserved domain near the C terminal end of the CG42666 protein with terms "Exonuclease" (IPR006055), "Ribonuclease H-like domain" (IPR012337), and "Exonuclease, RNase T/DNA polymerase III" (IPR013520). In each *prg* mutation, a single coding codon changed to a stop codon resulted in a truncated protein of 72

amino acids (prg^{16A}) and 373 amino acids (prg^{32}) (Figure 3.1). Both truncated proteins lack the predicted exonuclease domain.

To confirm that *prg* gene corresponds to CG42666, we carried out complementation tests of *prg* mutations with P-element insertions in CG42666. We tested for complementation between both *prg* mutant alleles (prg^{16A} and prg^{32}) and three P-element insertion lines available from Bloomington Stock Center. Two insertions, P{Mae UAS.6.11}$CG42666^{GG01337}$ (Mae) and P{EPgy2}$CG42666^{EY21466}$ (EPgy2), failed to complement either *prg* mutant allele. However, P{XP}$CG42666^{d10828}$ (XP) unexpectedly complemented both *prg* alleles. We confirmed by RT-PCR that this line had an insertion in CG42666 (Figure 3.2). Based on the gene structure described in *Flybase,* CG42666 contains six predicted isoforms (PE, PB, PD, PF, PC, PA). The insertions of Mae and EPyg2 are disrupted in all six isoforms, suggesting the universal effects of these two lines; however, XP is only inserted into regions found in one RNA isoform (PE). The simplest explanation is that XP insertion does not eliminate function of CG42666 gene, if some isoforms are still expressed normally and produce functional PRG protein. Whether functions of CG42666 isoforms can compensate for each other requires further study, but the results from Mae and EPgy2 insertion lines confirm that CG42666 is the *prg* gene.

RT-PCR shows that *prg* (CG42666) is expressed in both males and females, and is present during early embryogenesis (Figure 3.3). High-throughput expression studies confirm this finding (Chintapalli et al., 2007).

Oocytes from prg mutant mothers fail to undergo vitelline membrane reorganization

Egg activation in laid eggs from *prg* mutant mothers was first studied in the Lipshitz lab (Tadros et al., 2003). There, embryos from *prg* mothers were observed to undergo proper vitelline membrane (VM) reorganization (crosslinking to create a hard, impenetrable eggshell)

Figure 3.1 Schematic representation of *prg* alleles. Wild-type CG42666 gene (isoform A) encodes a protein of 761 a.a. prg^{16A} and prg^{32} have nonsense mutations in the coding region that results in truncated protein of 72 a.a. and 373 a.a. respectively.

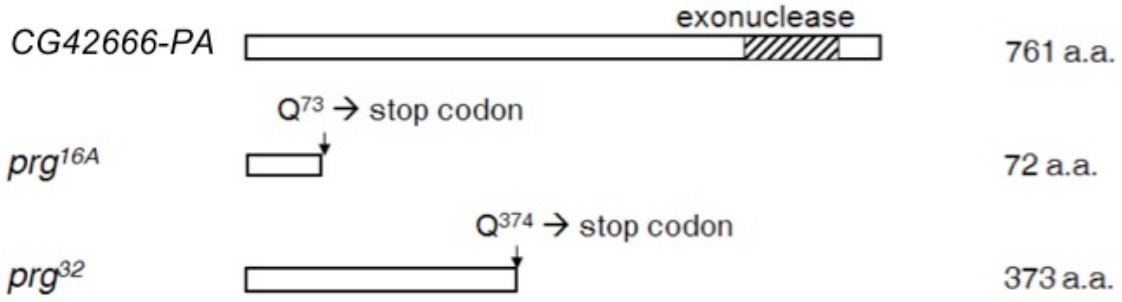
exonuclease
CG42666-PA
761 a.a.
Q73 → stop codon
prg16A
72 a.a.
Q374 → stop codon
prg32
373 a.a.

Supplementary Figure A.1 A map of P-element insertions relative to *prg* gene (CG42666) structure. Six isoforms (PE, PB, PD, PF, PC and PA) are shown in different lengths for both transcripts and cDNAs (CDS). The insertion sites of three P-element strains (P{XP}CG42666d10828, *P*{Mae-UAS.6.11}CG42666GG01337 and P{EPgy2}CG42666EY21466) are shown in a left to right order on the map (blue arrowhead). P{XP}CG42666d10828 only inserted into one gene isoform (PE) as described in the text. Map modified from *Flybase* (http://flybase.org/).

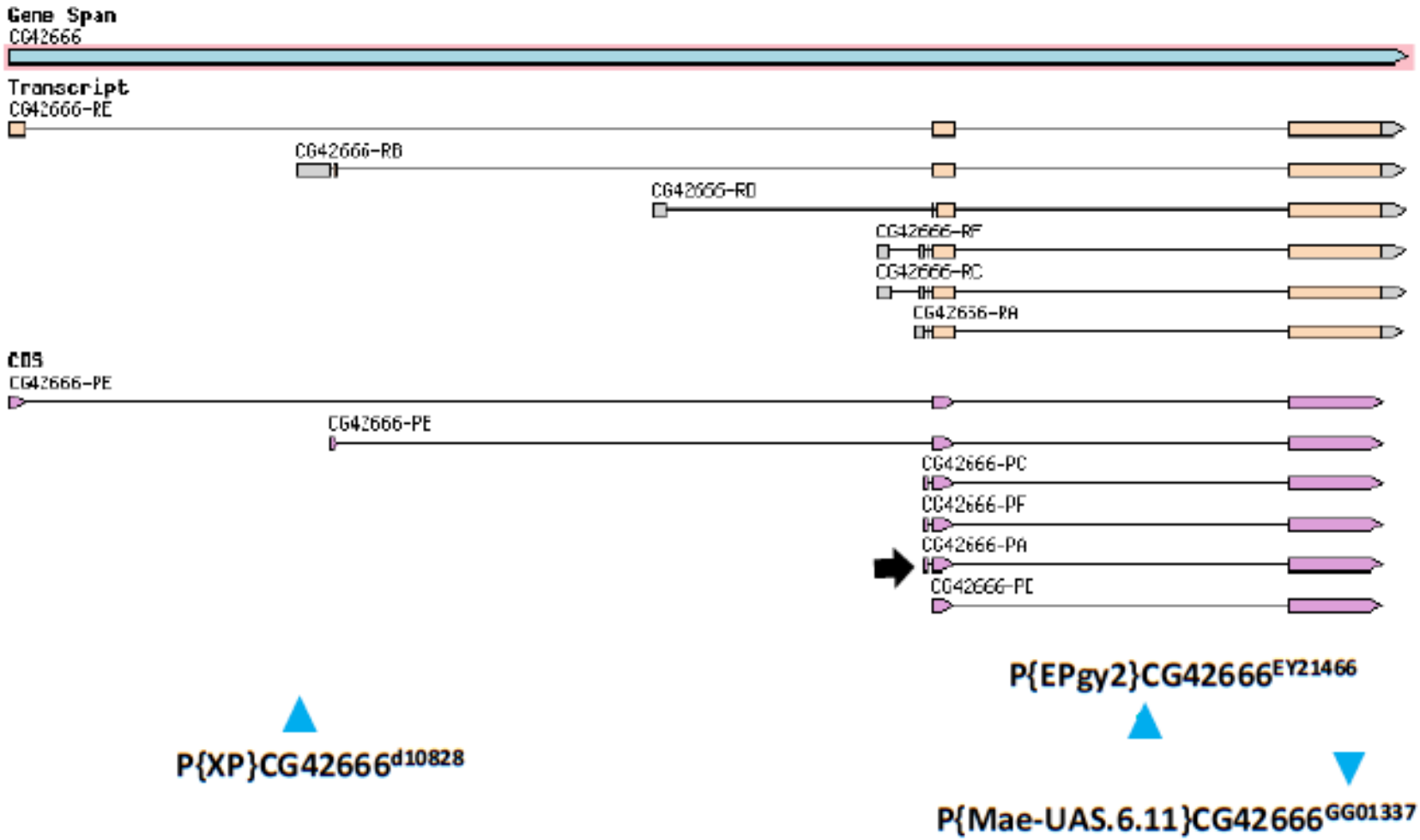
Gene Span
CG42666
Transcript
CG42666-RE
CG42666-RB
CG42666-RD
CG42666-RF
CG42666-RC
CG42666-RA
CDS
CG42666-PE
CG42666-PE
CG42666-PC
CG42666-PF
CG42666-PA
CG42666-PD
P{EPgy2}CG42666EY21466
P{XP}CG42666d10828
P{Mae-UAS.6.11}CG42666GG01337

Figure 3.2 Presence of insertion, P{XP}CG42666^{d10828}, in CG42666. (Yun-Wei Lai)

Genomic DNA was extracted from ten 3-4 day old adult males and used for PCR analysis. RPL32 was used as an internal control for evaluating the relative amounts of cDNAs. Three different combinations of *prg* primers shown in the simplified diagram (upper) were used to detect *prg* transcripts: P1&P2 - test for the presence of CG42666 gene; P1&P3 - test for the presence of P-element insertion; P1&P3 - negative control. P{XP}CG42666^{d10828} is located in the predicted site, suggesting the presence of the insertion.

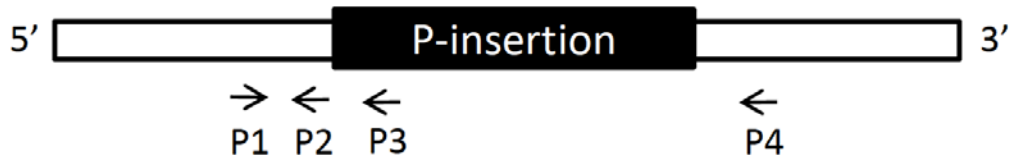
5'
P-insertion
3'
P1
P2
P3
P4

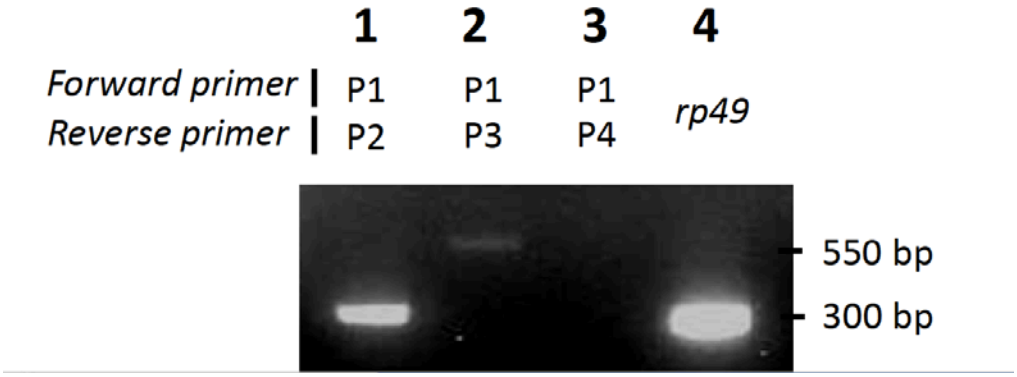
1
2
3
4
Forward primer
Reverse primer
P1
P2
P1
P3
P1
P4
rp49
550 bp
300 bp

Figure 3.3 Expression patterns of *prg* transcripts. (Yun-Wei Lai)

RT-PCR shows that *prg* is expressed in both whole males and females, and during early embryogenesis. RPL32 (rp49) is used as an internal control.

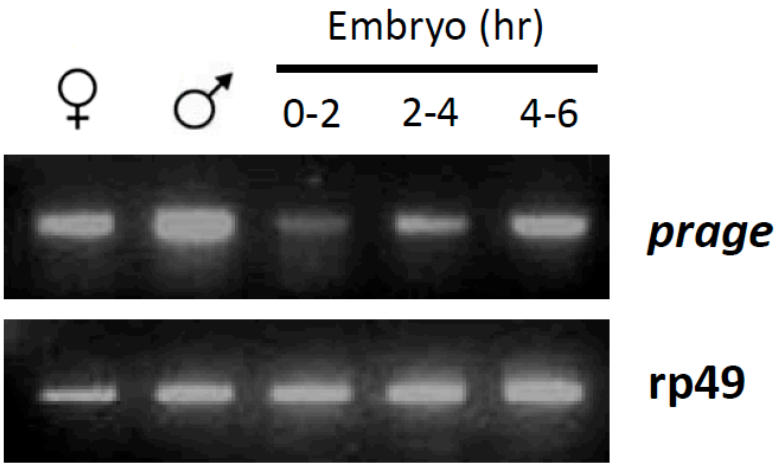
Embryo (hr)
♀
♂
0-2
2-4
4-6
prage
rp49

and to resume and complete meiosis (Tadros et al., 2003). However, when we started working with the *prg* mutation, we observed that laid eggs from *prg* mothers do not behave the same as wild-type with regard to VM crosslinking events. To test eggs for activation, we and others use the "bleach resistance" test: incubate the eggs or embryos in a 50% bleach solution for two minutes; eggs that have activated should have undergone VM crosslinking, which makes them impenetrable to bleach, while eggs that have not activated will lyse in the bleach solution. I repeated these experiments with each mutant line (prg^{16A} and prg^{32}) separately and found that the eggs of females from neither mutant line were bleach resistant to wild-type levels. It is possible that each line gained some mutation over the last decade of maintenance in our lab, so I also tested laid eggs from transheterozygotic mutant mothers (prg^{16A}/prg^{32}) for bleach resistance. I found that while eggs from mutant mothers do not completely dissolve in a bleach solution like unactivated eggs, none of them appeared normal. After bleach treatment, 84 of 146 (57%) of the eggs from prg^{16A}/prg^{32} mothers had not lysed completely, compared to 93 of 95 (98%) bleach resistance in wild-type samples.

However, the "resistant" *prg* eggs did not appear normal. In wild-type, activated eggs that have undergone bleach treatment appear swollen and taut like oblong balloons. Furthermore, they are opaque white and have a distinct sheen on their surface. The *prg* eggs that did not dissolve after bleach treatment did not appear like wild-type: instead, they appeared deflated and translucent. Upon closer inspection with a dissecting scope, I noticed that some of the "eggs" appeared to have holes and tears in an otherwise intact but rough-looking membrane: they looked like ripped empty bags, as if the yolk had seeped out imperfections in the membrane (can be seen in confocal imaged in Fig 3.4C,D). I conclude that VM reorganization and possibly initial VM composition is not normal in eggs from *prg* mutant mothers.

Figure 3.4 Eggs from *prg* mutant mothers are defective for VM crosslinking and meiotic completion. Fertilized eggs collected 0-1 hour after egg laying normally show many dividing nuclei in wild type (A,B), indicating that egg activation has occurred normally and embryogenesis is underway. Eggs collected from *prg* mutant mothers 0-1 hour after egg laying do not contain mitotically dividing nuclei (C,D). Furthermore, many eggs have ripped or burst (asterisk in D), and the cell surface (vitelline membrane) appears rough and perforated.

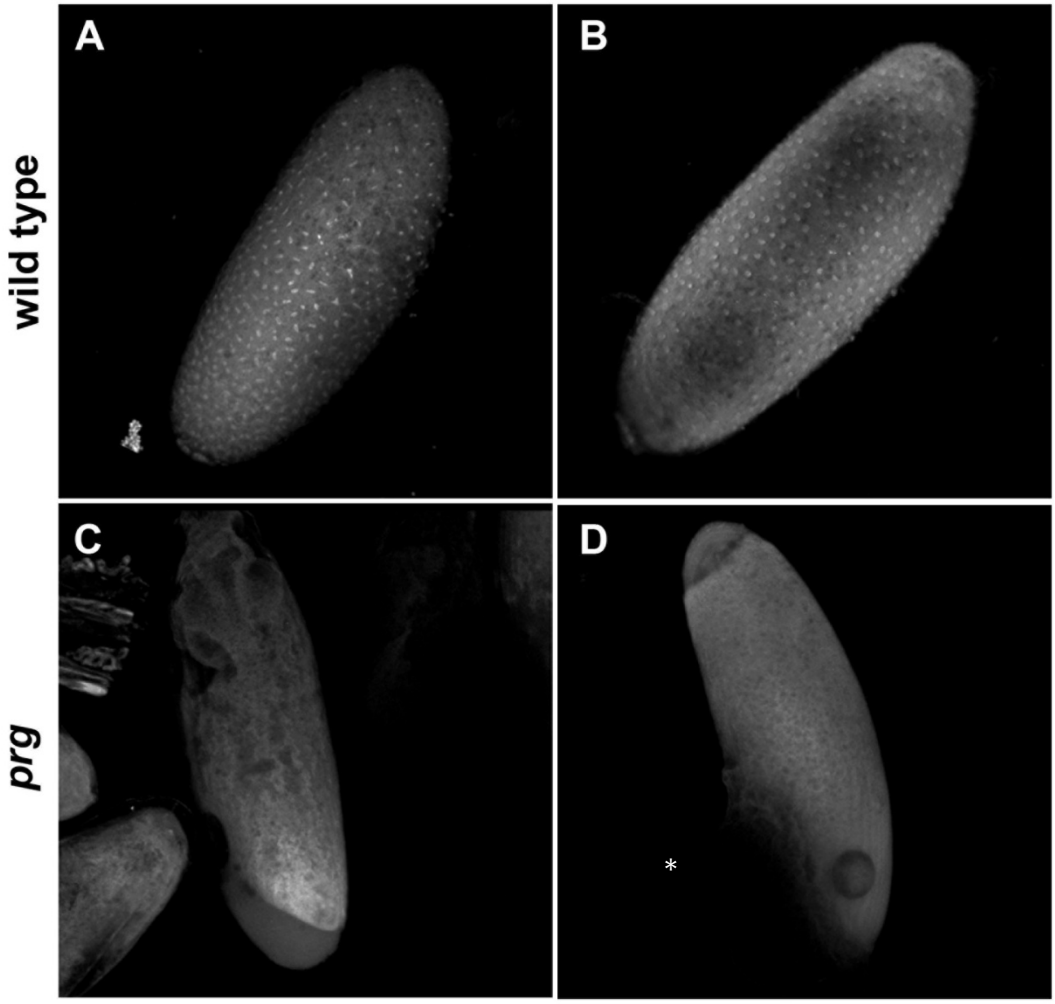
A
B
wild type
C
D
prg
*

Oocytes from prg mutant mothers fail to complete meiosis

Tadros and colleagues (2003) previously observed that meiosis does not occur normally in eggs from *prg* mutant mothers, but did not provide any evidence to this point. I tested whether fertilized laid eggs from *prg* mutant mothers were able to being mitotic divisions. I bleached eggs from *prg* and ORP2 mated females 0-1 hour after egg laying, permeabilized and fixed them using heptane/methanol, and stained nuclei with DAPI. I was able to observe many mitotically dividing nuclei in eggs from wild-type mothers (Figure 4A,B), but was not able to detect nuclei in eggs from *prg* mothers (Figure 4C,D). I conclude that eggs from *prg* mutant mothers cannot enter mitotic divisions, and likely are defective for meiotic resumption.

RNA-seq reveals putative targets of degradation by PRG

Because *prg* encodes a putative exonuclease, we hypothesized that egg activation fails in *prg* mutants due to an inability to destabilize maternal transcripts at the appropriate time during development. To explore this hypothesis, we performed RNA-seq analysis to compare the presence of maternally deposited transcripts between mutant and wild-type samples. We sampled transcripts from freshly-laid unfertilized eggs (0-30 minutes after egg laying), aged unfertilized eggs prior to zygotic genome activation (ZGA) (2-2.5 hours after egg laying), and aged fertilized eggs prior to ZGA (2-2.5 hours after egg laying). While we did not observe great differences in transcript abundance in freshly laid unfertilized eggs, a modest number of genes showed excess transcripts in the *prg* mutant in aged unfertilized eggs (Table 3.1). Notably, among these was *Hsp83*. In the initial screen that first identified the *prg* mutation, Tadros and colleagues (2003) used *Hsp83* maternal transcript degradation as a diagnostic marker of normal egg activation. They found that in *prg* mutants, *Hsp83* transcripts are not properly destabilized at egg activation. Thus, the fact that *Hsp83* is among the small number of genes identified in our RNA-seq

Table 3.1 Significant hits from comparison of unfertilized eggs from wild-type and *prg* mutant mothers 2-2.5 hours after egg laying. q-value is a representation of the p-value adjusted for multiple hypothesis testing.

gene	control	*prg*	fold change	test_stat	p_value	q_value
dhd	145.78	12997.2	6.47827	-5.73233	9.91E-09	0.000182838
Hsp26	82.5635	3390.87	5.36001	-5.21289	1.86E-07	0.00147069
26-29-p	19.5269	1294.82	6.05114	-5.1774	2.25E-07	0.00155735
Hsp83	57.0172	1615.41	4.82436	-4.99563	5.86E-07	0.00249784
CG6770	38.3399	3318.75	6.43565	-4.98725	6.12E-07	0.00251206
osk	7.54558	374.58	5.6335	-4.3505	1.36E-05	0.0116145
alphaTub67C	8.64095	692.788	6.32508	-4.24339	2.20E-05	0.0158069
Hsp27	77.6815	1241.62	3.99851	-4.09153	4.29E-05	0.0246486
Ahcy13	14.527	548.305	5.23817	-4.05857	4.94E-05	0.0269885
RnrS	4.96371	650.018	7.03292	-4.02383	5.73E-05	0.0292221
Gapdh2	18.6506	1868.32	6.64638	-4.01889	5.85E-05	0.0293002

comparisons serves as an internal validation of our results. On the other hand, while comparisons between the aged fertilized groups also showed differences in mRNA levels for many genes, many of these results are not significant in the expected direction (i.e., greater abundance in *prg* than in controls) and are likely due to the possibility that *prg* embryogenesis has stalled before this timepoint while fertilized wild-type embryos are able to continue development.

3.4 Discussion

Egg activation in Drosophila is a complex set of events, the interdependency of which is not yet fully understood. At this critical period, the cell undergoes several major changes, including vitelline membrane restructuring, meiotic resumption, protein modification, and transcript turnover through degradation or polyadenylation/translation. While there is some evidence regarding the timing of the onset of each of these events, we do not yet know whether one event depends upon proper completion of any of the other events. In Drosophila, the initial trigger for egg activation is likely a mechanical stimulus that is exerted upon the oocyte during its passage through the oviduct (Heifetz et al., 2001; Horner and Wolfner, 2008a). The mechanical stimulus is believed to trigger the influx of calcium from the external environment, which then acts as the activating signal for all of the events of egg activation (Horner and Wolfner, 2008; Sartain et al., *in prep*). The incoming calcium signal may activate several pathways that independently result in each separate egg activation event, or the pathways may be linked such that a mutant that cannot properly reorganize the vitelline membrane will also not be able to complete meiosis. Alternatively, a mutant that has some fundamental flaw in the vitelline membrane may not be able to properly transmit the signal from the mechanical stimulation during passage through the oviduct, as proposed by Tadros and colleagues (2003). In the case of *prg*, there seems to be some fundamental problem with vitelline membrane reorganization during

egg activation, but the flaw is not completely debilitating: While the activated egg does not appear “normal” like control samples (i.e., laid eggs from *prg* mutant mothers do not take on the sheen of wild-type eggs after bleach incubation), the egg does not completely lyse in bleach like unactivated eggs. It appears that eggs from *prg* mutant mothers can initiate some vitelline membrane crosslinking, but reorganization is not completely normal.

Our RNA-seq data failed to return data that indicate that *prg* plays a major role in mRNA degradation during egg activation. According to previous studies, approximately 55% of the entire Drosophila genome is represented as mRNA in the mature oocyte (Tadros et al., 2007). Approximately 20% of maternally stored mRNA is degraded upon egg activation due to female components alone (i.e., occurs in unfertilized eggs without contribution from the sperm). We know that two-thirds of these destabilized transcripts are regulated through SMG and are enriched for elements critical for cell cycle regulation. The remainng one-third are enriched for genes required for oogenesis (Tadros et al., 2007). However, PRG targets identified by our RNA-seq were not enriched for these categories. Interestingly, among the top hits in the RNA-seq data, some have previously been identified as SMG targets of degradation (*deadhead*, *Hsp83*), while others are cited as SMG-independent (*oskar*) (Tadros et al., 2007). Thus, it is possible that PRG acts independently of SMG, but the two are not mutually exclusive: for example, the exonuclease could act in concert with several different repressive elements to destabilize transcripts at egg activation. On the other hand, our RNA-seq data at may reflect secondary effects of *prg* loss-of-function: If *prg* function is needed upstream of SMG machinery, then some of the hits are likely not direct targets of PRG (assuming PRG indeed acts as an exonuclease). Alternatively, we may consider the fact that *smg* mRNA must be translated upon egg activation, and this is regulated by PNG (and likely the PNG complex, which includes PLU and GNU) (Tadros et al., 2007); our

RNA-seq data indicate that GNU is present in greater amounts in eggs from *prg* mutant mothers. Therefore, *smg* mRNA may be translated to a greater extent in eggs from *prg* mothers, which may explain why SMG targets are identified in our RNA-seq.

It is possible that the true requirement of *prg* is actually during oogenesis rather than egg activation. Our results indicate that *prg* is expressed in the female, in both the germline and the soma, and may be active in the ovary during oogenesis. If this is the case, *prg* might be required during the final stages of oogenesis, when the vitelline membrane and eggshell are synthesized around the oocyte. Here, the oocyte may still appear to have undergone normal development when observed in dissected ovaries, but any defects in eggshell composition may not become apparent until egg swelling and activation. Further analysis of timing of PRG function during development will be required to test this possibility.

In conclusion, our study has further demonstrated that *prg* is necessary for egg activation. The vitelline membrane may not crosslink properly, meiosis fails to complete, and there are differences in the abundances of several mRNAs. Though the PRG protein contains an exonuclease domain, the extent to which PRG is required for degradation of maternal transcripts at egg activation is unclear. More experiments will be necessary to determine the precise role of PRG during egg activation.

CHAPTER 4

CYTOPLASMIC POLYADENYLATION IS A MAJOR mRNA REGULATOR DURING OOGENESIS AND EGG ACTIVATION IN DROSOPHILA.[4]

4.1 Introduction

Most eukaryotic mRNAs are polyadenylated at their 3' terminus in a nuclear process that is coupled to their transcription. The presence of a poly(A) tail on a transcript both enhances its cytoplasmic stability and promotes its translation. In some cell types, a subset of transcripts has been shown to undergo further poly(A) tail adjustment in the cytoplasm. Typically, these transcripts undergo poly(A) tail shortening, which attenuates their translation, yet they remain stably 'stored' in the cytoplasm. In response to the appropriate cellular signals, these transcripts can then be induced to undergo cytoplasmic poly(A) tail lengthening, enabling their subsequent translation. As such, cytoplasmic polyadenylation of stored transcripts allows for rapid protein production in the absence of *de novo* transcription, enabling a potent mechanism for regulating gene expression.

The mechanism by which cytoplasmic polyadenylation is controlled has been studied in Xenopus oocytes (Mendez and Richter, 2001). Here, transcripts designated for poly(A) tail adjustments in the cytoplasm are marked by two cis-elements in the 3'UTR that interact with regulatory protein complexes, which include a poly(A) polymerase (PAP) as well as a ribonuclease that shortens the poly(A) tail. Upon a signal to activate translation, phosphorylation events within the protein complex cause the ribonuclease to be released (Kim and Richter, 2006).

[4] In revision as J. Cui, CV Sartain, JA Pleiss, MF Wolfner (2013) *Developmental Biology*.

The cytoplasmic PAP is then free to elongate the poly(A) tail of the transcript, thus promoting its translation.

Important cellular and developmental transitions such as those during germline development rely on cytoplasmic poly(A) tail adjustments. For example, during late oogenesis and early embryogenesis prior to the maternal-zygotic transition, the transcriptional machinery of the cell is largely silent. Growing oocytes accumulate a large pool of maternal RNA molecules whose translation is repressed after their production and then activated post-transcriptionally through cytoplasmic polyadenylation for subsequent developmental progression during oogenesis and embryogenesis (Tadros and Lipshitz, 2005). Cytoplasmic polyadenylation that occurs in the germline is often mediated by the GLD-2 family of cytoplasmic PAPs. GLD-2 homologs have been identified in many species, including worms, flies, mice and frogs (Benoit et al., 2008; Cui et al., 2008; Kwak et al., 2004; Nakanishi et al., 2006; Sartain et al., 2011). The GLD-2-type PAP in the Drosophila female germline is encoded by the *wispy (wisp)* gene (Benoit et al., 2008; Cui et al., 2008). In the absence of *wisp* function, several transcripts necessary for development do not undergo poly(A) tail lengthening and as a result these mRNAs fail to become translated in a *wispy* null mutant (Benoit et al., 2008).

A candidate gene approach was previously used to identify specific maternal mRNAs that are subject to WISP-dependent cytoplasmic poly(A) regulation during Drosophila oocyte/embryo development (Benoit et al., 2008; Cui et al., 2008). Those studies focused on cell cycle regulators and maternal transcripts necessary for embryonic development as important WISP targets for cytoplasmic polyadenylation. However, the extent to which this process controls genome-wide regulation remained unknown. Here we describe a microarray-based approach designed to identify the full subset of maternal mRNAs that are targeted for WISP-

dependent cytoplasmic polyadenylation. Our results indicate that WISP-dependent cytoplasmic polyadenylation is a major mechanism that regulates a wide spectrum of maternal mRNAs in the Drosophila female germline.

4.2 Materials and Methods

Drosophila stocks and sample collection: Male flies carrying the *wisp* null allele, *wisp*^{41} (Cui et al., 2008) were crossed to *Df(1)RA47/FM7c* female flies. *wisp*^{41}*/FM7c* (wild type control) or *wisp*^{41}*/Df* (*wisp*-deficient) virgin female progeny were separated from males and aged on standard yeast/glucose medium until use. Stage 14 oocytes were hand dissected from 3- to 5-day-old virgin females in hypertonic isolation buffer (Page and Orr-Weaver, 1997), which does not activate eggs. Virgin females that were 3 to 4 days old were mated to wild-type Oregon-R males and early embryos were collected 0- to 1-hr post egg deposition.

Sample preparation and hybridizing of microarrays: For global transcript analysis, we prepared total RNA as well as polyA$^+$-selected RNA for microarray analysis. For each sample, total RNA was extracted from ~2000 stage 14 oocytes or 0- to 1-hr embryos using the TRIzol reagent (Invitrogen, Carlsbad, CA). Polyadenylated RNA was then isolated from total RNA using the Oligotex mRNA isolation kit (Qiagen, Valencia, CA) according to the manufacturer's instruction. Sample preparation and hybridizing of microarrays was done as described (Pleiss et al., 2007), using 40 μg of total RNA or 800 ng of poly(A)-selected mRNA for cDNA synthesis. The purified cDNA was divided into halves. One half was conjugated to Cy3 and the other to the Cy5 fluorescent dye (GE Healthcare, Piscataway, NJ) to generate dye-swap pairs. Dye conjugation was performed as described (Pleiss et al., 2007).

Drosophila oligonucleotide microarrays (Agilent Design ID 18972, Agilent, Foster City, CA) were hybridized with labeled cDNA as described (Pleiss et al., 2007). Four groups of

comparisons were performed: WT vs. *wisp* total RNA from oocytes, WT vs. *wisp* total RNA from fertilized eggs, WT vs. *wisp* poly(A)-selected RNA from oocytes, WT vs. *wisp* poly(A)-selected RNA from fertilized eggs. Each comparison consisted of three independent RNA extractions and each experiment was done with dye-swap pairs as two technical replicates.

Image processing, data pre-processing and analysis: Microarray images were acquired and analyzed as described (Pleiss et al., 2007). The six different experimental replicates (three independent biological samples with dye-flipped technical replicates of each) comparing the total RNA samples of wild type and *wisp* mutant samples were processed largely according to standard procedures (Smyth and Speed, 2003). For each of the six microarrays, 'within array' normalization was accomplished using the LOESS implementation in the marray package in Bioconductor. No 'between array' processing was required to compare the six microarrays to one another. Processed data were then filtered according to expression level, excluding those features whose A-values were lower than 7.25 or greater than 15, and the remaining data were subsequently analyzed using Significance Analysis of Microarrays (SAM) to identify those genes whose expression was significantly changed in the mutant sample.

Microarrays comparing poly(A)$^+$ RNAs were processed differently. Our initial analyses of these data suggested that there was good correlation between each of the different experimental replicates, but that the dynamic range varied significantly between them (Figure S1). Because each of these samples was subject to poly(A)$^+$ purification, the effectiveness of which cannot be easily assessed, the absolute level of 'enrichment' detected for any given transcript is likely to vary from one microarray to the next. To account for these different dynamic ranges, quantile normalization was used to adjust the data from each of the six experimental replicates (Smyth and Speed, 2003). Briefly, the data from each replicate

experiment were ranked from highest to lowest enrichment. From these lists, an average value was determined for each of the ranked positions. The average values were then re-assigned to the individual transcripts from each experiment according to their ranks (Figure S1). The validity of this approach was empirically confirmed using PCR-based polyA tail assays, as described below and in the Results section. After quantile normalization, we used SAM to identify genes that showed either enrichment or depletion within the poly(A)$^+$ pool of *wisp* RNAs. Lists of enriched or depleted genes were tested by the DAVID Functional Annotation Bioinformatics Microarray Analysis (http://david.abcc.ncifcrf.gov/) to reveal over-represented Gene Ontology (GO) groups of annotated genes (Dennis et al., 2003).

Quantitative PCR and poly(A) tail assay: Total RNA was prepared as described above. Synthesis of cDNA was done using the SuperScript II Reverse Transcriptase kit (Invitrogen) according to the manufacturer's protocol. Quantitative real-time PCR was performed using an ABI Prism 7000 system (Applied Biosystems, Foster City, CA). Each reaction was prepared in a 25 µl mixture containing 5 µl cDNA template, 0.2 µM of each primer and 1X SYBR Green Super Mix (Applied Biosystems).

PCR-based polyA tail (PAT) assay was performed as previously described (Cui et al., 2008). PCR was performed on the PAT cDNAs using a gene-specific primer and the oligo(dT)$_{12}$-anchor to assess the length of the poly(A) tail of a specific mRNA. PCR products from the PAT assay were separated on 8% acrylamide gels.

Cross-linking and RNA immunoprecipitation: Early embryos (0- to 1-hr post deposition) were collected from Oregon-R P2 flies as previously described. These embryos were permeabilized and cross-linked by shaking at room temperature in a 1:3 mixture of 1.8% formaldehyde cross-linking solution [50 mM HEPES (pH 8.0), 100 mM NaCl, 1 mM EDTA, 0.5

Figure 4.S1 False-colored representation of (A) the raw oocyte poly(A)$^+$ data, and (B) the same data after quantile normalization. In each case, the three biological replicates are indicated, along with their dye-flipped technical duplicates (labeled + and -). Our initial analyses of the raw data suggested a strong correlation between the six experiments, but also demonstrated the different range of enrichment values that were detected. In order to account for these between array variations we used a quantile normalization approach.

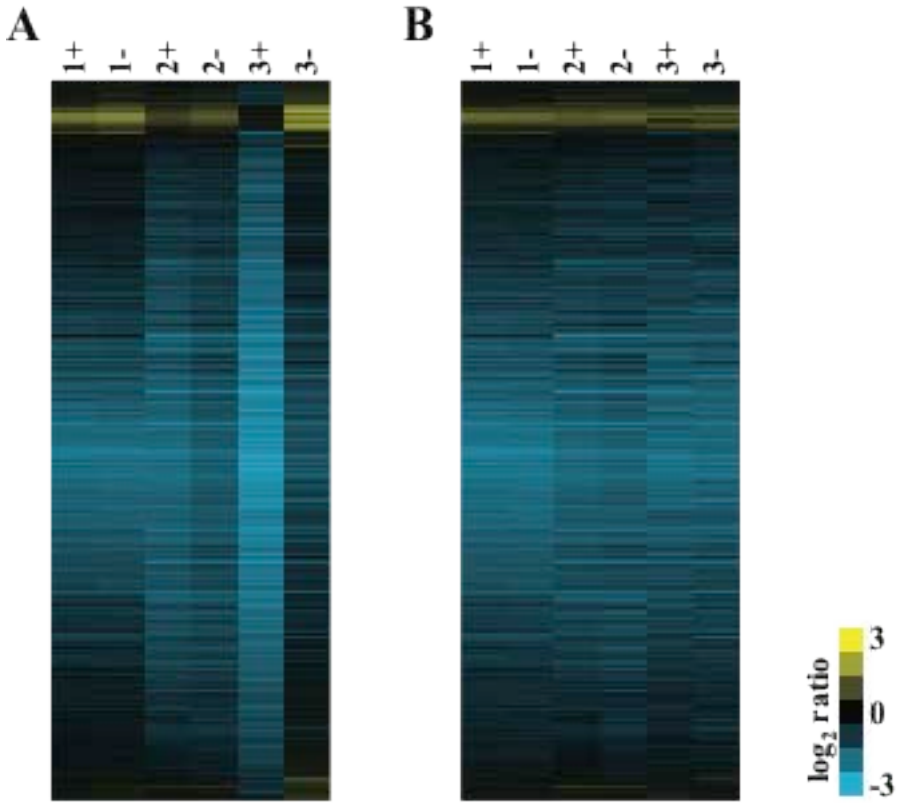
A
1+
1-
2+
2-
3+
3-
B
1+
1-
2+
2-
3+
3-
log2 ratio
3
0
-3

mM EGTA, 1.8% formaldehyde] and heptane. RNA immunoprecipitation was done using the method in (Keene et al., 2006) with modification. Cross-linked embryos were washed in 1 X PBST with 125 mM glycine and homogenized in the homogenization buffer [10 mM HEPES (pH 7.0), 100 mM KCl, 5 mM $MgCl_2$, 0.5% Nonidet P-40 (NP-40, Sigma), 1 mM dithiothreitol (DTT), 100 U/ml RNasin RNase inhibitor (Promega), 2 mM vanadyl ribonucleoside complexes (VRC, Sigma), protease inhibitor cocktail (Roche)] at 4°C. Lysates were filtered using Miracloth (EMD Chemicals, Gibbstown, NJ) and then centrifuged at 1,500 g for 10 minutes at 4°C. Protein concentration of supernatants was adjusted to 2 mg/ml by diluting in the immunoprecipitation buffer as described (Keene et al., 2006).

Protein A Sepharose beads (Sigma) were washed in the immunoprecipitation buffer with gentle shaking and centrifugation for 30 sec at 1,500 g. Egg extracts were pre-cleared with 50 µl of beads for 1 hr at 4°C, centrifuged at 1,500 g for 30 sec. The supernatant containing 5 mg of total proteins was incubated with 10 µg of anti-WISP antibody (Cui et al., 2008) or pre-immune serum (as control) and 50 µl of clean beads at 4°C with gentle rotating for 16 hr. The beads were collected with centrifugation and washed four times with the immunoprecipitation buffer and then four times with the immunoprecipitation buffer supplied with 1 M urea.

Beads were incubated in the elution buffer [100 mM Tris-HCl (pH 8.0), 10 mM EDTA, 1% sodium dodecyl sulfate (SDS), 40 U/ml RNasin RNase inhibitor] for 10 min with vortexing at 37°C and centrifuged at 1,500 g for 30 sec. The supernatants were treated with proteinase K (Roche) for 1 hr at 42°C and incubated for 1 hr at 65°C to reverse the cross-links. RNA was purified using TRIzol as described above.

4.3 Results

The poly(A)$^+$ transcriptome is altered in the absence of WISP function

To determine the global changes in transcript polyadenylation status resulting from loss of WISP function, we used a microarray based approach to compare wild type and *wisp* null mutant samples at two different developmental stages: dissected stage 14 (mature) oocytes or fertilized activated eggs collected at 0- to 1-hr post egg deposition (hereafter referred to as "early embryos"). In an effort to distinguish between a change in the total level of a given transcript versus a change in its polyadenylation state, microarrays were performed that compared between the mutant and wild type flies either the total cellular RNA populations, or only those RNAs containing long poly(A) tails. Although conceptually similar to a previously described approach (Novoa et al., 2010), we undertook a different strategy to isolate these different populations (see Methods and/or SI for complete details). To compare levels of total RNA, independent of poly(A) state, between wild type and *wispy* strains, total cellular RNA was isolated and converted into cDNA using short, random oligonucleotides as primers for reverse transcriptase. Because these random primers initiate cDNA synthesis across the body of the transcript, conversion of RNA into cDNA occurs independent of the poly(A) status of the parent transcript. To address poly(A) state of these transcripts, portions of the same total cellular RNA preps were subjected to poly(A)$^+$ purification using Oligotex mRNA isolation columns. Here we expect mRNAs with long poly(A) tails to bind the column more efficiently than those with short poly(A) tails. Notably, we previously observed that poly(A) tail lengths of WISP targets can become shorter in *wisp* null mutants (Cui et al., 2008). Therefore, we reason that the large difference in poly(A) tail length of a given target transcript between mutant and wild-type samples will result in differences in binding efficiencies between samples, such that the columns

will efficiently recover transcripts with long poly(A) tails in a wild-type sample, but will poorly recover the same targets with shorter tails in the *wisp* null mutant. Multiple biological and technical microarray replicates were performed for each approach, and Significance Analysis of Microarrays (SAM) (Tusher et al., 2001)was used to identify RNAs whose total abundance was different between strains.

Relatively few changes in transcript abundance were detected between the total RNA samples at either developmental point (Fig. 1A, C). In the stage 14 oocytes, only 5 probes, corresponding to 2 genes, were enriched by more than two-fold between mutant and control samples (and none was more than three-fold enriched). By contrast, 560 (9%) probes were downregulated by more than two-fold (including 206 which were more than three-fold) (summarized in Table 1). For the early embryos, the number of misregulated genes was lower still, with only 203 (4%) probes downregulated more than two-fold (only 32 of which were downregulated by more than three-fold) and no probes were significantly upregulated by more than two-fold.

By contrast with our observations of the total RNA levels, the poly(A)$^+$ RNA population from wild type was remarkably different from that of the *wisp* null mutant (Fig.1B, D). In stage 14 oocytes, a total of 5849 probe sets (out of 14886, or 39%) detected on the microarrays were down regulated by at least two-fold, with 3298 of these showing down-regulation of at least three-fold. The 5849 probe sets further collapsed into 2613 unique genes (Table 1). Remarkably, early embryos showed even larger changes with 11567 probe sets (out of 13208, or 88%) detected on the microarrays showing down-regulation of at least two-fold, and 9492 of these showing down-regulation of at least three-fold. The 11567 probe sets represented transcripts from 4171 genes (Table 1).

There was significant overlap between the probes downregulated among total RNA samples and the probes downregulated among poly(A)$^+$ samples. In the oocyte dataset, where 560 probes are downreglated by 2-fold or more, 87% are also decreased in abundance in the poly(A)$^+$ dataset. In the embryo dataset, all 203 probes downregulated amongst total RNA are also downregulated in the poly(A)$^+$ dataset. For these probes, we cannot distinguish between the possibility that their depletion in the poly(A)$^+$ pools is a result of shortened poly(A) length leading to their degradation, versus a simple decrease in their overall abundance. Nevertheless, these results are consistent with our general expectation that difference in total mRNA expression between the mutant and wild type should be similarly reflected in the poly(A)$^+$ samples. By contrast, the remainder of the probes that are downregulated in the poly(A)$^+$ pool did not show a significant difference in total mRNA expression between the wild type and mutant strains, strongly suggesting that their behavior in these poly(A)$^+$ microarrays reflects a shortening of their poly(A) tails.

Among the 4171 putative WISP targets detected in early embryos, 2318 (56%) overlapped with the putative targets detected in stage 14 oocytes. These results are consistent with a model in which these RNAs have shorter poly(A) tails in *wisp* null mutants than controls during oogenesis, and the short poly(A) tails of these mRNAs are sustained in *wisp* mutants until after egg activation in the early embryos. However, we cannot rule out the possibility that they could be regulated by cytoplasmic polyadenylation during both oogenesis and egg activation. Some mRNAs such as the *cyclin B* transcript are known to undergo two rounds of polyadenylation (Benoit et al., 2005; Vardy and Orr-Weaver, 2007b). It is possible that other genes could be regulated in the same way as *cyclin B* mRNA. The remaining 1856 probe sets

Table 4.1 SAM analysis of genes that show ≥2-fold significant change in abundance.

	Higher in WT		Higher in *wisp*$^{-}$		Array Total	
	Probes	**Genes**	**Probes**	**Genes**	**Probes**	**Genes**
Oocyte Total	560	359	5	2	14886	6359
Oocyte polyA	5849	2613	2	2		
Embryo Total	203	133	0	0	13208	5697
Embryo polyA	11567	4171	0	0		

Figure 4.1 Polyadenylated transcriptome is altered in the absence of WISP function. Histograms of global comparisons between wild type and mutant show that for the majority of transcripts analyzed, total RNA abundance is not affected by the absence of WISP in stage 14 oocytes (A) or early embryos (C). However, within polyadenylated RNA populations, many transcripts are present in higher abundances in wild type than in *wisp* mutants in oocytes (B) and early embryos (D), indicating an overall downregulation of polyadenylated RNA in oocytes and embryos of *wisp* mutant mothers.

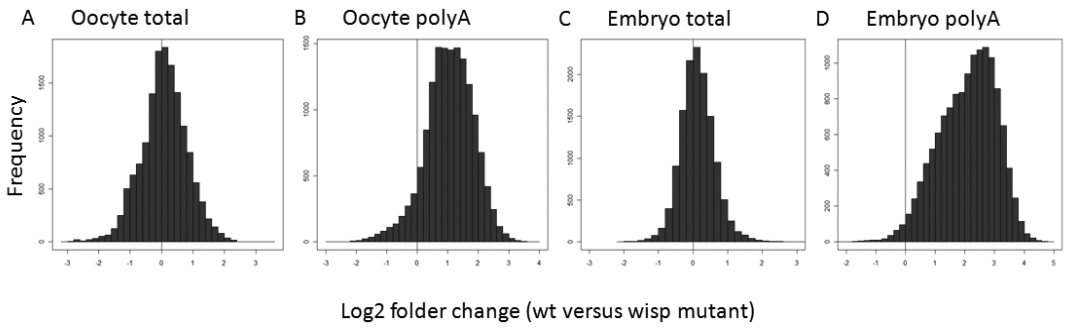
A
Oocyte total
B
Oocyte polyA
C
Embryo total
D
Embryo polyA
Frequency
Log2 folder change (wt versus wisp mutant)

were only detected as WISP regulated targets in early embryos, suggesting that their poly(A) tails undergo WISP-dependent elongation only upon egg activation.

Poly(A) tail length assays confirm the microarray results

Because of the challenges associated with analyzing the poly(A)$^+$ microarray data (see Materials and Methods), we sought to examine directly the poly(A) tail lengths of putative targets from each group using a PCR-based poly(A)-tail (PAT) test (Salles et al., 1994). We chose to test target sets that represented the full range of positive hits predicted by the microarray data, according to rank order of statistical significance as determined with SAM, and use these data to help establish the subset of high-confidence targets of WISP. For stage 14 oocytes, we chose nineteen putative WISP egg maturation targets identified above, ranging in rank from 6 to 4077 (Table 2): *CG4880, CG11971, Klp10A, CG8180, klp67A, CDC6, sced, mei-S332, geminin, AurB, sse, cyclin A, HSF, sce, psq, mr, bifocal, eIF4G, and CG5316*. Two previously known WISP-regulated RNAs, *dmos* and *cyclin B* (Benoit et al., 2008; Cui et al., 2008), appeared on our list (ranks 260 and 1083, respectively) and were included as positive controls. Similarly, in early embryos we chose twenty putative target mRNAs ranking in significance from 19 to 6551 (Table 2): *pimples, punt, spinster, CG8485, costa, Bj1, CG5262, CG2921, CG33298, Pp1a-96A, ubcE2h, tango11, Dsor1, CG8180, grapes, string, CG10209, mei-p26, CG8370, and CG34398*. Two previously known WISP-regulated RNAs, *bicoid* and *Toll* (Benoit et al., 2008; Cui et al., 2008), were also identified on our list (ranks 2293 and 3313, respectively) and included as positive controls. As shown in Figure 2 and Table 2, the poly(A) tail shortening of ~40 to ~120 nts was seen for all positive controls and the vast majority of the test mRNAs in the absence of WISP. Remarkably, the top 16 candidates in oocytes, representing the top ~3000 target transcripts, all showed shortened poly(A) tail length in *wisp* mutants by the PAT assay,

suggesting a high true positive discovery rate for the microarray data. Similarly, 17 of the 20 candidates tested in early embryos confirmed the shortened tail phenotype, demonstrating that upwards of ~6000 transcripts have shortened poly(A) tails in early embryos of the *wisp* null mutant.

Due to the difficulty associated with amplifying the entire length of the poly(A) tail for a given transcript of interest, the PAT assay itself is subject to a high false negative discovery rate. For example, previously uncharacterized alternative 3'UTR isoforms have been discovered in *C. elegans* and likely exist in other model organisms (Jan et al., 2011). Such alternative isoforms could impede PCR amplification of 3'UTR and poly(A) tail regions, causing the transcript-specific primers of the PAT assay to either not bind (shorter isoforms) or to be too far upstream for the allowed extension time (longer isoforms). As such, it remains unclear whether the few candidates that failed to show decreased poly(A)$^+$ tail lengths in the absence of WISP by PAT assay are, in fact, false positive discoveries from the microarray, or whether their true 3'UTRs are simply misannotated in the sequence databases, leading to unclear PAT assay results. In the oocyte set, all 16 of the tested candidates within the top ~3000 most enriched showed clear poly(A) tail shortening in the absence of WISP, after which the success rate dropped off (Table 2). For these data, we thus posit that the limit of the reliable microarray data is reached at or near the 3000 transcript mark. Interestingly, SAM revealed approximately 3000 transcripts that are upregulated by 3-fold or more among control poly(A)$^+$ RNA populations, thus supporting inclusion of data within this limit. By contrast, three of the transcripts from the early embryo set failed to demonstrate poly(A) tail shortening in the absence of WISP by the PAT assay in spite of sometimes strong enrichment on the microarrays. However, there is a strong overall confirmation rate within the early embryo data set through the entire list of ~6000 transcripts.

Table 4.2. PAT assay validation of selected candidate target mRNAs.

Oocyte

Gene name	Transcript ID	Rank	Score(d)	PAT assay
CG4880	CG4880-RA	6	4.76	+
CG11971	CG11971-RA	23	4.15	+
Klp10A	CG1453-RE	38	4.02	+
CG8180	CG8180-RA	39	4.01	+
klp67A	CG10923-RA	40	4.01	+
CDC6	CG5971-RA	83	3.82	+
sced	CG3273-RA	103	3.76	+
mei-S332	CG5303-RA	170	3.59	+
*dmos**	CG8767-RA	260	3.45	+
geminin	CG3183-RA	369	3.31	+
AurB	CG6620-RA	540	3.16	+
sse	CG10583-RA	709	3.05	+
*cyclin B**	CG3510-RA	1083	2.84	+
cyclin A	CG5940-RA	1247	2.77	+
HSF	CG5748-RD	1557	2.66	+
sce	CG5595-RA	1896	2.56	+
psq	CG2368-RI	2968	2.28	-
mr	CG3060-RA	3225	2.21	-
bifocal	CG1822-RB	3899	2.06	+
eIF4G	CG10811-RB	4013	2.03	+
CG5316	CG5316-RB	4077	2.02	-

Embryo

Gene name	Transcript ID	Rank	Score(d)	PAT assay
pimples	CG5052-RA	19	4.18	+
punt	CG7904-RA	197	3.76	+
spinster	CG8428-RB	300	3.67	-
CG8485	CG8485-RD	492	3.55	+
costa	CG1708-RA	600	3.48	-
bj1	CG10480-RA	737	3.43	+
CG5262	CG5262-RA	787	3.40	+
CG2921	CG2921-RA	998	3.33	+
CG33298	CG33298-RB	1087	3.30	-
Pp1alpha-96A	CG6593-RA	1376	3.21	+
ubcE2h	CG2257-RA	1569	3.16	+
tango11	CG30404-RB	1674	3.13	+
Dsor1	CG15793-RA	2146	3.03	+
CG8180	CG8180-RA	2164	3.03	+
*bicoid**	CG1034-RE	2293	3.00	+

grapes	CG17161-RA	2346	2.99	+
string	CG1395-RA	2477	2.96	+
*Toll**	CG5490-RA	3313	2.78	+
CG10209	CG10209-RA	3738	2.69	+
mei-p26	CG12218-RA	5702	2.29	+
CG8370	CG8730-RA	6476	2.13	+
CG34398	CG34398-RC	6551	2.11	-

*previously identified WISP target

+ Shift in electrophoretic mobility due to WISP

- No shift in electrophoretic mobility due to WISP

Figure 4.2. Poly(A) tails are shorter in the absence of WISP function. Poly(A) tail length of mRNAs was assessed in stage 14 oocytes (A) or activated eggs (B) using gene-specific primers in PAT assays, including four ribosomal protein mRNAs and ten mRNAs. Bars indicate the longest products produced by PAT. “Predicted targets” are those predicted from our microarray data. “Known targets” and “non-targets” were identified previously as WISP targets or WISP independent (respectively) by Benoit et al. (2008) and Cui et al. (2008).

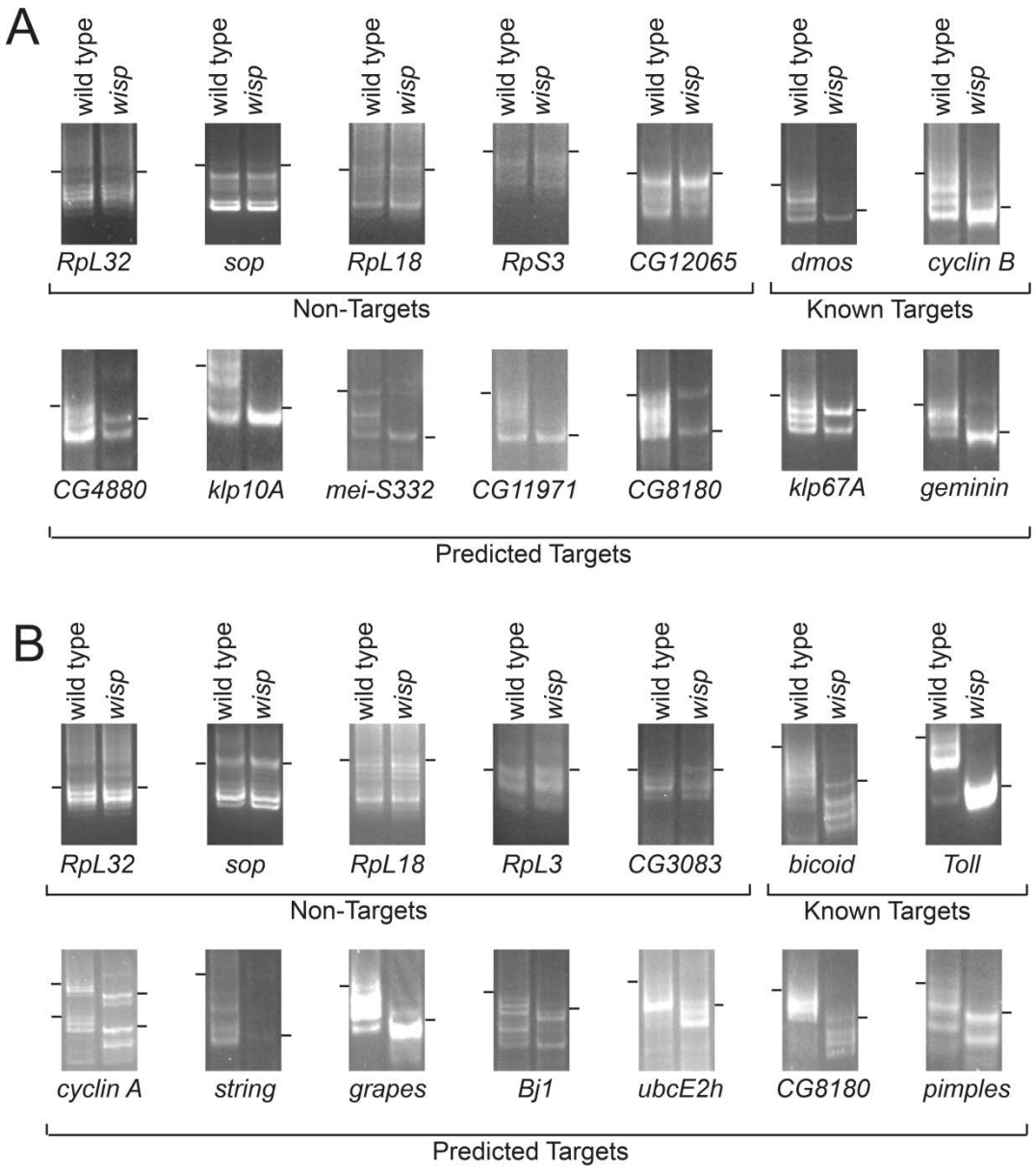
A
wild type
wisp
RpL32
sop
RpL18
RpS3
CG12065
dmos
cyclin B
Non-Targets
Known Targets
CG4880
klp10A
mei-S332
CG11971
CG8180
klp67A
geminin
Predicted Targets
B
wild type
wisp
RpL32
sop
RpL18
RpL3
CG3083
bicoid
Toll
Non-Targets
Known Targets
cyclin A
string
grapes
Bj1
ubcE2h
CG8180
pimples
Predicted Targets

SAM revealed more than 8000 transcripts that are present at levels 3-fold more or higher in the poly(A)$^+$ RNA population of controls compared to that of *wisp* mutants.

We noticed that in *wisp* deficient oocytes all the tested mRNAs retain a short poly(A) tail of ~10 to ~40 nt, depending on the specific mRNA. This observation has been reported previously for *bicoid* mRNA in *wisp* mutants (Cui et al., 2008). The residual tail likely results from the function of the nuclear poly(A) polymerase, encoded by the *hiiragi* gene, which is active in early oogenesis (Benoit et al., 2008).

qPCR also validates the shortened poly(A) tails in *wisp* mutants

To further validate the microarray results, we used real-time quantitative PCR (qPCR) to quantify the RNA levels of selected candidates in both the total RNA and poly(A)$^+$ pools. In stage 14 oocytes, seven mRNAs from the above list were chosen: *CG4880*, *klp10A*, *mei-S232*, *CG11971*, *CG8180*, *klp67A*, and *geminin*. *CG12065* was used as a negative control. Two previously known WISP-dependent RNAs, *dmos* and *cyclin B*, were used as positive controls (Benoit et al., 2008; Cui et al., 2008). We used qPCR to assess the abundance of poly(A) RNA versus total RNA for these mRNAs in wild type and *wisp* oocytes and plotted the ratio of poly(A)$^+$ RNA/total RNA for each transcript. As shown in Figure 3A, all seven putative targets and both positive controls, but not the negative control, showed a decreased ratio of poly(A)$^+$ RNA/total RNA in the *wisp* mutant compared to wild type, suggesting that *wisp* null mutant affected the poly(A) tail length of these mRNAs.

In early embryos, we tested seven candidates from the above list: *cyclin A*, *string*, *grapes*, *Bj1*, *ubcE2h*, *CG8180*, and *pimples*. *CG3083* was used as a negative control. Two previously known WISP-regulated RNAs, *bicoid* and *Toll* were used as positive controls in the experiment. As shown in Figure 3B, all seven putative targets and two positive controls, but not the negative

Figure 4.3. Polyadenylated transcripts are depleted in the absence of WISP. qPCR analysis measures the poly(A)$^+$ RNA abundance, shown as a proportion of the total RNA abundance in stage 14 oocytes (A) or activated eggs (B). Results from wild type oocytes (unfilled bars) and from *wisp* deficient oocytes (filled bars) are shown for two biological replicates and one technical replicate. Error bars indicate standard deviation.

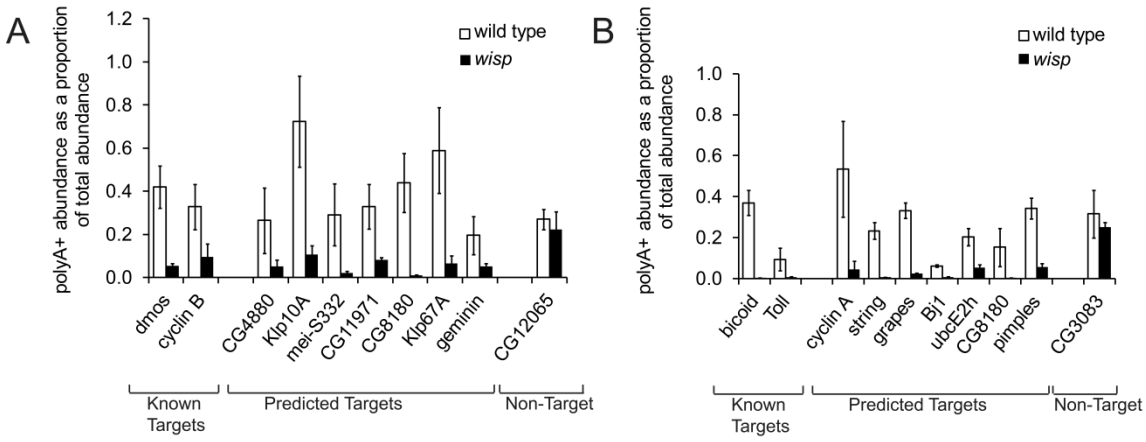
A
polyA+ abundance as a proportion of total abundance
1.2
1.0
0.8
0.6
0.4
0.2
0.0
wild type
wisp
dmos
cyclin B
CG4880
Klp10A
mei-S332
CG11971
CG8180
Klp67A
geminin
CG12065
Known Targets
Predicted Targets
Non-Target
B
polyA+ abundance as a proportion of total abundance
1.0
0.8
0.6
0.4
0.2
0.0
wild type
wisp
bicoid
Toll
cyclin A
string
grapes
Bj1
ubcE2h
CG8180
pimples
CG3083
Known Targets
Predicted Targets
Non-Target

control, showed a decreased ratio of poly(A)$^+$ RNA/total RNA in the *wisp* null mutant compared to wild type, suggesting that *wisp* mutant affected the polyadenylation of these mRNAs.

Functional relevance of genes regulated by WISP in stage 14 oocytes

We performed Gene Ontology (GO) annotation analysis to determine which functional groups of genes are over-represented in putative WISP targets in mature oocytes using DAVID (http://david.abcc.ncifcrf.gov/) (Dennis et al., 2003). Only genes whose poly(A)$^+$ transcript levels were greater by 2-fold or more in controls than in *wisp* mutants were included in this analysis. The total list of probes identified on the array for the mature oocyte poly(A)$^+$ sample was used as the background sample. GO analysis revealed that "cell cycle" related genes made up the top category within Biological Process (*P* value=1.23E-22; Bonferroni-adjusted=2.84E-19) [for a full list of terms see Tables B1 (>2-fold) and B2 (>3-fold)]. These groups include genes that encode cell cycle regulators, such as cyclins (cyclin A, cyclin B, cyclin B3, cyclin D and cyclin E) and checkpoint regulators (wee and polo kinases). The enrichment of cell cycle related genes can be linked to the phenotypes observed in oocytes produced from *wisp* mutant mothers. One such example is *klp3A,* which encodes a kinesin-like protein that is required for pronuclear migration at the end of meiosis (Williams et al., 1997). Previously we observed that the female pronucleus does not migrate in *wisp* mutant (Cui et al., 2008). This phenotype could be due to the lack of translation of *klp3A* mRNA when its poly(A) tail fails to lengthen in the absence of WISP function.

Top categories in Molecular Function are "DNA binding" (*P* value =3.71E-17; Bonferroni-adjusted 3.16E-14) and "zinc ion binding" (*P* value =2.75E-11; Bonferroni-adjusted 2.35E-08) (Table B2). Emerging evidence suggests that zinc is critical for proper development of oocytes. During maturation, mouse oocytes accumulate over twenty billion zinc atoms, which

are exocytosed in up to five rapid release events during egg activation (Kim et al., 2011). Zinc function is critical for progression of oocytes through the meiosis I–meiosis II transition in mouse oocytes (Bernhardt et al., 2011). In Drosophila oocytes, zinc-binding proteins are also enriched and are modulated by phosphorylation or dephosphorylation during egg activation (Krauchunas et al., 2012).

Using the KEGG pathway identifier in GO analysis, we found that members of the ubiquitination machinery were highly enriched among the WISP-regulated RNA groups in oocytes (P = 1.57E-07; Bonferroni-adjusted 1.38E-05) (Table B2). Among these are two E1 ubiquitin-activating enzymes, 14 E2 ubiquitin-conjugating enzymes, and most subunits of the two major multi subunit E3 ubiqitin ligase complexes, Cullin-Rbx and Anaphase-promoting complex (APC/C) (annotations from KEGG PATHWAY Database, http://www.genome.jp/kegg/pathway.html). Regulatory protein degradation plays important roles in oocyte development. In Xenopus oocytes, the E3 ubiquitin ligase APC/C degrades XErp1 protein, one component of the cytostatic factor, and this degradation causes the release of meiotic arrest (Wu and Kornbluth, 2008). The APC/C is also involved in the activation of meiotic progression in Drosophila oocytes. A mutation of the *cortex* gene, which encodes a female meiosis-specific activator of APC/C, results in the accumulation of Cyclin A protein and blocks meiotic progression (Pesin and Orr-Weaver, 2007). Polyadenylation of *cortex* mRNA occurs during oocyte maturation (Pesin and Orr-Weaver, 2007) and this polyadenylation depends on WISP function (Benoit et al., 2008). Our finding suggests that the ubiquitination machinery is probably activated as a consequence of cytoplasmic polyadenylation during late oogenesis, thus allowing cell cycle progression at egg maturation.

WISP-regulated RNAs are also associated with the "progesterone-mediated oocyte maturation" pathway (P = 1.16E-04; Bonferroni-adjusted 1.02E-2) (Table B2), a pathway that has been characterized previously in Xenopus (Belloc et al. 2008). In Xenopus, a signal from progesterone ultimately results in cytoplasmic polyadenylation and subsequent translation of stored mRNAs, which plays a central role in activating oocyte maturation in Xenopus (Belloc et al., 2008). Drosophila oocyte maturation does not involve progesterone, but the goal of oocyte maturation—release from one meiotic arrest point and progression to the next meiotic arrest point—remains conserved. Therefore, it is not surprising that some of the factors in the Xenopus progesterone-mediated oocyte maturation pathway, such as those that regulate cell cycle dynamics, would also be required during Drosophila egg maturation. Like the Xenopus oocyte maturation pathway involving MAPK and MOS, we have found that MAPK activity is high in Drosophila oocytes, and that *mos* mRNA is among WISP targets at egg maturation (Cui et al., 2008), further confirming conservation of key signaling events at egg maturation between Drosophila and Xenopus. In contrast to Xenopus, however, Drosophila MOS is not required for completion of meiosis (Ivanovska et al., 2004).

Genes that were identified as downregulated in the total RNA population (Table 1) are enriched for many of the same functional categories as those in the poly(A)$^+$ population, including cell cycle and chromosome organization categories (Table B3); this is expected, since many transcripts that are downregulated in total RNA are shared in the poly(A)$^+$ group.

Functional relevance of genes regulated by WISP in early embryos

We also searched for enriched functional groups among the genes that are WISP regulated in early embryos after egg activation. Enriched functional categories within Biological Process are indicative of cellular changes that occur during egg activation, including

"reproductive cellular process" (*P* value =4.32E-10; Bonferroni-adjusted 1.36E-06), "protein amino acid phosphorylation" (*P* value =6.36E-07; Bonferroni-adjusted 2.00E-3), and "pattern specification process" (*P* value =7.23E-06; Bonferroni-adjusted 2.25E-2) [for a full list of terms see Tables B4 (>2-fold) and B5 (>3-fold)]. Top-ranking categories in Cellular Compartment suggest that chromosome-related proteins are enriched in WISP targets (*P* value =1.36E-14; Bonferroni-adjusted 8.29E-12), which may reflect release from meiotic arrest and progression to embryonic mitotic cell cycles. Top categories in Molecular Function are "zinc ion binding proteins" (*P* value =7.16E-14; Bonferroni-adjusted 1.02E-10) and "protein kinase activity" (*P* value =2.41E-08; Bonferroni-adjusted 3.43E-05), which likely relate to the signaling events that initiate and coordinate the process of egg activation.

GO analysis identified the functional group "pattern specification process" (Table B5). This group includes components that function in patterning the embryo, such as *bicoid*, *Toll*, *torso*, *caudal*, *gurken*, *hunchback*, *nanos*, *oskar*, *pumilio*, and *trunk*. Posttranscriptional regulation of axis patterning genes in Drosophila embryos has been documented, and some of these genes' transcripts are already known to be regulated at the level of cytoplasmic polyadenylation. For example, translation of *oskar* mRNA in the embryo's posterior is activated by cytoplasmic polyadenylation (Castagnetti and Ephrussi, 2003; Chang et al., 1999). Additionally, the maternally supplied *hunchback* mRNA poly(A) tail elongates to about 70 nucleotides in early embryos; this correlates with the increase of its translation (Wreden et al., 1997). Furthermore, changes in poly(A) tail length of *bicoid* has been described previously (Salles and Strickland, 1999) and attributed to WISP function (Benoit et al., 2008; Cui et al., 2008). Although some of these pattern formation genes are already known to be targets of regulatory polyadenylation, it was not known that others are also regulated in a poly(A)-

dependent manner. Our GO analysis reveals that transcripts of pattern specification genes comprise a major class among the total number of WISP targets at egg activation.

Because some target transcripts identified in early embryos were also identified as WISP targets in mature oocytes, we additionally analyzed the subset of transcripts that are unique to the embryo array and were not identified as targets in the mature oocyte array. GO analysis indicates that transcripts from genes involved in embryogenesis and morphogenesis are enriched within this subset, but not to the level of our significance cut-off.

Functional relevance of RNAs that are not regulated by WISP

We also performed GO analysis on the sets of genes whose transcripts were not affected by WISP in oocytes and early embryos. Genes involved in mitochondrial cellular respiration were highly represented in both oocyte and embryo sets (Table B6). The most highly enriched functional categories within Biological Process include “oxidation reduction” for oocytes (*P* value =2.98E-9; Bonferroni-adjusted 8.51E-6) and “oxidative phosphorylation” for early embryos (*P* value =7.68E-21; Bonferroni-adjusted 7.19E-18) (Table B6). Similarly, enriched functional categories within Cellular Compartment included “mitochondrial respiratory chain” for both oocyte (*P* value =2.16E-5; Bonferroni-adjusted 1.21E-2) and embryo (*P* value =1.62E-17; Bonferroni-adjusted 3.99E-15). Genes within these groups for both data sets include subunits of cytochrome C oxidase (*CoIV, CoVa, CoVb, CoVIb,* and *CoVIIc*) as well as energy metabolism enzymes such as aldehyde dehydrogenase (*Aldh*) and glutamate dehydrogenase (*Gdh*). These results indicate that while WISP regulates many cellular changes during egg maturation and egg activation, genes and transcripts governing basic cellular energy requirements are not affected in a WISP-dependent manner. The mitochondrially-encoded gene *mt:ND2* was also found among

the genes that are not WISP-regulated, indicating that transcripts from the mitochondrial genome likely remain unaffected.

Target RNAs can be co-immunoprecipitated with WISP

With such a large part of the maternal transcriptome showing poly(A) tail shortening in the *wisp* mutant, the question arises whether these transcripts are direct targets of WISP. Although GLD-2-type poly(A) polymerases do not have RNA binding domains (Wang et al., 2002) and they are believed not to bind RNA directly, GLD-2 proteins can be recruited to the target mRNA by forming complexes with certain RNA binding proteins (Barnard et al., 2004; Kim et al., 2009; Wang et al., 2002). It has also been shown that WISP protein and RNA are in the same ribonucleoprotein (RNP) complex in ovarian extracts (Benoit et al., 2008). It is likely that mRNAs directly regulated by WISP will also be found in such WISP-containing RNP complexes.

We used RNA immunoprecipitation (Keene et al., 2006) to determine whether a subset of putative WISP targets were associated with WISP-containing RNPs. Cytoplasmic extracts were made from wild type early embryos, and WISP-containing RNPs were immunoprecipitated from these extracts using an immobilized polyclonal anti-WISP antibody (Cui et al., 2008); pre-immune serum was used in parallel as a negative control. We used real-time quantitative RT-PCR to examine the enrichment of RNA that was immunoprecipitated with WISP. Test mRNAs included seven known targets of WISP (Benoit et al., 2008; Cui et al., 2008) as well as three targets identified in this microarray study and confirmed with PAT assays in Figure 3C. All of the ten test mRNAs were enriched by >2-fold in the WISP IP compared with the mock IP (Fig. 4). Neither of the two negative control mRNAs, *rpA1* and *CG3083*, were significantly enriched

Figure 4.4. WISP forms a complex with candidate target mRNAs. Embryos collected at 0- to 1-hr post deposition from wild type flies were fixed and cross-linked in formaldehyde for RNA immunoprecipitation. Cytoplasmic extracts from these embryos were incubated with an immobilized polyclonal anti-WISP antibody or pre-immune serum (negative control). mRNAs enriched in the IPs were isolated and used to synthesize cDNA. RT-PCR was performed to test enrichment of mRNAs in the WISP IP vs. control IP. All data were normalized to *RpL32*. The average of two biological replicates and one technical replicate are shown. Error bars indicate standard deviation.

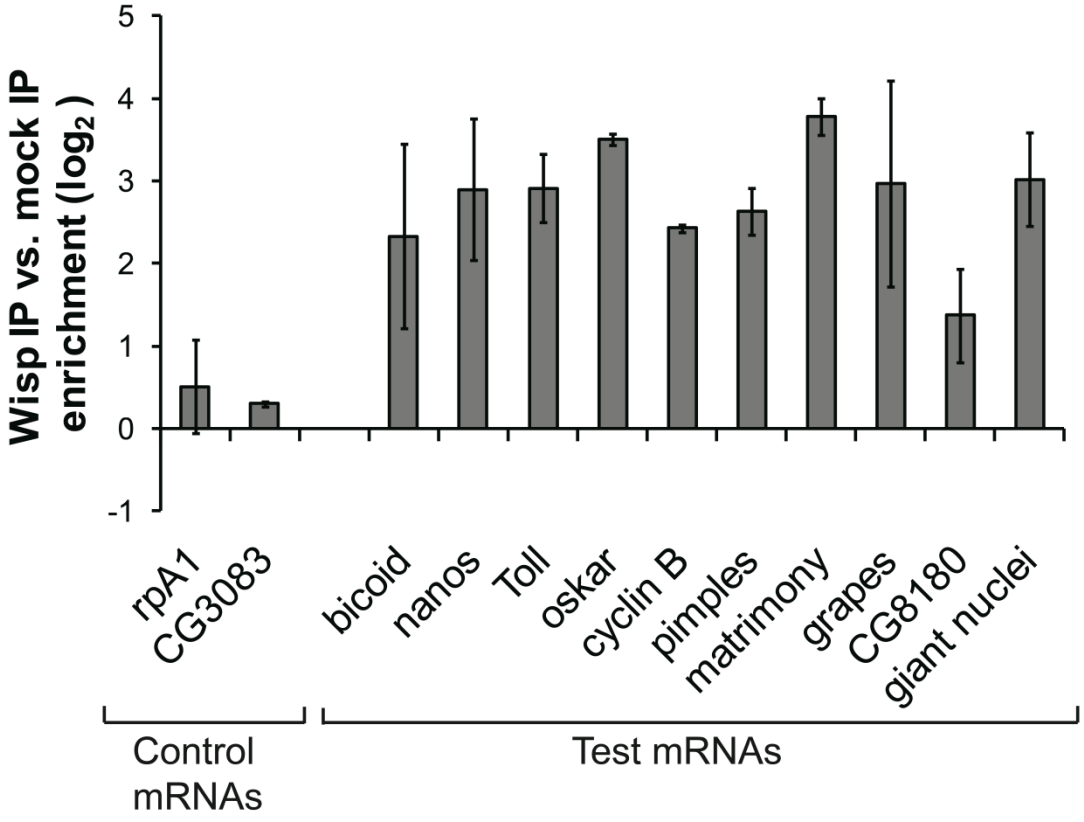
Wisp IP vs. mock IP enrichment (log2)
5
4
3
2
1
0
-1
rpA1
CG3083
bicoid
nanos
Toll
oskar
cyclin B
pimples
matrimony
grapes
CG8180
giant nuclei
Control mRNAs
Test mRNAs

in WISP IP. This suggests that the ten WISP-targeted mRNAs and WISP protein are co-present in the same RNPs and they are likely to be directly regulated by WISP.

4.4 Discussion

Our study demonstrates that cytoplasmic polyadenylation is a powerful mechanism for facilitating cellular change. Post-transcriptional control through poly(A) tail elongation has been observed previously on several maternal mRNAs in the cytoplasm of Drosophila oocytes and early embryos. Importantly, experimental evidence demonstrates that this polyadenylation is necessary for protein production: the test-case mRNAs that fail to get polyadenylated in *wisp* null mutants also fail to get translated in these mutants (Benoit et al., 2008). Previous studies of cytoplasmic polyadenylation in oocytes and embryos had tested a very limited number of candidate genes encoding transcripts that were expected to be WISP-regulated at these stage (e.g. cell cycle and patterning genes). In the study described here, we show that rather than being limited to a small group of specific maternal mRNAs, cytoplasmic polyadenylation is a major regulatory mechanism widely used on many maternal mRNAs at two distinct developmental stages in Drosophila. These mRNAs fail to elongate their poly(A) tails when the GLD-2 class cytoplasmic poly(A) polymerase WISP is not functional, suggesting these maternal mRNAs are putative targets of the cytoplasmic polyadenylation machinery during normal development.

During oogenesis, large amounts of gene products are packed into the developing oocyte, where they must remain quiescent until activation of embryonic development. However, there are changes that occur in the developing oocyte during late oogenesis that may require the activation of some of these gene products for completion of egg development. Prior to oocyte maturation in Drosophila, the oocyte arrests in prophase I of meiosis, and can remain arrested for several days. At maturation during late oogenesis, this arrest is relieved and the oocyte

progresses to metaphase I, where it will arrest once more until the mature oocyte is ovulated. It has been shown that oocyte maturation involves the polyadenylation and translational activation of some transcripts involved in cell cycle control: PAN GU kinase activates both polyadenylation and translation of *cyclin A* mRNA, which promotes cell cycle progression into prometaphase (Vardy et al., 2009). Poly(A) tail elongation of *cyclin B* mRNA also occurs during oocyte maturation. About 100 to 120 adenosine residues are added to its mRNA (Benoit et al., 2005; Vardy and Orr-Weaver, 2007b). This polyadenylation is mediated by the Drosophila homologs of known cytoplasmic polyadenylation machinery including WISP, and is believed to activate the translation of *cyclin B* for the exit from prophase I arrest. In the current study, we show that transcripts from over 2000 genes are likely regulated in a similar manner by WISP during late oogenesis. A substantial subset of these genes is involved in cell cycle control and chromosome organization, consistent with the cellular events that take place during oocyte maturation. Our validation studies confirm that most of the targets identified in our microarray, such as *separase* and *CDC6*, are indeed polyadenylated in a WISP-dependent manner during oogenesis. Interestingly, *heat shock factor* and the translation initiation factor *eIF4G* were also identified and confirmed as targets of WISP-dependent polyadenylation, indicating that activation of the more general regulators of cellular activity may also be critical while major cellular changes like maturation are underway.

After maturation, the Drosophila oocyte remains arrested at metaphase I of meiosis until the egg is ovulated. Ovulation induces a set of events collectively known as egg activation (Heifetz et al., 2001), which includes meiotic resumption, changes in stored proteins' phosphorylation states, and transcript degradation or translation. These events prepare an oocyte to begin embryogenesis. Using a candidate-based approach, previous studies have found that

transcripts of several genes involved in embryonic patterning are regulated by cytoplasmic polyadenylation, including *bicoid, torso, Toll,* and *hunchback* (Salles et al., 1994; Wreden et al., 1997). Our data suggest that over 4000 maternally-supplied transcripts undergo WISP-dependent polyadenylation in the cytoplasm of activating eggs, and translation of these transcripts likely facilitates the varied events of egg activation. In addition to embryonic patterning genes, mRNAs encoding cell cycle components such as *grapes* (Chk1 homolog), *string* (CDC25 homolog) and *Bj1* (Rcc1 homolog) also undergo poly(A) tail extension during this period, and likely participate in meiotic resumption or subsequent embryonic mitoses. A striking finding from our early embryo data is the prevalence of targets involved in signal transduction. In many species, egg activation is triggered by a rise in intracellular calcium, often induced by factors in the fertilizing sperm. This calcium rise sets off a signaling cascade that ultimately results in the events of egg activation. In Drosophila, fertilization is not necessary for egg activation (Doane, 1960; Heifetz et al., 2001), though calcium signaling is still required for most events including meiotic resumption (Horner and Wolfner, 2008a). It is plausible that cell signaling factors are translationally activated by WISP in order to carry out downstream signaling events. Our GO analysis identified enrichment of genes with functions relating to ion binding and phosphorylation, which may indicate changes in enzymatic function leading to signal transduction. In our validation tests, we positively identified the kinases *Dsor1* (MEK) and *Mekk1* as well as the phosphatase *Pp1α-96A* as WISP targets at egg activation. Activation of these classes of proteins could be responsible for signaling events at egg activation, as well as the wide range of changes in proteins' phosphorylation states following egg activation (Krauchunas et al., 2012).

Our microarray study has revealed that cytoplasmic polyadenylation can be a major regulator of cellular change. The regulation of oogenesis and egg activation by a GLD-2-dependent mechanism is not restricted to Drosophila, nor is the phenomenon of cytoplasmic polyadenylation in general unique to the female gametes. However, the number of WISP targets identified in our microarray—well into the thousands at two different developmental periods—is greater than any group of GLD-2 targets identified to date. The cytoplasmic polyadenylation machinery has been well dissected using Xenopus oocytes, where xGLD2 has been studied during oocyte maturation (Barnard et al., 2004). Here, similar to the case in Drosophila, xGLD2 is known to elongate the poly(A) tails of several mRNAs, such as those encoding Cyclin B and Mos, thus activating their translation (Barkoff et al., 2000; Stebbins-Boaz et al., 1996). Studies of the mouse GLD-2 homolog have also been performed. While mouse GLD-2 is present in the female germline during meiosis, knockout of mouse GLD-2 has no effect on egg maturation, suggesting that there may be a functionally redundant protein at play if cytoplasmic polyadenylation is a major regulator at this time (Nakanishi et al., 2006). As in Drosophila, *C. elegans* GLD-2 is involved in meiotic progression and embryogenesis (Kadyk and Kimble, 1998; Wang et al., 2002). Interestingly, *C. elegans* GLD-2 targets a different set of transcripts depending on the RNA-binding protein with which it is partnered (Kim et al., 2009; Kim et al., 2010). RIP-chip studies indicate that the *C. elegans* GLD-2 homolog has approximately 550 targets in whole adults, but the enzyme acts only on 335 of these when bound to the binding partner RNP-8 (Kim et al., 2010). Previous studies have identified the GLD-3 homolog Bic-C as a WISP binding partner in the Drosophila female germline (Benoit et al., 2008; Cui et al., 2008). Given a different binding partner, or in a different tissue, a GLD-2 enzyme may activate distinctive sets of target transcripts beyond those identified by our microarray study.

GLD-2s and other families of cytoplasmic PAPs also act outside of the female germline. The Drosophila genome encodes a second GLD-2 homolog, a paralog of *wispy*, that acts during post-meiotic spermatogenesis (Sartain et al., 2011). The same paralog has a second function in the brain, where it is required for long-term memory storage (Kwak et al., 2008), and there are other examples of vertebrate cytoplasmic PAPs that are required for gene expression at axon synapses (Rouhana et al., 2005). Finally, non-GLD-2 PAPs have also been identified in the mouse male germline (Kashiwabara et al., 2000). These findings indicate that the cytoplasmic polyadenylation system is a widely used mechanism for generating a quick protein production response in cell types that must undergo rapid changes, such as a firing neuron or an activating oocyte. Our findings that WISP regulates thousands of genes in this way demonstrates that the effects of cytoplasmic polyadenylation in a single cell can be very large-scale; thus, control of cytosolic mRNAs through cytoplasmic polyadenylation is a crucial mechanism for allowing coordinated, synchronous cellular change.

CHAPTER 5

THE POLY(A) POLYMERASE GLD2 IS REQUIRED FOR SPERMATOGENESIS IN DROSOPHILA MELANOGASTER[5]

5.1 Introduction

Spermatogenesis is a tightly controlled developmental process that requires stage-specific production of proteins. In animals, spermatogenesis begins when a diploid cell produced from the testis stem cell niche undergoes differentiation and proliferation though mitosis and meiosis to form many haploid spermatocytes. Post-meiotic development, called spermiogenesis, is a series of morphological changes that will determine the final shape and form of the mature sperm; the latter can vary greatly among taxa. One important phenomenon that is seen in spermatogenesis in many species is that transcription is silenced for part of the process: for example, transcription cannot occur after nuclear condensation in mice (Braun, 1998), and there is some evidence for transcriptional silencing during meiosis in *Drosophila* (Vibranovski et al., 2009). In such cases, any proteins that must be translated during the transcriptionally silent period must be synthesized from mRNAs that were transcribed earlier but remain untranslated until the appropriate stage of development. Furthermore, some transcripts needed for late spermiogenesis, such as those for *don juan* (Santel et al., 1997) and Mst87F (Schafer et al., 1990), are synthesized in spermatocytes, though they are not translated until much later.

Spermatogenesis in *Drosophila melanogaster* is well described. Testis gonial cells originating from germline stem cell divisions undergo synchronous mitosis and meiosis with incomplete cytokinesis, resulting in a cyst of 64 round haploid spermatids after the completion of meiosis (Fuller, 1993; Fuller, 1998) (Fig. 1). The spermatids undergo morphological changes

[5] Published and reprinted with permission: CV Sartain, J Cui, RP Meisel, MF Wolfner (2011) *Development* 138, **1619-1629**.

including flagellum extension and nuclear reshaping within the syncytium, until spermatid individualization occurs. The cells exit the testis as mature sperm.

During the final stages of spermatogenesis in *Drosophila*, as in many other invertebrate and vertebrate species, chromatin reorganization events cause the spermatid nuclei to become tightly compacted (Lewis et al., 2003). Histones associated with spermatocyte chromatin are ultimately exchanged for protamines, allowing the nucleus to condense up to 200-fold (Fuller, 1993). Two genes encoding protamines have been identified in *Drosophila* (Raja and Renkawitz-Pohl, 2006). Additionally, the gene tpl^{94D} demonstrates functional homology to mammalian transition proteins, which bind chromatin as an intermediate step between histone-based and protamine-based chromatin organization (Rathke et al., 2007). Therefore, nuclear compaction in *Drosophila* occurs as a two-step process: histones are first displaced by transition proteins, and transition proteins are later exchanged for protamines.

Soon after protamine incorporation, the spermatids in a cyst become separated from one another in a process called individualization. During this process, a cone-like structure composed of cross-linked F-actin assembles around each nucleus in the cyst. The 64 cones in the cyst move as a unit down the length of the sperm tails, simultaneously pushing out excess cytoplasm and wrapping each spermatid in an individual membrane (Fabrizio et al., 1998; Noguchi and Miller, 2003). The separated, mature sperm then roll into coils and exit the testis to be stored in the seminal vesicle (Tokuyasu et al., 1972).

In *Drosophila*, there are many examples of transcripts that are synthesized in spermatocytes, but are not translated until after meiosis, to such an extent that transcriptional activity in the developing *Drosophila* sperm cell was previously thought to be predominantly limited to early spermatocytes and spermatogonia (Barreau et al., 2008; Fuller, 1998; Olivieri

FIG. 5.1. Overview of spermatogenesis in *Drosophila melanogaster*. Asymmetric divisions from germline stem cells (GSC) produce a single primary spermatocyte. Spermatocytes undergo four rounds of mitosis, resulting in a cyst of 16 cells. After a period of growth, each mature primary spermatocyte in a cyst completes meiosis, resulting in a cyst of 64 round spermatids. Spermatids then undergo differentiation events: the centriole becomes the basal body, the axoneme is formed, and the cell undergoes morphological changes. Finally, spermatid nuclei become very compact and needle-shaped, and spermatids separate from one another through individualization.

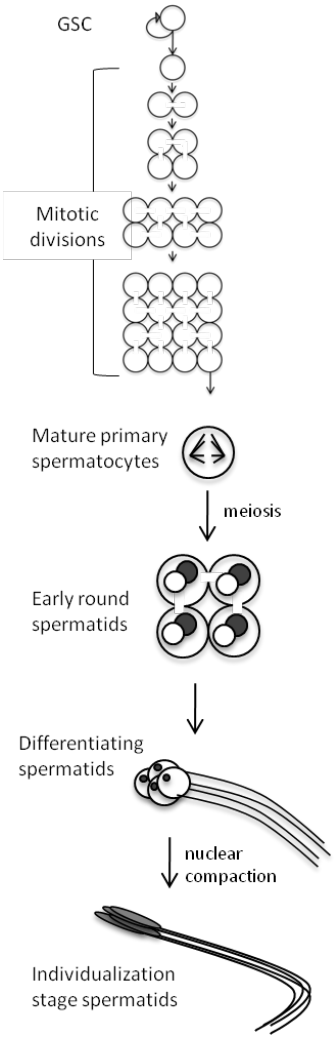
GSC
Mitotic divisions
Mature primary spermatocytes
meiosis
Early round spermatids
Differentiating spermatids
nuclear compaction
Individualization stage spermatids

and Olivieri, 1965; Rathke et al., 2007; Schafer et al., 1990). However, recent evidence demonstrates that transcriptional activity occurs post-meiotically as well (Barreau et al., 2008; Vibranovski et al., 2010). For those transcripts that remain quiescent until post-meiotic stages, a translational control mechanism must be in place.

Many cell types including oocytes and neurons achieve translational regulation through adjusting the length of a transcript's poly(A) tail in the cytoplasm (Benoit et al., 2008; Cui et al., 2008; Galili et al., 1988; Kwak et al., 2008; Preiss et al., 1998). A long poly(A) tail promotes translation of the transcript through recruitment of translation initiation factors, while a transcript with a short poly(A) tail remains untranslated or is degraded. Most mRNAs are extensively polyadenylated in the nucleus; however, for some transcripts that will be held in an untranslated state for a period of time, poly(A) tail modifications occur outside the nucleus (Kim and Richter, 2006). In *Xenopus*, transcripts destined for post-transcriptional poly(A) tail adjustment contain two consensus sequences in their 3'UTR: a cytoplasmic polyadenylation element (CPE) and the hexamer AAUAAA, which will recruit a complex of proteins to alter poly(A) tail length (Mendez and Richter, 2001; Pique et al., 2008). In *Xenopus*, CPE is bound by CPE binding protein (CPEB) (Hake and Richter, 1994; Stebbins-Boaz et al., 1996). The cleavage and polyadenylation specificity factor (CPSF) binds to the hexamer (Dickson et al., 1999; Mendez et al., 2000). CPEB and CPSF recruit a cytoplasmic poly(A) polymerase (PAP) as well as a deadenylase, both of which work on the transcript simultaneously (Kim and Richter, 2007). However, the deadenylase is slightly more efficient than the PAP, so the net effect is a poly(A) tail that remains short. Upon a signal to activate translation, CPEB is phosphorylated, causing the deadenylase to dissociate from the complex; the PAP is then free to elongate the poly(A) tail (Kim and Richter, 2007).

PAPs that act in the cytoplasmic complex differ from nuclear PAPs. One family of cytoplasmic PAPs called Gld-2 (*g*erm*l*ine *d*evelopment 2) has been described in *C. elegans, Xenopus,* and *Drosophila* (Barnard et al., 2004; Benoit et al., 2008; Cui et al., 2008; Wang et al., 2002). While nuclear PAPs contain a catalytic domain and a RNA binding domain, Gld-2 family members have only a catalytic domain (Bard et al., 2000; Martin et al., 2000). For RNA specificity, Gld-2 associates with an RNA-binding protein, typically a Gld-3, to form a heterodimer which acts as a cytoplasmic PAP (Wang et al., 2002).

Gld-2 family members have been shown to play roles in oogenesis in several organisms. In worms, a Gld-2 homolog is involved in the mitosis/meiosis decision to make both male and female germ cells (Kadyk and Kimble, 1998). In *Drosophila*, the X-linked Gld-2 homolog *wispy (wisp)* is necessary for oogenesis and egg activation (Benoit et al., 2008; Cui et al., 2008). WISP is present in ovaries but not in testes, and is necessary for completion of meiosis in oocytes. WISP has been shown to polyadenylate transcripts of *cortex*, which is required for proper meiotic progression (Benoit et al., 2008). WISP also polyadenylates several developmental transcripts whose protein products are needed for early embryogenesis such as *bicoid, Toll*, and *torso* (Benoit et al., 2008; Cui et al., 2008).

The *Drosophila* genome contains an autosomal paralog of *wispy* called *Gld2*. Previous studies of *Gld2* have demonstrated a role in long-term memory and show that GLD2 acts as a poly(A) polymerase in vitro (Kwak et al., 2008). Here, we show that *Gld2* is expressed in the male, but not female, germline. It is required for completion of spermatogenesis, specifically for elongation and individualization stages. In GLD2-knockdown testes, the first disruption observed is post-meiotic, at the onset of spermatocyst elongation. In these testes, the nuclei in developing cysts scatter, and basal bodies are not observed near nuclei. F-actin-containing

individualization complexes do not assemble, and nuclear compaction does not complete. Additionally, protamines are not incorporated, and transcripts for both dynamin and the transition protein are undetectable. Our findings indicate that *Gld2* arose from duplication of the *wispy* locus, and that this derived paralog was likely maintained in the genome due to its necessary role in spermatogenesis.

5.2 Materials and Methods

Evolutionary analysis: Orthologs of *wispy* and *Gld2* within the *Drosophila* genus were identified from sequences obtained from The *Drosophila* 12 Genomes Consortium (Clark et al., 2007). Orthologs in other insect species were identified via best reciprocal BLASTp hits between non-redundant protein databases at the NCBI BLAST server (http://blast.ncbi.nlm.nih.gov/Blast.cgi), using either GLD2 or WISPY protein sequence as the query.

***Drosophila* stocks:** All strains were raised on standard yeast-glucose media at 22°C. OregonR P2 was used as the wild-type stock. The stock *bam*-GAL4-VP16 (Chen and McKearin, 2003), which expresses a GAL4 driver by the *bag-of-marbles* (*bam*) promoter, was kindly provided by C. Baker and M.T. Fuller (Stanford University, Palo Alto, CA). The stock carrying an X-linked transgenic protamine-B-eGFP transgene (Manier et al., 2010) was kindly provided by J. Belote (Syracuse University, Syracuse, NY). Lines carrying UAS-driven snapback RNA against *Gld2* (CG5732) transcripts were obtained from the Vienna *Drosophila* RNAi Center (VDRC ID#52042 and VDRC ID#51605) (Dietzl et al., 2007). Both lines carry the same construct, and prediction programs detect no off-targets. We crossed virgin females from the VDRC line to males carrying *bam*-GAL4-VP16 to achieve knockdown of GLD2 specifically in the gonads of the progeny. To observe protamine B in knockdown and control flies, we crossed protamine-B-

eGFP; P{*tubP-GAL4*}LL7/TM3,*Sb* virgin females to males from the VDRC line using methods described by Avila and Wolfner (2009); the Sb^{+} progeny were the knockdown group, and their *Sb* siblings were the control group. Expression of the protamineB-GFP construct was confirmed by RT-PCR.

Fertility tests: To assess fertility, 3-5 day old GLD2 knockdown males and females created by the cross described above were singly mated to 3-5 day old wild-type males or females. In vials, single pairs were observed until completion of mating, and the male of each couple was then removed. The females from each mating were transferred to new vials for three consecutive 24-hour periods. The number of eggs laid during each period was recorded, and the number of progeny resulting from those eggs was also recorded.

Phase-contrast microscopy: Testes were dissected in cold Ringer's solution (Ashburner, 1989) and squashed in a drop of solution on a slide under the weight of a cover slip. Squashes were examined under phase-contrast using a Zeiss Axioskop compound microscope. Images were captured using Hamamatsu ORCA-ER camera equipment and software.

Fluorescence microscopy: To detect actin individualization cones and nuclei, testes of 3-5 day old males were prepared for phalloidin staining as described by Fabrizio et al. (1998). For immunostaining of GLD2, an affinity-purified polyclonal antibody was generated against GLD2 by using a 329 amino acid region (residues 480-808) of the protein as antigen, using methods previously described (Cui et al., 2008). Testes were dissected in cold PBS (10 mM Na phosphate buffer pH 7.4, 150 mM NaCl). Dissected testes were then squashed and fixed in 4% paraformaldehyde in PBS as described by Fabrizio et al. (1998). Squash preparations were then washed with PBS, blocked, and stained as described by Hurst et al. (2003). A 1:1000 dilution of primary GLD2 antibody or a 1:500 dilution of primary γ-tubulin (#GTU88, Sigma, St. Louis,

MO, USA) was used, and a 1:1000 dilution of AlexaFluor® 488 anti-rabbit or anti-mouse secondary antibody (Invitrogen, Carlsbad, CA, USA) was used. Squashes were incubated with propidium iodide for 30 minutes or DAPI for 5 minutes at room temperature following secondary antibody incubation.

To detect monomeric G-actin, squashes were fixed and washed as described above. Squashes were incubated with Alexa-488 conjugated DNase I (Invitrogen) for 1 hour at room temperature and then washed with PBS.

Coverslips with a drop of anti-fade mounting solution (10 mM N-propyl gallate in 75% glycerol) were placed on stained squash preparations. Preparations were examined using a Leica TCS SP2 confocal microscope or Zeiss Axioscop compound microscope.

RNA extraction and RT-PCR: Total RNA was extracted from hand-dissected testes of 3-5 day old males using TRIzol (Invitrogen) and reverse transcribed using SuperScript II reverse transcriptase (Invitrogen) according to the manufacturer's instructions. The GoTaq PCR system (Promega, Madison, WI, USA) was used for PCR analysis of cDNA.

Western blot: For each sample prepared for Western blot analysis, testes from five 3-day-old males or ovaries from two 3-day-old females were dissected in cold PBS and homogenized by rapid pipetting in sample buffer. Samples were boiled for 5 minutes and run on a 7.5% SDS polyacrylamide gel, and proteins were transferred to a Millipore Immobilon membrane. The membrane was then blocked with 5% milk in TBST for 1 hour before adding primary GLD2 antibody (1:1000) overnight at 4°C. The membrane was then washed 4 times in TBST and incubated with secondary HRP antibody (Jackson Laboratories, Bar Harbor, ME, USA) for 1 hour at room temperature. ECL-Plus (Amersham) was added to the membrane per the manufacturer's instructions to expose the film.

Poly(A) Tail assay: Poly(A) tail (PAT) assays were performed as described by Salles and Strickland (1999). For PAT assay of low-abundance transcripts, nested PAT PCR experiments were performed. Here, the first PCR was run using a gene-specific primer 500-600 base pairs upstream of the 3' end of the transcript of interest, plus the anchor primer. Product from this reaction was used as template in a second PAT PCR using a primer 200-400 base pairs upstream of the 3' end of the transcript of interest, plus the anchor primer. Products were resolved on a 2% agarose gel or 8% polyacrylamide gel. Primer sequences are available upon request.

Yeast two-hybrid analysis: Yeast two-hybrid analysis was performed as described by Cui et al. (2008). Briefly, we cloned full length coding sequences from *Gld2* and *Bic-C* into vectors of the Matchmaker yeast two-hybrid system (Clontech, Mountain View, CA, USA). In-frame fusions of each coding region were generated in both the DNA-binding domain vector pGBKT7 and the activation domain vector pGADT7. Yeast cells co-transformed with pGBKT7 and pGADT7 derivatives were grown on -Trp -Leu synthetic medium and tested for growth on -Trp -Leu -His and -Trp -Leu -His -Ade synthetic media.

5.3 Results and Discussion

Evolutionary history of *Gld2* and *wispy*: The *Drosophila* genus can be divided into subgenera, and genome sequences are available from two subgenera: *Sophophora* (containing *D. melanogaster*) and *Drosophila* (containing species that diverged from *D. melanogaster* ~63 million years ago (Tamura et al., 2004)). We identified *wispy* and *Gld2* orthologs in species from both subgenera. The *wispy* orthologs in *D. melanogaster*, *D. mojavensis* and *D. virilis* have female-biased expression, while the *Gld2* orthologs from *D. melanogaster*, *D. simulans*, *D. secchelia*, *D. yakuba*, *D. pseudoobscura*, and *D. mojavensis* are male-biased (Zhang et al., 2007). This is consistent with the conservation of the oogenesis and spermatogenesis functions of WISP

and GLD2, respectively, across the entire genus. All other insect species with sequenced genomes (including *Anopheles gambiae* and *Aedes aegypti*, the closest relatives to *Drosophila* with completely sequenced genomes) possess only a single ortholog of *wispy*/*Gld2*, based on best reciprocal BLAST searches. Therefore, a duplication event occurred after the most recent common ancestor (MRCA) of *Drosophila* and mosquitoes—but prior to the MRCA of the genus *Drosophila*—to give rise to either *wispy* or *Gld2* (depending on which locus is ancestral and which is derived). A phylogenetic reconstruction of the evolutionary relationships of the insect protein coding sequences supports this hypothesis (Fig. 5.S1). Furthermore, the *wispy*/*Gld2* ortholog in *A. gambiae* has female-biased expression, based on microarray data from whole males and females (Marinotti et al., 2005). We hypothesize that the ancestral germline function of this gene family is in ovaries, and the testis-specific function of GLD2 (see below) is derived.

We examined the conservation of flanking genes on both local and global scales to determine whether *wispy* or *Gld2* is the ancestral locus. On the local scale, *wispy* is in close proximity to *Upf1*, and the *A. gambiae* ortholog is in close proximity to the ortholog of *Upf1*. Assuming conserved synteny, this suggests that *wispy* is the ancestral copy. On a more global scale, the *A. gambiae* ortholog is located on chromosome 2R. This arm has homology to both the X chromosome and 3R of *D. melanogaster* (Fig. 5.S2A). *wispy* is X-linked and *Gld2* is found on 3R. However, the local region of *A. gambiae* 2R that contains the *wispy*/*Gld2* ortholog is enriched for genes that are X-linked in *D. melanogaster* (Fig. 5.S2B). This provides further evidence that *wispy* is the ancestral copy. Additionally, *Gld2* is missing introns found in both *wispy* and the other insect orthologs (Fig. 5.S3), suggesting that *Gld2* may have arisen via the retrotransposition of *wispy* from the X to the autosome.

FIG. 5.S1. The duplication giving rise to *wispy*/*Gld2* occurred after the divergence of the *Drosophila* and mosquito lineages. Phylogenetic trees show the relationship between the *D. melanogaster* WISP and GLD2 protein sequences and orthologous genes from other insects. We constructed phylogenies using the neighbor joining algorithm (Saitou and Nei, 1987) implemented in MEGA 4.0 (Tamura et al., 2007). Divergence was estimated using Poisson corrected amino acid differences and alignment gaps were excluded from all comparisons. Bootstrap percentages (estimated with 1000 replicates) are given at the nodes. Scale bars indicate the number of substitutions per site along the branches. The *A. gambiae* gene is incompletely annotated, and phylogenies were constructed both with (A) and without (B) this sequence; the same evolutionary relationships are recovered regardless of whether the *A. gambiae* gene is included.

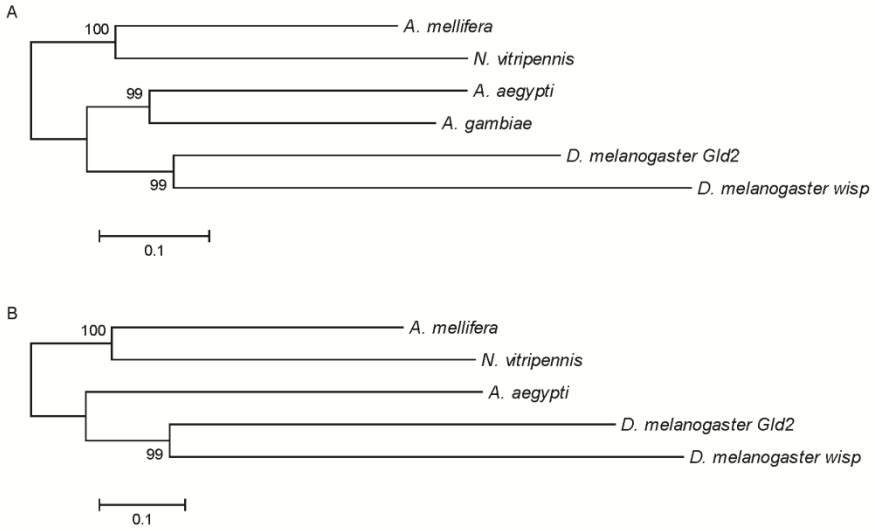
A
100
A. mellifera
N. vitripennis
99
A. aegypti
A. gambiae
D. melanogaster Gld2
99
D. melanogaster wisp
0.1
B
100
A. mellifera
N. vitripennis
A. aegypti
D. melanogaster Gld2
99
D. melanogaster wisp
0.1

FIG. 5.S2. The *A. gambiae* ortholog of *wispy*/*Gld2* is in a region of the genome most resembling the *D. melanogaster* X chromosome. We used reciprocal best protein blast hits to identify one-to-one orthologs between *D. melanogaster* and *A. gambiae*. The x-axis represents chromosome 2R in *A. gambiae*, and the red lines indicate the position of the *A. gambiae* ortholog of *wispy*/*Gld2*. Histograms show the number of genes mapping to each of the five major chromosome arms in *D. melanogaster* for windows along *A. gambiae* chromosome 2R (A). Looking closely at the proximal region of *A. gambiae* chromosome 2R (B), each circle represents a gene, with the y-axis indicating the chromosome arm in which the gene is located in *D. melanogaster*.

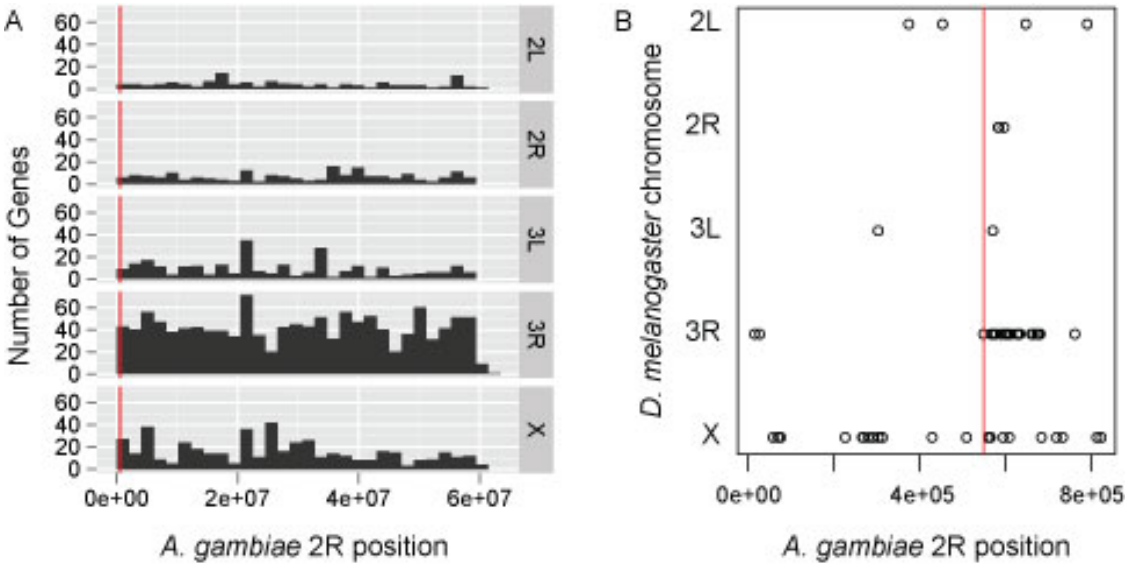
A
Number of Genes
60
40
20
0
2L
2R
3L
3R
X
0e+00
2e+07
4e+07
6e+07
A. gambiae 2R position
B
D. melanogaster chromosome
2L
2R
3L
3R
X
0e+00
4e+05
8e+05
A. gambiae 2R position

FIG. 5.S3. *D. melanogaster Gld2* is missing introns that are conserved between *wispy* and the mosquito Gld-2 ortholog. Rectangles represent protein-coding exons and lines represent introns in the annotated *Gld2*, *wispy*, *A. aegypti*, and *A. gambiae* genes (non-coding exons have been omitted). Diagonal lines between genes connect the end-points of homologous exonic sequences. The truncated *A. gambiae* gene is most likely an annotation error. Note that introns 5 and 6 of *wispy* are conserved in both mosquito genes but missing in *Gld2*. Introns 1 and 2 of *wispy* are near introns found in at least one mosquito gene. The gene structures of *wispy* and *Gld2* are largely conserved within the *Drosophila* genus.

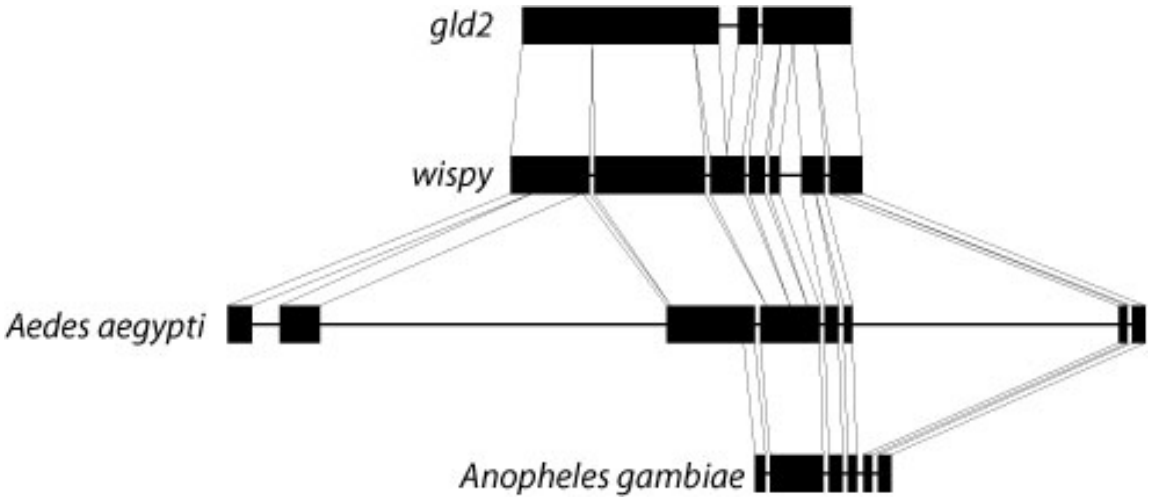
gld2
wispy
Aedes aegypti
Anopheles gambiae

The phenomenon of meiotic sex chromosome inactivation (MSCI) may have contributed to duplication of the *wispy* gene and subsequent retention of *Gld2*. During spermatogenesis in *Drosophila* and other animals, the X chromosome is transcriptionally silenced prior to autosomal silencing (Hense et al., 2007; Turner, 2007; Vibranovski et al., 2009). Therefore, genes located on the X chromosome have a limited capacity to encode proteins involved in spermatogenesis. Interestingly, an excess of genes has been retrotransposed from the X to the autosomes, and the autosomal derived copies are hypothesized to allow for the "escape" from X-inactivation (Betran et al., 2002; Meisel et al., 2009). The testis biased expression (Chintapalli et al., 2007) and spermatogenic functions (see below) of *Gld2* suggest that it was selectively retained because it performs a function unavailable to *wispy* because of MSCI.

***D. melanogaster Gld2* is expressed in the testis and localizes to elongating spermatogenic cysts:** To determine the normal expression pattern of *Gld2*, we performed RT-PCR and immunoblots of RNA and protein from dissected tissues as well as from whole wild-type flies. *Gld2* transcripts were detected in larvae, pupae, and adults. The signal was quite robust in males, whereas expression was barely detectable in whole females (Fig. 5.2A). Western blotting with affinity-purified GLD2 antibody revealed GLD2 presence in the testes of the adult, and did not detect GLD2 in the remainder of the male or the female body (Fig. 2B). *Gld2* has previously been reported to be expressed and function in the *Drosophila* nervous system (Kwak et al., 2008); apparently this expression was below the detection limits of our western blots. We believe it is the source of the low levels of expression we see in RT-PCR of whole females. We did not detect GLD2 in the ovaries of wild-type females (Fig. 5.2C).

FIG. 5.2. GLD2 is expressed in the testes, and is not detectable in the female. RT-PCR for GLD2 shows expression in male larvae, pupae, and adult stages, while expression is not detected in the female (A). RPL32 is used as a positive control. Western blot with anti-GLD2 shows expression is robust in the testes, but is not detected in the remainder of the male (carcass) or in whole females (B). Western blot with anti-GLD2 and anti-WISPY show that GLD2 is expressed in testis but not ovary, and WISPY is expressed in ovary but not testis (C). Membranes were probed with anti-a-tubulin as a loading control. Immunostaining of whole testis squashes using anti-GLD2 shows the breadth of GLD2 expression (D). GLD2 first appears in primary spermatocytes (E) at the distal tip of the testis, and persists at the distal ends of spermatogenic cysts in late stages of spermiogenesis (F). Arrowheads in E indicate the start of the region of the testis containing weakly labeled primary spermatocytes. Arrows in F indicate the distal ends of elongated spermatogenic cysts. Scale bars, 40mm.

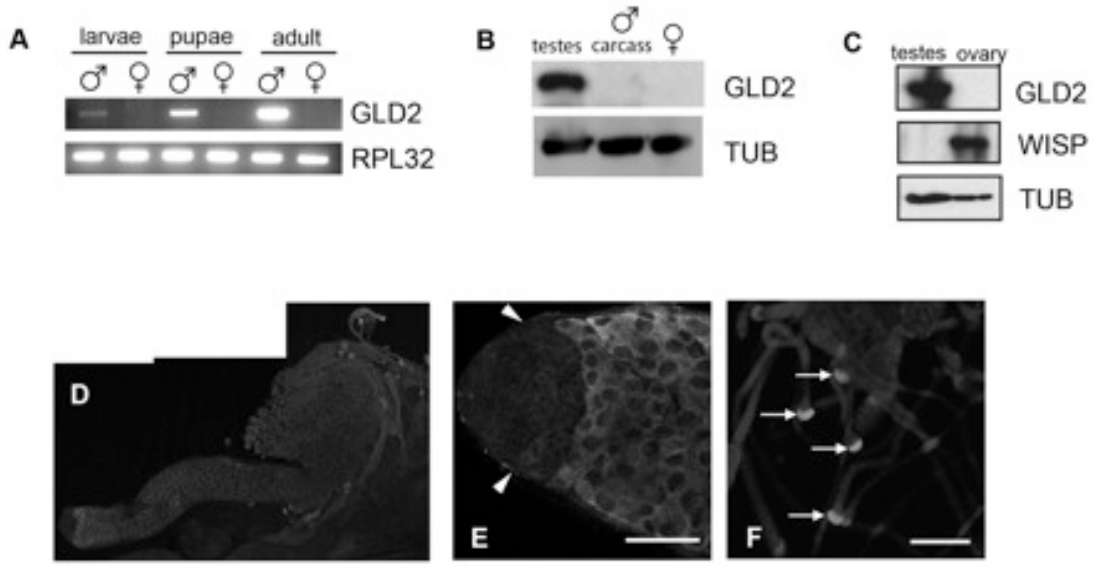
A
larvae
pupae
adult
♂ ♀ ♂ ♀ ♂ ♀
GLD2
RPL32
B
testes carcass
♂ ♀
GLD2
TUB
C
testes ovary
GLD2
WISP
TUB
D
E
F

Immunostaining of adult testis shows that GLD2 localizes to the cytoplasm in primary spermatocytes, throughout meiosis, and in early round spermatids, consistent with its proposed action as a cytoplasmic PAP in the male germline (Fig. 5.2D). GLD2 first appears in early spermatocytes, with robust expression in mid-primary spermatocytes (Fig. 5.2E). In later stages of spermatogenesis, GLD2 is detectable in elongated spermatogenic cysts and is specifically localized to the distal end of the cysts (Fig. 5.2F). This region of the cyst is where polarized growth of the cyst occurs in accordance with axoneme extension (Fuller, 1993; Tates, 1971); additionally, a group of mRNAs that are transcribed post-meiotically have been shown to localize to the distal end of the spermatogenic cyst (Barreau et al., 2008). Interestingly, one of these late-transcribed genes is *orb*, which encodes the *Drosophila* ortholog of CPEB, the protein necessary for cytoplasmic polyadenylation in *Xenopus* (Barnard et al., 2004; Richter, 2007). The presence of both the CPEB homolog ORB and the cytoplasmic poly(A) polymerase GLD2 at the end of the cyst where growth is occurring may indicate GLD2's involvement in late spermatocyst growth. Taken together, these data suggest that the distal end of the cyst may be a major production center for cyst growth, with necessary mRNAs regulated post-transcriptionally through cytoplasmic polyadenylation.

GLD2 has the ability to bind the *Drosophila* Gld-3 homolog Bic-C: GLD2, like its *Drosophila* homolog WISP and other Gld-2 family members (Kwak et al., 2004; Kwak and Wickens, 2007), does not contain any predicted RNA recognition motifs. In *C. elegans*, binding of GLD-2 to mRNA is mediated by an RNA binding protein GLD-3 through formation of a heterodimer (Wang et al., 2002). In *Drosophila*, the Gld-3 homolog is encoded by *bicaudal-C (BicC)*. Previous studies have shown that the *Drosophila* Gld-2 homolog WISP, a known

cytoplasmic poly(A) polymerase, can interact with Bic-C in yeast two-hybrid assays (Cui et al., 2008), though co-immunoprecipitation experiments suggest that this interaction is RNA-dependent (Benoit et al., 2008; Cui et al., 2008).

Using a yeast two-hybrid assay, we found that GLD2 can interact with Bic-C. GLD2 in an activation domain (AD) fusion can interact with Bic-C in a binding domain (BD) fusion but not with the BD alone. We only observed interaction between GLD2 and Bic-C in this orientation. The two-hybrid interaction we observed between GLD2 and Bic-C suggests that GLD2 might function, analogous to WISP and other Gld-2 family members, by forming a protein complex with an RNA binding subunit. Bic-C is expressed in the testis as well as in the ovary (Chintapalli et al., 2007), so GLD2 has the opportunity to associate with Bic-C, thus supporting the case for the role of GLD2 as a PAP during spermatogenesis.

GLD2 is necessary for late spermatogenesis: To assess the function of GLD2 in the testes, we examined flies expressing dsRNA against GLD2 transcripts specifically in the germline. Efficiency of GLD2 knockdown was confirmed by RT-PCR (not shown) and Western blot (Fig. 5.3A); we did not detect GLD2 in these animals. We analyzed the GLD2-knockdown phenotype using two different RNAi lines (see Methods) as well as two different drivers, *bam*-VP16-GAL4 and *tubulin*-VP16-GAL4. All four RNAi-driver line combinations gave the same phenotype in our experiments (data not shown). The results reported here are from RNAi progeny resulting from a cross between VDRC line #52042 and *bam*-GAL4-VP16, unless otherwise stated.

The most striking effect of GLD2-knockdown in the germline is that knockdown males are completely sterile, whereas knockdown females display normal fertility in our fertility tests, even though the same RNAi is produced in their germlines (data not shown). Wild-type females mated to GLD2-knockdown males produced a normal number of eggs, but no eggs from these

matings hatched. The reciprocal cross, in which GLD2-knockdown females were mated to wild-type males, produced normal numbers of eggs and progeny, indicating that females do not require GLD2 for fertility. The same fertility effect is observed when GLD2 RNAi is driven globally using a *tubulin*-GAL4 driver as when GLD2 RNAi is driven exclusively in the male and female reproductive tracts using a *bam*-GAL4 driver.

Because the fertility phenotype of GLD2-knockdown is male specific, we checked knockdown testes for proper sperm development. Phase-contrast images of GLD2-knockdown testis squashes show that in spermatozoa and spermatocytes, mitosis and meiosis proceed normally, producing spermatogenic cysts containing 64 spermatids after completion of meiosis II (Fig. 5.3B,C). Each early spermatid contains one nucleus and one associated mitochondrial derivative, indicating no obvious morphological defects during meiosis and mitochondrial development. However, spermatids within elongated cysts show several abnormalities. Testes and seminal vesicles from GLD2 knockdown males are devoid of mature or motile sperm, thus resulting in male sterility. Instead, fully elongated cysts in GLD2-knockdown males still contain syncytial spermatids, indicating that spermatogenic individualization did occur (Fig. 5.3D,E). Bulges of material that accumulate along the tails of the elongated spermatids can be seen in squash preparations of GLD2-knockdown testis to a considerably higher degree than is seen in control squashes prepared in the same way (panels 3D and 3E are typical of what we see in control and knockdown, respectively); bulges of similar appearance have been observed in testis squash preparations of mutants that fail to complete spermatogenic individualization (Fabrizio et al., 1998). We speculate that these bulges are cytoplasmic aggregates freed from the cyst during the squash preparation, and because the GLD2-knockdown sperm tail is not contained within a membrane the droplet of cytoplasm can adhere to it.

We stained testis squash preparations from knockdown and wild-type males with DAPI and rhodamine-conjugated phalloidin, in order to detect nuclear bundles and actin individualization complexes, respectively. Individualization complexes appear as groups of cone-like structures composed of F-actin that assemble around bundled nuclei; each nucleus is associated with one actin cone. During the individualization process, these actin cones move as a complex down the length of the cyst, wrapping each spermatid in an individual membrane (Noguchi and Miller, 2003; Tokuyasu et al., 1972). In wild type, cysts isolated from ruptured testis tissue contain all 64 spermatid nuclei at their apical ends, and many of these nuclear bundles are closely associated with assembled individualization complexes (Fig. 5.4A). Testes of GLD2-knockdown males show dramatic differences from the wild-type. Their spermatogenic cysts never contain bundled nuclei or assembled F-actin-containing individualization complexes. Instead, nuclei of spermatogenic cysts from RNAi-treated flies are evenly scattered throughout the cyst, without a tendency for greater nuclear density at the apical end of any cyst (Fig. 5.4B). A scattered nuclear phenotype is common in many individualization mutants (Fabrizio et al., 1998). Such scattering has usually been attributed to malformation of the actin individualization complexes. It has been proposed that in those mutants, a malformed individualization complex will drag nuclei along as the complex moves down the length of the cyst (Fabrizio et al., 1998). However, in such mutants, even in cysts containing scattered nuclei there is a higher density of nuclei at the apical end. This pattern suggests that nuclear bundles may have been formed initially, but later became scattered by malformed individualization complexes. The phenotype of GLD2 knockdown cysts differs from this: since individualization complexes are apparently unassembled, nuclear scattering cannot be due to the previously-described dragging effect. Instead, because nuclei are scattered uniformly across the length of the spermatogenic cyst,

FIG. 5.3. RNAi knockdown of GLD2 results in defective late spermatogenesis. GLD2 knockdown was achieved by driving UAS-snapback RNA against GLD2 transcripts specifically in the testes using a *bam*-GAL4 driver. Reproductive tracts of GLD2-knockdown (KD) and control males were assayed for GLD2 expression using western blot (A). Testis squashes under phase-contrast microscopy show that meiosis completes normally in spermatogenic cysts of knockdown (C) testes compared to those of wild-type controls (B), so that each cyst contains 64 nuclei (light phase), and each nucleus is associated with one mitochondrial derivative (dark phase). Late spermatogenesis becomes disrupted, resulting in lack of individualized spermatids in knockdown testes (E) compared to wild-type testes (D). Arrowheads in E indicate cytoplasmic bulges. Scale bars, 40mm.

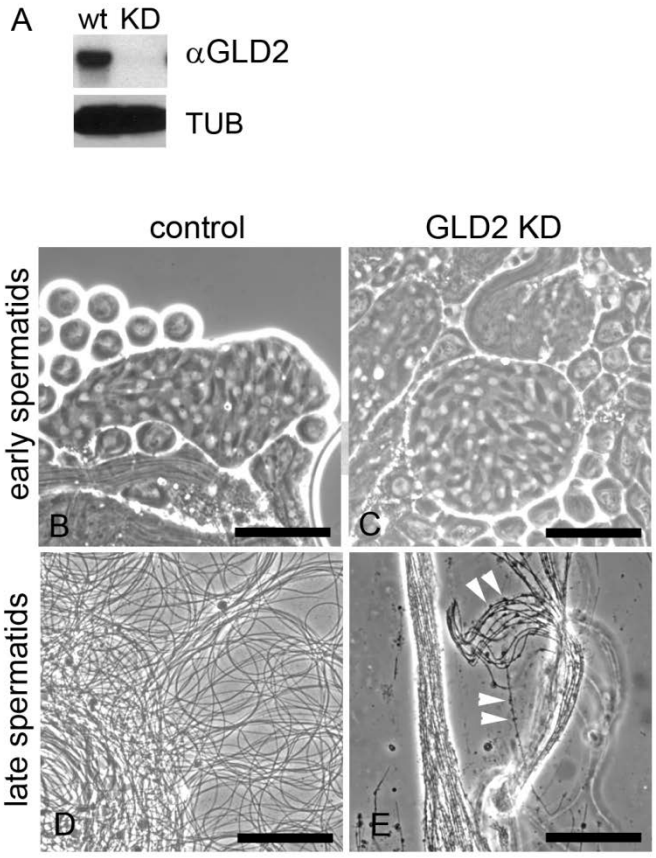
A
wt KD
αGLD2
TUB
control
GLD2 KD
early spermatids
late spermatids
B
C
D
E

FIG. 5.4. Nuclei are scattered throughout spermatogenic cysts and individualization cones do not form in GLD2 knockdown testes. Testes squashes were fixed and stained with DAPI and rhodamine-conjugated phalloidin to detect nuclei (blue) and F-actin individualization cones (red), respectively. In wild-type controls (A), individualization cones assemble around bundled nuclei in late spermatogenic cysts. In GLD2-knockdown testes, nuclei of late spermatogenic cysts are scattered uniformly throughout the cyst (its extent is visible with the phase-contrast overlay), and individualization cones are absent (B). Furthermore, higher magnification of nuclei shows that nuclei in late spermatogenic cysts of the knockdown (D) are noticeably less condensed than those of wild-type (C). Nuclei shown in (D) are representative of the most highly condensed nuclei that we see in knockdown testes. Examination of pupal testes with propidium iodide staining shows that nuclei (red) begin to bundle at the onset of cyst elongation in wild-type (E); at early elongation stages in GLD2-knockdown, nuclei are already scattered (F). Outlines denote early elongation cyst. Scale bars, 10mm.

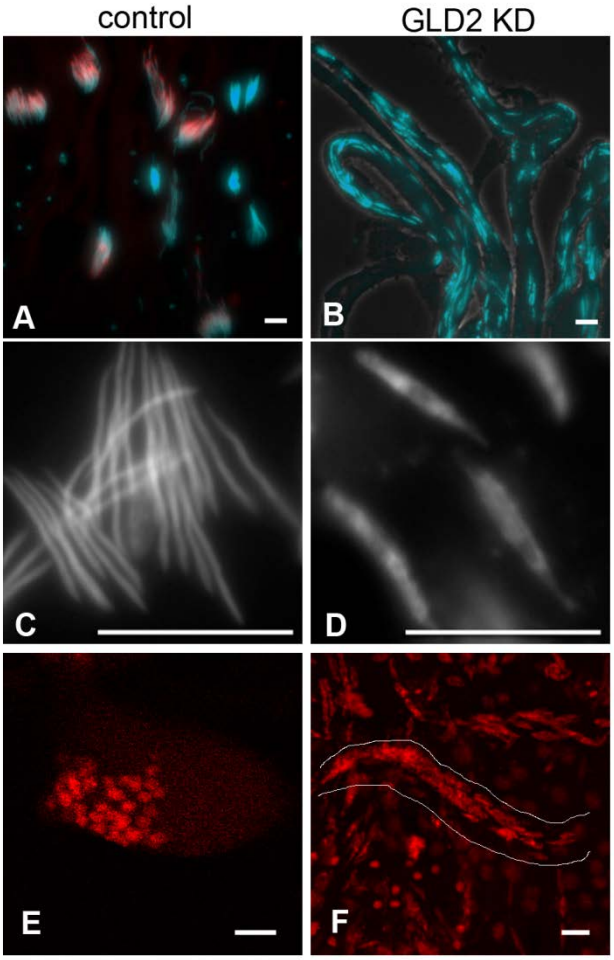
control
GLD2 KD
A
B
C
D
E
F

nuclei were likely not bundled in initial stages of spermiogenesis, and defects may be apparent even before onset of individualization complex assembly. Therefore, we looked in preceding spermatogenic stages to search for earlier visible defects in the absence of GLD2.

Many post-meiotic spermatogenic cysts within adult *Drosophila* testis have already undergone substantial flagellar extension and cyst elongation, making the smaller, early post-meiotic cysts difficult to identify. In order to observe cysts that are just beginning to elongate, we examined testes of wild-type and GLD2-deficient pupae. Tissues were dissected 3-4 days after pupation and stained for nuclei and GLD2 localization as was done with adult tissues. In wild-type preparations, nuclear bundling at one end of elongating cysts was observed at the onset of elongation (Fig. 5.4E); however, such nuclear bundles are never observed in GLD2 knockdown preparations from the pupae. GLD2-knockdown pupal testes showed nuclear scattering within cysts even in the earliest stages of spermatocyst elongation (Fig 5.4F). This indicates that GLD2 is necessary for some aspect of post-meiotic nuclear localization. Previous studies have indicated a requirement for dynein and dynactin at apical ends of elongating cysts for nuclear retention and bundling (Ghosh-Roy et al., 2004). Additionally, interfering with phosphoinositide signaling can affect cyst polarity (Fabian et al., 2010). It is possible that GLD2 is required for proper nuclear localization by mediating dynein-dynactin dependent anchoring and/or phosphoinositide-dependent cyst polarity.

Basal body docking is defective in GLD2-deficient spermatogenesis: After completion of meiosis, haploid round spermatids undergo differentiation events before entering the spermatid elongation period. One important event is the formation of the basal body derived from the centriole. During meiosis II, the centrosome undergoes reductive division so that each post-meiotic spermatid nucleus is associated with only one centriole. Upon spermatid differentiation

soon after meiosis, the centriole inserts into a groove in the nuclear membrane at the base of the nucleus (a process called basal body docking), where it becomes the spermatid basal body (Fuller, 1993; Tokuyasu, 1974). Nuclear scattering has previously been described in mutants affecting basal body docking (Anderson et al., 2009; Texada et al., 2008).

To assess whether the basal body could form and dock properly in the absence of GLD2, we compared staining patterns of g-tubulin in adult testes of GLD2-deficient and control males. In wild-type testes, g-tubulin stains centrosomes throughout meiotic phases, and stains basal bodies associated with nuclei in elongated spermatids (Fig. 5.5A). In GLD2-knockdown testes, centrosomal g-tubulin staining can be seen in meiotic spermatocytes (data not shown); however, g-tubulin is not consistently detected at or near the nuclei of elongated spermatids (Fig. 5.5B). This result indicates that centrioles were unable to attach to the nuclear membrane after meiosis, resulting in post-meiotic spermatids that lack basal bodies at the nucleus. In examining the full length of the testis, some intermittent staining can be detected, but staining does not appear to be associated with nuclei, nor does it appear as succinct puncta as in the wild-type. It is unclear what happens to centrosomal derivatives in elongated cysts. The presence of axonemes raises the possibility that centrosome-derived structures are intact at least in early spermatids, since the basal body is required for axoneme assembly (Fuller, 1993). However, our confocal microscopy scans of late spermatogenic cysts of knockdown testes failed to detect distinct g-tubulin staining, which would have indicated the presence of properly-formed basal bodies; we did detect such basal body staining in wild-type (Fig. 5.S4).

FIG. 5.5. Basal body docking is defective in GLD2-knockdown testes. Basal body formation was examined by immunostaining for γ-tubulin. In wild-type control testes (A), γ-tubulin staining (green) can be seen at the base of each nucleus (stained with propidium iodide, red), indicating proper differentiation of basal bodies. In GLD2-knockdown testes (B), concentrated γ-tubulin staining cannot be observed near nuclei. Scale bars, 10mm.

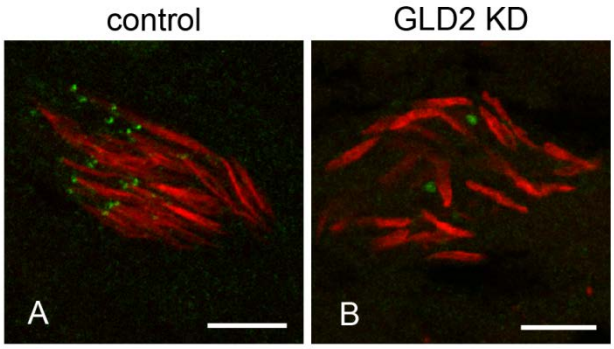
control
GLD2 KD
A
B

Nuclear compaction is disrupted in GLD2-deficient spermatogenesis: DAPI staining indicated that, in addition to the nuclear scattering phenotype, nuclei in elongated spermatocysts of GLD2-knockdown testes were less condensed than those of wild-type testes (Fig.5. 4C,D), suggesting a nuclear compaction defect. We found that the nuclei that were the most condensed in GLD2-knockdown testes had not progressed past the canoe stage (Fig. 5.4D). One possible explanation is that the translation of nuclear compaction proteins requires GLD2. To investigate whether spermatids in GLD2-knockdown flies are able to exchange histones for protamines, we examined spermatid nuclei of GLD2-knockdown males carrying a protamineB-eGFP construct. In this cross, snapback RNA against GLD2 was driven by *tubulin*-GAL4, which yields a knockdown testis phenotype identical to RNAi achieved by *bam*-GAL4 (data not shown). While many spermatid nuclear bundles and all nuclei of free-swimming sperm in control testis showed clear GFP signal (Fig. 5.6A,B), there was no GFP signal detectable anywhere in knockdown testis (Fig. 5.6C,D). However, RT-PCR shows the presence of protamineB-eGFP transcripts, indicating that the construct is present and transcribed in these flies (Fig. 5.6E). Therefore, we performed PAT assays for protamine A and protamine B on control and knockdown flies, and we found no difference in poly(A) tail length of protamine transcripts between the two groups (Fig. 5.6F).

To further investigate why nuclei fail to condense fully in the GLD2-knockdown, we tested for presence of transcripts of the *Drosophila* transition-protein tpl^{94D} (CG31281) by RT-PCR. The gene encoding the *Drosophila* transition protein is transcribed in spermatocytes, and its protein appears only transiently during nuclear remodeling (Rathke et al., 2007). Thus tpl^{94D} is a candidate for post-transcriptional regulation at the transcript's 3' sequence. *Drosophila*

tpl^{94D} transcripts were detectable in wild-type testes, but were not detectable in GLD2-knockdown testes (Fig. 5.7). This result could indicate that the gene is not being transcribed, or that the transcript is synthesized but is unstable. Such instability could arise from a poly(A) tail elongation defect; however, because the transcript is not detectable in GLD2-knockdown samples, we could not measure its poly(A) tail length or otherwise test these hypotheses.

These data suggest that GLD2 acts upstream of protamine B translation. Given that no effects of GLD2 on poly(A) tail length of protamine transcripts were detected, it seems likely that removing GLD2 causes a block in the spermatogenic developmental pathway at a stage before protamine transcripts would normally be translated. Rathke and colleagues (2007) showed that protamines are incorporated into the spermatid chromatin after the onset of transition protein incorporation, so it is possible that lack of transition protein causes a developmental block in GLD2-knockdown testes, and the lack of protamine translation in these testes reflects that block. There is evidence that protamine transcripts are translationally repressed for a few days after their transcription, and this repression is dependent upon elements in the 5'UTR (Raja and Renkawitz-Pohl, 2006). GLD2 alternatively could be responsible for controlling translation of a critical element that affects the release of repressor binding at the protamine 5'UTR repression element, while not affecting poly(A) tail status of the protamine transcript itself.

Although no effect of GLD2 on protamine transcripts was observed, we found an interesting result that has not been reported before in *Drosophila* spermatogenesis. The poly(A) tail of the protamine A and protamine B transcripts is approximately 30 nucleotides longer in larval testes than in adult testes (Fig. 5.6F). Larval testes are comprised mostly of primary spermatocytes and have not yet developed the protamine-based nuclear configurations that are

seen in adult testes (Fuller, 1993). Therefore, the difference in protamine poly(A) tail length between larval and adult testes indicates that deadenylation accompanies spermatid differentiation, and may promote protamine translation. While this seems contradictory to what is known about the role of the poly(A) tail in regulating translational efficiency, deadenylation has been known to accompany translation in some cases. In mice, transition protein and protamine transcripts are synthesized in primary spermatocytes and are translationally repressed for several days. The translationally inactive, non-polysome-bound forms of the mouse protamine transcripts are considerably longer than the active polysome-bound forms, and this difference in transcript length reflects differences in amount of poly(A) (Kleene et al., 1984).

Absence of dynamin may contribute to F-actin assembly defect in GLD2-deficient spermatogenesis: In wild-type adult testes, F-actin individualization complex formation follows protamine incorporation. As described above, actin individualization complexes do not develop in the absence of GLD2. Lack of F-actin at nuclear bundles could be due to a failure to regulate actin transcripts, a failure to stabilize G-actin, or a failure to assemble G-actin into individualization cones in GLD2-knockdown testes. To distinguish between these possibilities, we performed tests at each level.

We tested for expression of two actin genes, *act42a* and *act87e*, that are reported to be highly expressed in testis tissue (Chintapalli et al., 2007). We were able to detect both transcripts in wild-type and GLD2-knockdown testes; however, poly(A) tail (PAT) assays indicated no change in polyadenylation state in the absence of GLD2 (Fig. S5A). To test whether actin transcripts were being translated, we stained adult testes for monomeric G-actin using AlexaFluor-labeled DNase1. DNase1 binds to G-actin and is an indicator of G-actin levels (Philip et al., 1992; Snabes et al., 1981). There was no noticeable difference in the staining

FIG. 5.6. Protamines are transcribed, but not incorporated in GLD2-knockdown testes. We examined protamine incorporation by crossing in eGFP-tagged protamine B and staining for DNA using DAPI. In control testes, many nuclear bundles of late spermatogenic cysts (A) contain protamine-based chromatin, visualized here as GFP (B). Late-stage nuclei in GLD2-knockdown testes (C) are only partially condensed. Lack of GFP signal in GLD2-knockdown testes (D) indicates that protamine B is not incorporated. RT-PCR specifically for the protamineB-eGFP construct shows that the construct is expressed in knockdown and control testes (E). PAT assay (F) shows that both protamines are expressed in wild-type male larvae (L), wild-type male adults (A+) and GLD2-knockdown male adults (A-). The transcripts of both protamines are larger in larvae than in adults, and there is no difference in transcript length between wild-type and GLD2-knockdown adults. Scale bars, 40mm.

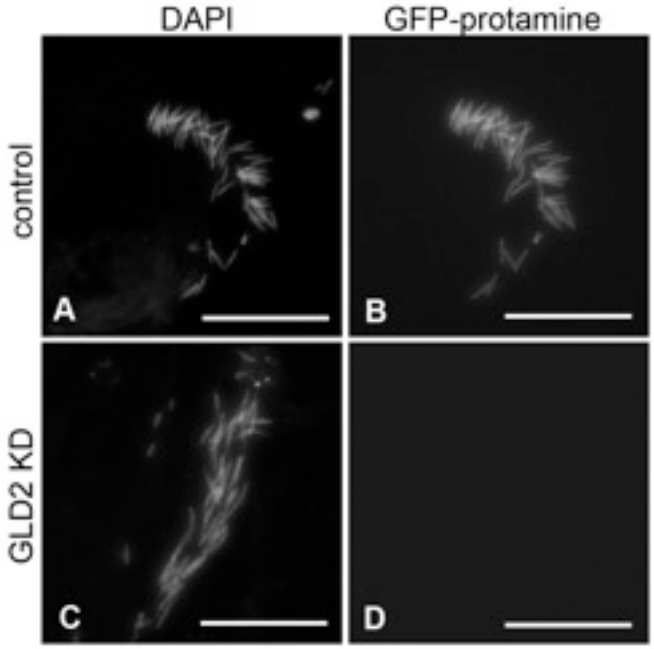
DAPI
GFP-protamine
control
GLD2 KD
A
B
C
D

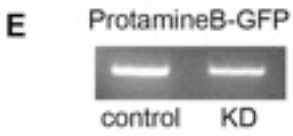
E
ProtamineB-GFP
control
KD

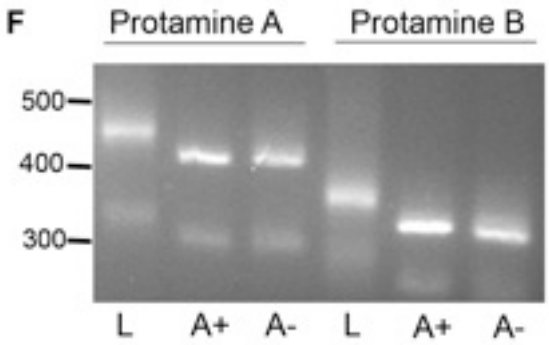
F
Protamine A
Protamine B
500
400
300
L
A+
A-
L
A+
A-

FIG. 5.S4. g-tubulin staining shows centrosomal derivatives throughout many stages of spermatogenesis in whole wild-type testes. g-tubulin stains centrosomes throughout spermatocyte stages of spermatogenesis (distal testis), and stains basal bodies in post-meiotic spermatogenesis (basal testis). Centrosomal staining is bright and can be seen at lower magnification; however, basal body staining is fainter and requires higher magnification (inset).

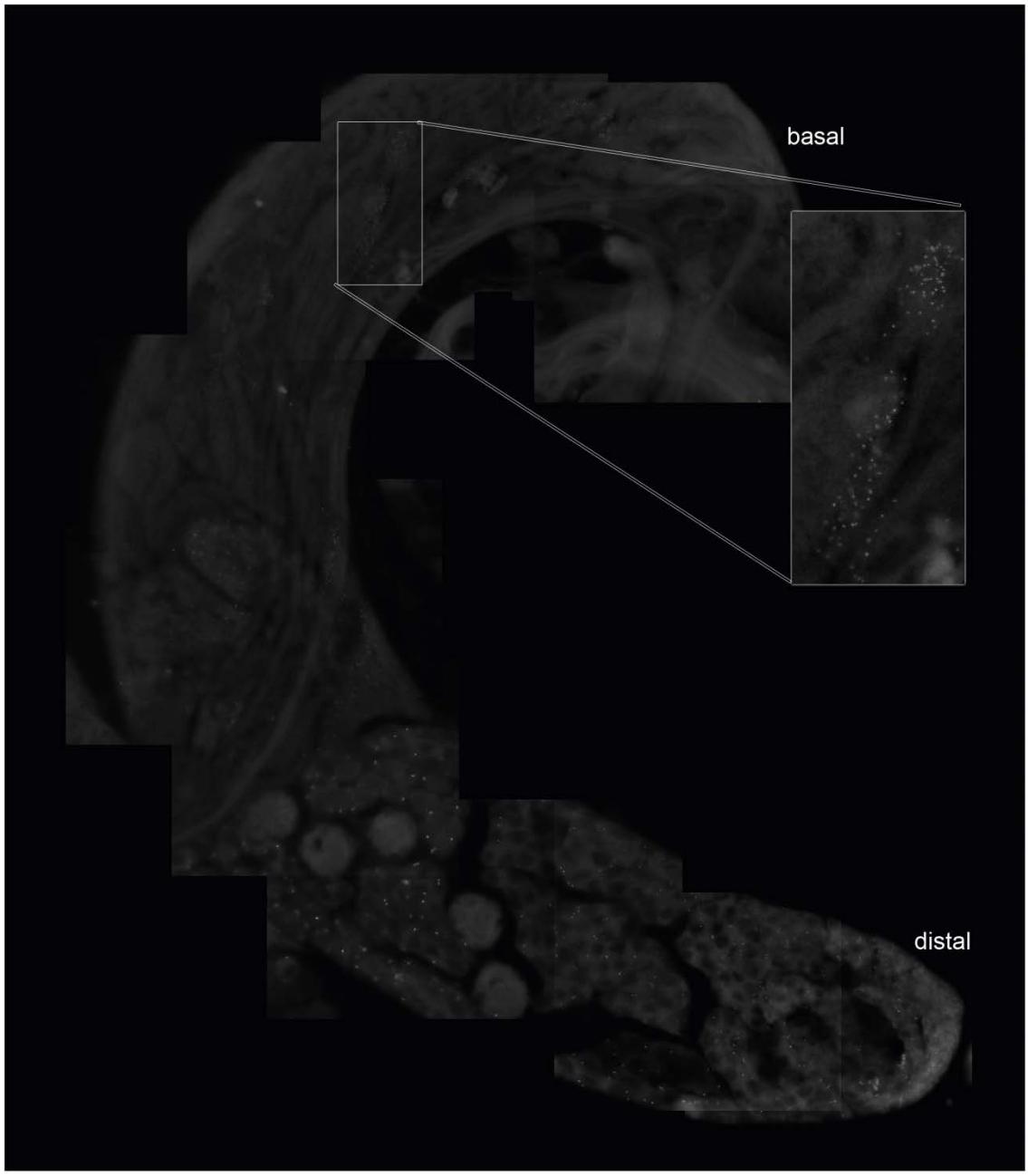
basal
distal

FIG. 5.S5. G-actin levels appear normal in GLD2 knockdown. PAT assay of Act42a and Act87e from testes cDNA samples indicates no difference in mRNA levels or length of these actin transcripts (A). Cellular G-actin protein levels do not differ between control (B) and knockdown (C) testes, as indicated by intensity of Alexa 488-conjugated DNase1 staining (green). Scale bars, 150mm.

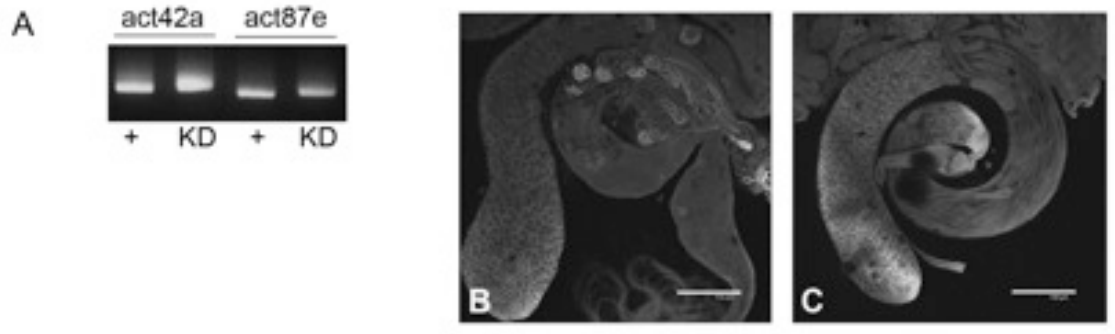
A
act42a
act87e
+
KD
+
KD
B
C

FIG. 5.7. Transition protein and dynamin transcripts are absent from GLD2-knockdown testes. RT-PCR shows that the dynamin (dyn) transcript is present in control adult testes, but absent from GLD2-knockdown testes; additionally, transition protein *tpl94D* transcript is present in control adult testes, but absent from GLD2-knockdown testes. RPL32 is used as a positive control.

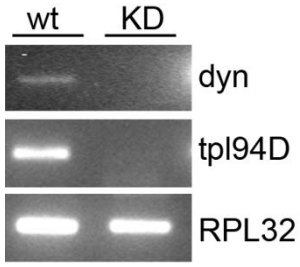
wt
KD
dyn
tpl94D
RPL32

pattern detected between wild-type and GLD2-deficient testes, indicating that G-actin is present in apparently equal amounts (Fig. S5B,C). These data indicate that the loss of F-actin in GLD2-knockdown testes is likely not due to a deficit of available G-actin, but could possibly be attributed to missing F-actin assembly machinery in the GLD2-knockdown.

Therefore, we tested for the presence of a number of factors known to be involved in F-actin formation, including profilin and dynamin. RT-PCR showed that dynamin was expressed in wild-type, but not in GLD2-deficient, testes (Fig. 5.7). Dynamin has previously been shown to be necessary in late spermatogenesis for assembly of F-actin cones at spermatid nuclei (Ghosh-Roy et al., 2005). The absence of dynamin in GLD2-deficient testes may account for the lack of F-actin individualization cones in late-stage spermatids; however, as with the transition protein transcript, we cannot determine whether the absence of the dynamin transcript is a direct result of lack of polyadenylation by GLD2, or rather a secondary result of a block to spermatogenesis occurring upstream of dynamin regulation.

Candidate target testing: We have tested candidate transcripts for changes in poly(A) tail length due to GLD2 by PAT assay, but thus far have not found a change in the polyadenylation status in GLD2 knockdowns for any mRNA tested (Table 5.1). Candidates were chosen based on the phenotype of the GLD2 knockdown; specifically, gene transcripts known to be necessary for the affected late spermatogenesis events such as basal body formation, nuclear anchoring, nuclear compaction, or individualization were tested by PAT assay. A change in poly(A) tail length due to amount of GLD2 would indicate a positive hit. We did not identify any targets of GLD2 using this candidate approach. All transcripts that were tested by PAT assay (with the exception of *tpl94D* and *dynamin*, see above) were present in GLD2-knockdown and control testes, and variation in transcript length between GLD2-knockdown and control samples was not

Table 1. Transcripts that tested negative for GLD2-dependent polyadenylation by PAT assay

Annotation	Gene (synonym)	Function (reference)
CG12051	*Actin 42A*	Actin
CG18290	*Actin 87E*	Actin
CG2092	*anillin* (*scraps*)	Actin-associated at male fusome (Hime et al., 1996; Fabian et al., 2010)
CG6814	*asunder* (*Mat89Bb*)	Basal body docking (Anderson et al., 2009)
CG4760	*boule*	G2/M in male meiosis (Castrillon et al., 1993; Eberhart et al., 1996)
CG9012	*Clathrin heavy chain*	Individualization (Fabrizio et al., 1998)
CG10536	*crossbronx*	Individualization, E2 Ub-conjugating enzyme (Fabrizio et al., 1998)
CG9206	*dynactin* (*Glued*)	Spermatid nuclear anchoring (Ghosh-Roy et al., 2004)
CG6998	*dynein light chain* (*cut up*)	Spermatid nuclear anchoring (Ghosh-Roy et al., 2004)
CG1765	*Ecdysone receptor* (*lie*)	Individualization (Fabrizio et al., 1998)
CG10192	*eIF4G2*	Male-specific translation initiation factor (Baker and Fuller, 2007)
CG7570	*hale-bopp*	Comet protein, late spermiogenesis (Barreau et al., 2008)
CG7788	*Ice*	Caspase (Arama et al., 2003)
CG18584	*klaroid*	Nuclear anchoring (Starr and Fischer, 2005)
CG17046	*klarsicht*	Nuclear anchoring (Starr and Fischer, 2005)
CG10701	*Moesin*	Actin-associated during spermatogenesis (Fabian et al., 2010)
CG33715	*Msp-300*	Nuclear anchoring (Yu et al., 2006)
CG4479	*Mst35Ba*	Protamine A (Raja and Renkawitz-Pohl, 2006)
CG4478	*Mst35Bb*	Protamine B (Raja and Renkawitz-Pohl, 2006)
CG3354	*Mst77F*	Linker histone-like protein (Raja and Renkawitz-Pohl, 2006)
CG17956	*Mst87F*	Polyadenylated in cytoplasm during spermiogenesis (Schafer et al., 1990)
CG5695	*myosin VI* (*jaguar*)	Individualization (Hicks et al., 1999; Noguchi et al., 2006)
CG10523	*parkin*	Mitochondrial morphogenesis (Riparbelli and Callaini, 2007)
CG9553	*profilin IV* (*chickadee*)	F-actin assembly (Verheyen and Cooley, 1994; Fabrizio et al., 1998)
CG14472	*purity of essence*	Individualization, E3 Ub ligase (Fabrizio et al., 1998)
CG3766	*scattered*	Individualization (Fabrizio et al., 1998)
CG9985	*skittles*	Spermatid cyst polarity (Fabian et al., 2010)
CG6589	*spag4*	Basal body differentiation (Kracklauer et al., 2010)
CG1977	*Spectrin*	Polarized localization in spermatid cyst (Hime et al., 1996; Fabian et al., 2010)
CG31281	*Transition protein-like 94D*	Transition protein (Rathke et al., 2007)
CG10113	*walker cup*	Cup protein, late spermiogenesis (Barreau et al., 2008)
CG31732	*yuri gagarin*	Basal body docking (Texada et al., 2008)

detected. However, it is conceivable that because some of the candidate genes have multiple transcript isoforms, a change in some minor isoform could have gone undetected. Additionally, it is possible that *tpl94D* and *dynamin* transcripts, which are not detectable in GLD2 knockdown testes, are true targets of GLD2. Without GLD2, target transcripts would have short poly(A) tails, which may cause increased susceptibility to degradation in the cytoplasm by exonucleases. Another possibility is that GLD2 is responsible for polyadenylation of a master regulator of spermiogenesis, such as a transcription factor, and the many aspects of the GLD2 phenotype occur as a result of one missing regulatory step.

5.4 Conclusions

We have shown that in the absence of GLD2, spermiogenesis is severely compromised in *Drosophila*. The earliest defects are seen in early post-meiotic spermatids, when the basal body fails to attach and the nuclei begin to scatter. Many downstream events are also affected, including protamine translation and F-actin cone formation, as well as stability of dynamin and transition protein transcripts. However, without identifying the direct targets of GLD2, we cannot determine whether later defects are directly due to GLD2, or they are a result of improper nuclear positioning or malformed basal bodies.

Based on results by Kwak and colleagues (2004) showing that GLD2 has poly(A) polymerase activity, it is very likely that GLD2 functions as a cytoplasmic poly(A) polymerase during spermatogenesis. GLD2 could be responsible for turning on a single or small number of master regulators for post-meiotic spermatid development. Alternatively, GLD2 could act on a suite of transcripts required in early spermatids, and perhaps even another subset of transcripts needed later at the distal end of the spermatogenic cyst. The fact that there is a long period during which some transcripts must remain stable and untranslated in the cytoplasm, as well as

the fact that the CPEB homolog *orb* is turned expressed during late spermatogenesis (Barreau et al., 2008), supports the hypothesis that GLD2 is a cytoplasmic poly(A) polymerase important for spermatogenesis.

It is interesting that *Gld2* is critical for post-meiotic spermatogenesis in *Drosophila*, yet all Gld-2 family members analyzed so far in *Drosophila* and other species play roles specifically at meiosis. We hypothesize that GLD2's male germline function reflects its evolutionary origin: duplication of the X-linked *wispy* locus allows for a testis-expressed derived autosomal copy that can be expressed during MSCI. Although this is the first example of a Gld-2 family member with a role solely in spermatogenesis, other species may have developed similar mechanisms of translational control in the testes; for example, spermatogenesis in mice is regulated in part by a cytoplasmic poly(A) polymerase outside of the Gld-2 family called TPAP (Kashiwabara et al., 2002). Further investigation and identification of GLD2 targets in *Drosophila* testes will help to elucidate how spermatogenesis can be regulated through cytoplasmic polyadenylation.

CHAPTER 6

THESIS SUMMARY AND PERSPECTIVES

Egg activation is a highly conserved set of events among animals, yet Drosophila is just emerging as a viable model for studying this process. The results described in this dissertation show that like in other organisms, Drosophila oocytes experience an increase in cytosolic Ca^{2+} levels as a trigger for egg activation. Furthermore, high-throughput biochemical analysis, phenotypic analysis, and evolutionary analysis has demonstrated the versatility of this organism in approaching important questions of egg activation. In this chapter, I discuss the implications of the work presented in this dissertation and provide perspectives pertaining to future studies.

A convergent Ca^{2+} influx as a trigger for egg activation

Until relatively recently—only seven years ago—it was unknown whether calcium played a role in egg activation in Drosophila. Because the trigger for egg activation is quite different in fruitflies and some other insects, Drosophila has been somewhat overlooked as a model system for this process. However, some important discoveries have been made concerning the requirement for and source of the calcium, the relationship of calcium to the trigger of the release from the ovary into the oviduct, and the components of the subsequent signaling pathway. Taken together, calcium is absolutely required for egg activation in Drosophila, and many of the downstream signaling components are conserved among species. Furthermore, without the fertilizing sperm, their egg activation events are driven solely by maternal components within the oocyte, affording a different view of egg activation than can be observed

in other organisms. Thus, I posit that Drosophila is not only viable but also uniquely valuable as a model system for egg activation, especially given the availability of genetic tools and ease of rearing and manipulation in this organism.

The work I have presented in Chapter 2 focuses on visualizing a calcium influx during egg activation in live Drosophila oocytes. In mice and other vertebrate species, the fertilizing sperm sparks a rise in cytosolic Ca^{2+} levels, and this event triggers egg activation events. In mice, several different types of calcium channels work together to propagate the influx that occurs upon egg activation (Malcuit et al., 2006). While the first calcium transient results from Ca^{2+} release from the ER following sperm-induced phosphoinositide signaling, further oscillations depend upon a number of different calcium channels and ion pumps. When Ca^{2+} levels are depleted from ER stores, sarco/endoplasmic reticulum Ca^{2+}-ATPase (SERCA) pumps on the ER membrane must actively transport Ca^{2+} from the cytosol back into the ER. Furthermore, plasma membrane Ca^{2+}-ATPase (PMCA) pumps on the cell surface move Ca^{2+} out of the cell to restore normal cytosolic Ca^{2+} levels. Thus, for each oscillation, the intracellular Ca^{2+} levels are elevated for several minutes. In organisms whose oocytes undergo multiple waves at fertilization, oscillations following the initial sperm-induced transient rely not only upon Ca^{2+} from the ER, but also Ca^{2+} influx from the external environment (Miao et al., 2012). On the other hand, not all organisms' oocytes undergo multiple oscillations: in the large eggs of frogs and fish, for example, only a single large calcium transient is produced (Stricker, 1999).

My work shows that the Ca^{2+} requirement for egg activation is conserved in Drosophila. However, the mode of Ca^{2+} elevation is different from that of most other organisms studied. Notably, I found that release of calcium from intracellular stores is not required for calcium wave propagation: inhibition of members of the phosphoinositide signaling pathway does not

compromise the cytosolic calcium increase during egg activation. Instead, Ca^{2+} from the extracellular environment enters the oocyte through TRP family mechanosensitive channels. However, it is unclear exactly which type of TRP channel mediates the Ca^{2+} influx, or which channels are present on the egg cell surface. Several members of the TRP family of calcium channels (reviewed in (Montell, 2005)) are activated by mechanical stress, including *nompC* (which is activated by cytoskeletal tension (Walker et al., 2000)), *nanchung,* and *inactive* (both activated by hypoosmolarity (Gong et al., 2004; Kim et al., 2003)). Although transcripts encoding these particular TRP channels are not detectable by RT-PCR in the adult ovary (Horner and Wolfner, 2008a), and thus cannot be the sensors for the egg activation trigger, a fourth TRP protein that may be responsive to mechanical stimuli, TRPA encoded by the *painless* gene, is expressed in the ovary (Horner and Wolfner, 2008a), but it has not yet been tested for a role in egg activation. In addition, mechanosensitive channels of a different class, the DEG/ENaC family are expressed in ovaries and thus are candidates for involvement in egg activation. Only one member of this family, *ripped pocket* (*rpk*), had been tested, and its mutant exhibited normal fertility (Horner and Wolfner, 2008a). However, that mutant is not null so it is not possible to conclusively rule out a role for *rpk* in egg activation. Additional mechanosensitive channels of the TRP and DEG/ENaC families are expressed in the ovary (Chintapalli et al., 2007; McQuilton et al., 2012). An important direction for future study is to assess the roles of these ovary-expressed channels in egg activation and their localization, if any, to the egg cell surface.

One surprising result that came from the study is the form of the influx itself. In most organisms, the calcium influx initiates from the point of sperm entry and traverses across the egg. However, Drosophila does not require sperm entry for egg activation. Therefore, before we began this study we could imagine several possible scenarios: (1) If the Drosophila oocyte opens

stretch-activated calcium channels as a result of fluid uptake in the oviduct, which likely exerts pressure across all parts of the egg membrane uniformly, we would expect an isometric rise in cytoplasmic calcium levels, instead of a wave initiating from a single point (as occurs in systems that require sperm entry for activation). (2) Since the posterior pole of the oocyte enters the oviduct first, and thus pressure is first exerted posteriorly, a calcium rise may initiate from the posterior and propagate anteriorly *in vivo*. (3) The calcium rise may initiate from the micropyle (the small opening through which the sperm enters) on the anterior end of the oocyte, which is analogous to the point of sperm entry in oocytes of other organisms, even though the Drosophila egg activation does not require fertilization. In this case, a calcium wave would propagate from the anterior to the posterior.

However, none of these scenarios was observed in my *in vitro* studies. Instead, I observed an increase originating from either pole and moving inward to finally converge at the center of the egg. Typically, a rise in Ca^{2+} levels would be visible first at the anterior pole, followed by an increase at the posterior pole. The high Ca^{2+} regions would expand towards the interior and plateau for several minutes, after which time levels would then fall to baseline first from the poles and lastly in the interior. The question remains whether these particular dynamics are specific to *in vitro* egg activation or if the wave occurs in the same way *in vivo.* An *in vivo* imaging technique will need to be developed to answer this question.

Perhaps the most interesting question is, what happens after the Ca^{2+} influx? What are the biochemical pathways involved in connecting the initial Ca^{2+} increase to all of the major egg activation events (meiosis resumption, transcript turnover, etc.)? The initial steps of this process are likely conserved in many species. I believe that the calcium-binding protein calmodulin (CaM) is involved as a first step and then interacts with downstream calcium-dependent kinases

(likely CaMKII) and phosphatases (calcineurin) to spark signaling pathways. However, studying the requirement for CaM and CaMKII has been difficult in Drosophila. One challenge for such genetic analysis is that global knockout of either CaM or CaMKII is lethal to the animal, so, tissue-specific knockdowns must be tested. CaM-deficient germline clones were generated to study CaM's role in oogenesis and embryogenesis, but surprisingly, the germlines of these flies were not depleted of CaM protein. Though the germline cells were indeed *CaM*-null, it appeared that CaM protein was able to enter the germline cells from the surrounding somatic cells (Andruss et al., 2004). Thus, it was not possible to determine definitively whether CaM plays a role at egg activation. However, Andruss and colleagues observed that some mature oocytes absorbed less somatic CaM than others (anywhere between 28% and 76% that of heterozygous controls), and those that received relatively little somatic CaM show severe defects upon embryogenesis, though oogenesis occurs relatively normally (Andruss et al., 2004). These latter results support the idea that CaM plays a role in the egg-to-embryo transition, although further experiments are needed to fully prove this hypothesis.

It has not yet been possible to test for a role for CaMKII in Drosophila egg activation because the location of the CaMKII gene, on Drosophila's fourth chromosome, has precluded the generation of germline clones. However, a method to generate mitotic clones for fourth chromosome genes in the soma has just been reported (Sousa-Neves and Schinaman). Future tweaks to this system may make it possible to induce loss of CaMKII expression in the germline while maintaining normal expression in the soma.

Because generating germline clones deficient for CaM or CaMKII has not yet been possible, attempts have been made to knock down the amount or activity of these proteins using other means. Interfering RNA (Harvard Medical School, TRiP) or inhibitory peptides targeted

against CaM (VanBerkum and Goodman, 1995) or CaMKII (Griffith et al., 1993) can be expressed in the germline. Preliminary experiments of this type have not produced an effect on egg activation or fertility (A. Krauchunas, K. Kumar, Y. Lai, K. Sackton, C. Sartain, and M. Wolfner, unpublished data), but it is possible that the abundant maternal stores of CaM or CaMKII in oocytes cannot be sufficiently inhibited by these methods. Thus, at present we cannot evaluate whether CaM and CaMKII are essential for egg activation. We expect that new genetic techniques for germline analysis will allow us to study these proteins' roles in the future.

Transcript regulation downstream of the activating signal

Through as of yet unknown signaling pathways, the trigger for egg activation eventually results in major changes to the pool of maternal mRNAs stored within the cytoplasm. Approximately 55% of the entire Drosophila genome is represented among the stored transcript pool in mature oocytes (transcripts from an estimated 7745 genes), where they remain in a stored, quiescent state (Tadros et al., 2007). Upon egg activation, these transcripts must become active and are either translated or degraded as the egg transitions to embryogenesis. Previous studies have demonstrated that about 20% of the transcripts present in mature oocytes are degraded at egg activation in eggs from virgin females: this represents the degradation that occurs as a direct result of egg activation (Tadros et al., 2007). Our studies on the cytoplasmic poly(A) polymerase *wispy* indicate that approximately 73% of transcripts present at egg activation get polyadenylated in a *wisp*-dependent manner (Chapter 4). Polyadenylation has been shown to promote translation, as in the case of *bicoid* transcripts (Benoit et al., 2008). With these numbers taken together, we have a broad view of the fates of stored transcripts upon egg activation.

The specific mechanism regulating each transcript may require more work. Previous studies have shown that approximately two-thirds of the transcripts destined for degradation are targets of SMG, a conserved posttranscriptional regulator (Tadros et al., 2007). SMG targets have sequence elements in the 3'UTR that recruit SMG (Smaug Repressive Element, SRE), which promotes deadenylation and degradation if repression is not relieved (Vardy and Orr-Weaver, 2007a). There are a handful of other repressive elements that may lie in the 3'UTR, signaling repression by other translational inhibitors such as PUMILIO and BRUNO (Vardy and Orr-Weaver, 2007a). These may regulate the other one-third of degraded transcripts that are SMG-independent.

We were unable to find a sequence element that signals for WISP-dependent cytoplasmic polyadenylation. Like other Gld-2 family members, WISP does not have RNA-binding capabilities by itself and must pair with a binding partner (BIC-C, the Drosophila Gld-3 homolog) in order to bind RNA (Wang et al., 2002). We searched for shared sequence motifs among the targets of WISP identified in our microarray data, but we were unable to find a consensus sequence using these methods. In frogs, for example, there is a known element in the 3'UTR that binds CPEB (Drosophila ORB), and GLD-2 (Drosophila WISP) is a part of this complex (Kim and Richter, 2007). However, there are far fewer GLD-2 targets in other species (for example, 550 in worms (Kim et al., 2010)), so finding statistical significance for a single consensus sequence may be less confounding. Better computational methods will be required to identify a sequence element for WISP-dependent polyadenylation in Drosophila.

The *prg* and *wisp* mutations were both identified in a screen for X-linked mutations that caused failure of egg activation and particularly failure to degrade key transcripts at egg activation (Tadros et al., 2003). Jun Cui mapped *wisp* to a poly(A) polymerase and classified its

action at egg activation (Cui et al., 2008), and mapped *prg* to a predicted exonuclease with no known function (Chapter 3). I had originally hypothesized that PRG might be responsible for destabilization of repressed transcripts at egg activation through its predicted exonuclease activity. To this end, I ran RNA-seq to detect differences in stored transcript abundance prior to zygotic genome activation (ZGA) in activated eggs (Chapter 3). Unfortunately, my data did not reveal any large-scale changes in transcript abundance between wild-type and *prg* mutant samples. However, Hsp83 was among the significant hits returned by the data analysis; this is an important internal control, since *prg* was first identified using Hsp83 degradation as a diagnostic marker (Tadros et al., 2003). Therefore, I believe that the data are reliable, but using an FDR cutoff of 0.05 I may be obtaining a large number of false negatives. My data lack biological replicates, which may drive the P-values to non-significant levels. Ideally, we would run more replicates to get a more accurate view of the true positives; however, we will likely get a close approximation by doing a simpler screening of the data returned by this RNA-seq experiment. I propose running qPCR on a range of hits by either P-value or fold-change (similar to what was done to conform the WISP microarray data, Chapter 4) to narrow down (or in this case, to broaden) our window of how many transcripts change abundance in a PRG-dependent manner.

The egg activation phenotype of eggs from *prg* mutant mothers is also questionable. When *prg* was originally identified, the authors claimed that vitelline membrane reorganization occurred normally but meiosis failed to complete (Tadros et al., 2003). They used the same bleach-resistance assay as I have used and found that *prg* eggs did not lyse during incubation with bleach. On the contrary, I found that *prg* eggs are extremely fragile. While the eggs did not completely dissolve in bleach in the same way unactivated eggs do, eggs from *prg* mutant mothers were markedly different from their wild-type counterparts after bleach incubation

(Chapter 3). Additionally, I attempted manual chorion removal using double-sided tape, which is possible with activated eggs that have undergone proper VM crosslinking; I found that the *prg* eggs were extremely fragile. I often destroyed the eggs, and in the few instances in which I was able to remove the outer chorion, I could not touch the egg or it would burst. This indicates that the VM is especially fragile, but the "empty bag" appearance they take on after bleach incubation suggests that some crosslinking may have occurred. I believe it is likely that there is some role for PRG during oogenesis, possibly in the somatic cells that synthesize the eggshell components. It might be useful to separate somatic and germline functions (i.e., knockout *prg* everywhere except the germline or ectopically express *prg* in somatic cells of a *prg* mutant) in order to narrow down the precise egg activation defects in eggs from *prg* mutant mothers.

Cytoplasmic polyadenylation during spermatogenesis

In our lab's original *wispy* study, Jun Cui noticed that the Drosophila genome encoded a gene closely related to *wispy*: CG5732, now called *Gld2* (Cui et al., 2008). As a rotation project, I studied the role of this gene as a cytoplasmic poly(A) polymerase similar to *wispy* (Chapter 5). Unexpectedly, *Gld2* played no role in female gametogenesis, but instead had roles in spermatogenesis. Unlike eggs, sperm do not need to contribute many nutrients to embryogenesis; instead, sperm cells should be compact and nimble, essentially a nucleus with a propeller. During spermatogenesis in Drosophila and other organisms, some transcripts are synthesized early, during premeiotic spermatocyte growth phases, but are not translated until after meiosis has completed. This is likely where GLD2 is required, but I was unable to provide direct evidence of any transcript that undergoes GLD2-dependent polyadenylation. Whatever the targets of GLD2 in spermatogenesis, they are essential to this process: without GLD2, males cannot complete proper spermatogenesis and thus are completely sterile. Ideally, I would like to perform a high-

throughput experiment in order to identify all the targets of GLD2 during spermatogenesis. Though we were able to successfully globally identify WISP targets using microarrays, I would recommend RIP-chip for future studies of this kind, since this single experiment allows identification of an RNA directly bound within the GLD-2 protein complex, whereas our microarray is a more indirect measure that we must assume is GLD-2 dependent. However, we did not perform this experiment on the sperm GLD2 because of issues obtaining great enough amounts of material from the Drosophila testes. Additionally, because we are traditionally not a spermatogenesis lab, such a time-consuming experiment is not a high priority for us at this point.

It is interesting that Drosophila has independently developed two GLD-2 homologs with separate functions, whereas most GLD-2 homologs studied act solely in the female germline (with the exception of hermaphroditic worms). In collaboration with Richard Meisel in Andy Clark's lab, I found that *wisp* and *Gld2* are paralogous genes that have uniquely arisen in the Drosophila genus. *Gld2* appears to be the derived copy while *wisp* lies in the ancestral chromosomal location. However, because in Drosophila the original GLD-2 homolog was on the X chromosome, it may have required duplication to an autosome in order to maintain expression during meiosis (MSCI avoidance, Chapter 5). It would be interesting to explore the requirement of GLD-2 homologs in males of other species to see if the same GLD-2 is required in both male and female germlines, or if this is a unique property of Drosophila GLD2.

Summary

My work has tied up some outstanding questions in Drosophila egg activation, and also opens doors to new research questions. I have made significant advances in examining calcium dynamics. Using the flies generated by the Aigaki lab, I have developed a method for successfully imaging calcium waves in Drosophila eggs, and have for the first time shown that a

calcium influx occurs in eggs of this species. This work pushes Drosophila forward as an important and useful model system for this process. I have also further classified the defects in eggs of *wisp* and *prg* mutant mothers, allowing for a more comprehensive view of RNA regulation during egg activation.

APPENDIX A.

SUMMARY AND RESULTS OF CALCIUM DRUGS TESTED

To aid in future investigations of Ca^{2+} dynamics during egg activation in *Drosophila melanogaster*, I have compiled a list of all pharmacological inhibitors tested on activating oocytes to date (Table A1). Many of the inhibitors tested prior to January 2013 were only tested for their ability to inhibit vitelline membrane crosslinking using the bleach assay (described in Chapter 3 of this dissertation). I believe the bleach assay to be a less reliable assay for testing various aspects of the calcium influx; these reagents should be retested using the treatment and microscopy methods described in Chapter 2 instead.

Table A1. Pharmacological agents tested on activating oocytes.

Drug	Function	Method	Result	Who	Date
U-73122	PLC inhibitor	10-20μM in bleach assays	No effect	VLH	May-03
		10-20μM GCaMP microscopy	No effect	CVS	Mar-13
wortmannin	PI3K inhibitor	1-5μM GCamP microscopy	No effect	CVS	Mar-13
GdCl3	SA channel blocker	100μM in bleach assays	Inhibits	VLH	Oct-03
		100-400μM GCaMP microscopy	Inhibits	CVS	Mar-13
		10μM GCaMP microscopy	No effect	CVS	Jul-13
Amiloride	Blocks Na/H exchanger	10-100μM in bleach assays	No effect	VLH	Nov-03
Ryanodine	Receptor channel on ER	50μM in bleach assays	no effect	VLH	Dec-04
Ruthenium Red	Blocks RyR, some TRP	10μM in bleach assays, meiosis	no effect	VLH	Dec-04
		10μM GCaMP microscopy	No effect	CVS	Jul-13
XestosponginC	Blocks IP3	350nM in bleach assays	no effect	VLH	Dec-04
thapsigargin	Blocks SERCA pump	100-400μM in bleach assays	inconsistent	CVS	2012
verapamil	L-type blocker	50μM in bleach assays	poor controls	YWL	Jan-10
NiCl2	R-type blocker	1-5mM in bleach assays	trend	YWL	Jan-10
CdCl2	channel blocker	10mM in bleach assays	Inhibits	YWL	Jan-10
SNX-482	Block R-type channel	30nM in bleach assays	poor controls	YWL	Dec-09
w-conotoxin	channel blocker	3μM in bleach assays	no effect	YWL	Jan-10
nifedipine	L-type blocker	10μM in bleach assays	no effect	YWL	Jan-10
MRS-1845	SOC inhibitor	5μM in bleach assays	poor controls	MO/CVS	Aug-12
Calmidazolium	CaM inhibitor	10μM in bleach assays	moderate	MO/CVS	Aug-12
ACA	TRP blocker, broad	20μM in bleach assays	No effect	MO/CVS	Aug-12
		10-20μM GCaMP microscopy	Inhibits	CVS	May-13
BAPTA	Ca2+ chelator	Chelate Ca in buffer to <50nM			
		GCaMP microscopy assays	inhibits	CVS	May-13
		Bleach assay	inhibits	VLH	2008

VLH = Vanessa Horner
CVS = Caroline Sartain
YWL = Yun Wei Lai
MO = Misato Okajima (Tokyo Metropolitan University)

APPENDIX B

DAVID ANALYSIS OF WISPY MICROARRAYS

The following tables are the full results of gene ontology analysis using the program DAVID on subsets of genes identified in our WISPY microarray study (Chapter 4).

Table B1. Oocyte DAVID analysis, transcripts ≥2-fold higher in control than *wisp*

Term	Count	*P* value	Bonferroni
Biological process			
GO:0051276~chromosome organization	133	2.76E-30	7.46E-27
GO:0006259~DNA metabolic process	105	3.03E-24	8.19E-21
GO:0007049~cell cycle	209	1.46E-23	3.94E-20
GO:0000278~mitotic cell cycle	141	1.50E-22	4.06E-19
GO:0022402~cell cycle process	181	4.63E-19	1.25E-15
GO:0048285~organelle fission	76	4.41E-19	1.19E-15
GO:0007010~cytoskeleton organization	161	4.37E-19	1.18E-15
GO:0000087~M phase of mitotic cell cycle	74	8.43E-19	2.28E-15
GO:0007067~mitosis	73	1.49E-18	4.01E-15
GO:0008104~protein localization	141	2.20E-18	5.94E-15
GO:0000280~nuclear division	73	3.88E-18	1.05E-14
GO:0006260~DNA replication	55	1.74E-17	4.69E-14
GO:0007059~chromosome segregation	62	2.06E-17	5.57E-14
GO:0051301~cell division	86	1.07E-15	3.00E-12
GO:0000226~microtubule cytoskeleton organization	111	1.27E-15	3.30E-12
GO:0043933~macromolecular complex subunit organization	106	2.25E-15	6.00E-12
GO:0022403~cell cycle phase	157	1.98E-14	5.37E-11
GO:0051726~regulation of cell cycle	71	1.38E-13	3.73E-10
GO:0033043~regulation of organelle organization	54	1.36E-13	3.67E-10
GO:0006325~chromatin organization	72	1.64E-13	4.44E-10
GO:0000279~M phase	149	4.09E-13	1.11E-09
GO:0034621~cellular macromolecular complex subunit organization	80	6.37E-13	1.72E-09
GO:0007017~microtubule-based process	131	8.67E-13	2.34E-09
GO:0046907~intracellular transport	108	1.09E-12	2.96E-09
GO:0006261~DNA-dependent DNA replication	35	1.91E-12	5.16E-09
GO:0007051~spindle organization	84	4.80E-12	1.30E-08
GO:0045184~establishment of protein localization	99	6.98E-12	1.89E-08
GO:0048610~reproductive cellular process	149	1.95E-11	5.28E-08
GO:0065003~macromolecular complex assembly	88	2.04E-11	5.51E-08
GO:0015031~protein transport	96	2.22E-11	6.00E-08

GO:0044265~cellular macromolecule catabolic process	82	3.70E-11	9.99E-08
GO:0007242~intracellular signaling cascade	99	1.03E-10	2.77E-07
GO:0016568~chromatin modification	50	1.40E-10	3.79E-07
GO:0000819~sister chromatid segregation	29	1.84E-10	4.97E-07
GO:0009057~macromolecule catabolic process	93	2.66E-10	7.19E-07
GO:0007052~mitotic spindle organization	72	2.64E-10	7.13E-07
GO:0032989~cellular component morphogenesis	149	3.37E-10	9.11E-07
GO:0048477~oogenesis	153	5.44E-10	1.47E-06
GO:0000070~mitotic sister chromatid segregation	28	6.25E-10	1.69E-06
GO:0007292~female gamete generation	154	7.84E-10	2.12E-06
GO:0000902~cell morphogenesis	130	1.18E-09	3.20E-06
GO:0003006~reproductive developmental process	144	1.59E-09	4.30E-06
GO:0033554~cellular response to stress	65	2.75E-09	7.44E-06
GO:0019953~sexual reproduction	193	2.71E-09	7.32E-06
GO:0007346~regulation of mitotic cell cycle	43	6.22E-09	1.68E-05
GO:0006323~DNA packaging	33	6.64E-09	1.79E-05
GO:0007276~gamete generation	187	7.09E-09	1.91E-05
GO:0006281~DNA repair	44	7.53E-09	2.03E-05
GO:0051656~establishment of organelle localization	36	7.84E-09	2.12E-05
GO:0034622~cellular macromolecular complex assembly	61	8.66E-09	2.34E-05
GO:0051640~organelle localization	38	9.22E-09	2.49E-05
GO:0010605~negative regulation of macromolecule metabolic process	98	1.16E-08	3.13E-05
GO:0030182~neuron differentiation	119	1.33E-08	3.59E-05
GO:0006270~DNA replication initiation	14	1.31E-08	3.54E-05
GO:0006350~transcription	130	1.56E-08	4.21E-05
GO:0006974~response to DNA damage stimulus	47	1.66E-08	4.49E-05
GO:0045449~regulation of transcription	203	1.79E-08	4.84E-05
GO:0010564~regulation of cell cycle process	38	2.05E-08	5.54E-05
GO:0048666~neuron development	104	2.39E-08	6.45E-05
GO:0007264~small GTPase mediated signal transduction	45	2.46E-08	6.64E-05
GO:0016192~vesicle-mediated transport	114	2.50E-08	6.75E-05
GO:0070727~cellular macromolecule localization	79	4.23E-08	1.14E-04
GO:0051225~spindle assembly	21	5.11E-08	1.38E-04
GO:0030163~protein catabolic process	68	5.20E-08	1.40E-04
GO:0019941~modification-dependent protein catabolic process	59	1.61E-07	4.36E-04
GO:0010604~positive regulation of macromolecule metabolic process	52	1.79E-07	4.84E-04
GO:0043632~modification-dependent macromolecule catabolic process	59	2.03E-07	5.49E-04
GO:0016071~mRNA metabolic process	71	2.12E-07	5.72E-04
GO:0007143~female meiosis	30	2.18E-07	5.89E-04
GO:0031175~neuron projection development	87	2.26E-07	6.10E-04
GO:0044257~cellular protein catabolic process	62	2.52E-07	6.81E-04
GO:0051603~proteolysis involved in cellular protein catabolic process	62	2.52E-07	6.81E-04

GO:0045935~positive regulation of nucleobase, nucleoside, nucleotide and nucleic acid metabolic process	46	3.00E-07	8.10E-04
GO:0051173~positive regulation of nitrogen compound metabolic process	46	3.00E-07	8.10E-04
GO:0065004~protein-DNA complex assembly	25	3.60E-07	9.72E-04
GO:0000904~cell morphogenesis involved in differentiation	90	3.71E-07	0.00100
GO:0048812~neuron projection morphogenesis	86	3.93E-07	0.00106
GO:0006357~regulation of transcription from RNA polymerase II promoter	63	7.08E-07	0.00191
GO:0044087~regulation of cellular component biogenesis	34	7.63E-07	0.00206
GO:0009968~negative regulation of signal transduction	40	8.11E-07	0.00219
GO:0007281~germ cell development	75	8.08E-07	0.00218
GO:0010557~positive regulation of macromolecule biosynthetic process	47	9.03E-07	0.00244
GO:0031328~positive regulation of cellular biosynthetic process	53	9.89E-07	0.00267
GO:0009891~positive regulation of biosynthetic process	53	9.89E-07	0.00267
GO:0048667~cell morphogenesis involved in neuron differentiation	85	1.10E-06	0.00295
GO:0010648~negative regulation of cell communication	40	1.08E-06	0.00293
GO:0032504~multicellular organism reproduction	190	1.16E-06	0.00313
GO:0048609~reproductive process in a multicellular organism	190	1.16E-06	0.00313
GO:0043067~regulation of programmed cell death	42	1.23E-06	0.00333
GO:0060284~regulation of cell development	47	1.49E-06	0.00400
GO:0007088~regulation of mitosis	22	1.95E-06	0.00524
GO:0051783~regulation of nuclear division	22	1.95E-06	0.00524
GO:0030261~chromosome condensation	18	1.97E-06	0.00532
GO:0007098~centrosome cycle	20	2.11E-06	0.00567
GO:0016044~membrane organization	91	2.17E-06	0.00584
GO:0010628~positive regulation of gene expression	43	2.19E-06	0.00591
GO:0007293~germarium-derived egg chamber formation	28	3.20E-06	0.00860
GO:0010629~negative regulation of gene expression	76	3.46E-06	0.00930
GO:0010941~regulation of cell death	42	3.53E-06	0.00949
GO:0030030~cell projection organization	100	4.57E-06	0.01227
GO:0045941~positive regulation of transcription	42	4.53E-06	0.01218
GO:0031023~microtubule organizing center organization	23	4.51E-06	0.01211
GO:0006397~mRNA processing	61	5.16E-06	0.01384
GO:0007444~imaginal disc development	110	5.22E-06	0.01400
GO:0007163~establishment or maintenance of cell polarity	40	5.50E-06	0.01475
GO:0051254~positive regulation of RNA metabolic process	35	5.57E-06	0.01495
GO:0051960~regulation of nervous system development	35	5.57E-06	0.01495
GO:0012501~programmed cell death	51	5.73E-06	0.01537
GO:0006403~RNA localization	44	5.96E-06	0.01599
GO:0008356~asymmetric cell division	26	6.51E-06	0.01743
GO:0008219~cell death	53	6.73E-06	0.01803

GO:0034613~cellular protein localization	57	7.22E-06	0.01932
GO:0070271~protein complex biogenesis	54	7.97E-06	0.02131
GO:0006461~protein complex assembly	54	7.97E-06	0.02131
GO:0016265~death	53	8.21E-06	0.02193
GO:0009798~axis specification	62	8.44E-06	0.02254
GO:0006644~phospholipid metabolic process	33	8.52E-06	0.02276
GO:0045893~positive regulation of transcription, DNA-dependent	34	9.17E-06	0.02447
GO:0022604~regulation of cell morphogenesis	42	9.35E-06	0.02495
GO:0007062~sister chromatid cohesion	12	1.03E-05	0.02733
GO:0035220~wing disc development	80	1.05E-05	0.02801
GO:0051129~negative regulation of cellular component organization	25	1.12E-05	0.02979
GO:0048469~cell maturation	44	1.18E-05	0.03140
GO:0051252~regulation of RNA metabolic process	164	1.30E-05	0.03443
GO:0019637~organophosphate metabolic process	36	1.33E-05	0.03539
GO:0042981~regulation of apoptosis	36	1.33E-05	0.03539
GO:0051297~centrosome organization	21	1.38E-05	0.03660
GO:0030707~ovarian follicle cell development	62	1.41E-05	0.03736
GO:0006277~DNA amplification	13	1.46E-05	0.03873
GO:0045132~meiotic chromosome segregation	25	1.61E-05	0.04256
GO:0006333~chromatin assembly or disassembly	25	1.61E-05	0.04256
Cellular compartment			
GO:0005694~chromosome	134	1.96E-24	1.05E-21
GO:0044427~chromosomal part	107	2.02E-19	1.09E-16
GO:0005654~nucleoplasm	106	1.67E-15	8.98E-13
GO:0044451~nucleoplasm part	95	1.35E-13	7.28E-11
GO:0005819~spindle	40	2.53E-12	1.37E-09
GO:0012505~endomembrane system	81	4.65E-10	2.51E-07
GO:0031981~nuclear lumen	123	1.04E-09	5.63E-07
GO:0031974~membrane-enclosed lumen	163	9.66E-09	5.21E-06
GO:0043232~intracellular non-membrane-bounded organelle	245	1.17E-08	6.32E-06
GO:0043228~non-membrane-bounded organelle	245	1.17E-08	6.32E-06
GO:0043233~organelle lumen	158	2.48E-08	1.34E-05
GO:0070013~intracellular organelle lumen	158	2.48E-08	1.34E-05
GO:0005635~nuclear envelope	40	2.32E-08	1.25E-05
GO:0000775~chromosome, centromeric region	27	1.83E-07	9.88E-05
GO:0005700~polytene chromosome	40	2.17E-07	1.17E-04
GO:0000228~nuclear chromosome	35	4.10E-07	2.21E-04
GO:0044454~nuclear chromosome part	32	8.40E-07	4.53E-04
GO:0032993~protein-DNA complex	22	1.34E-06	7.21E-04
GO:0000785~chromatin	44	1.86E-06	0.00100
GO:0005813~centrosome	26	2.12E-06	0.00114
GO:0005876~spindle microtubule	14	3.88E-06	0.00209
GO:0005815~microtubule organizing center	28	4.15E-06	0.00224

GO:0000922~spindle pole	15	1.23E-05	0.00663
GO:0000932~cytoplasmic mRNA processing body	9	1.36E-05	0.00730
GO:0005656~pre-replicative complex	9	1.36E-05	0.00730
GO:0015630~microtubule cytoskeleton	69	1.45E-05	0.00779
GO:0005856~cytoskeleton	98	4.34E-05	0.02312
GO:0016585~chromatin remodeling complex	19	4.74E-05	0.02520
GO:0005938~cell cortex	30	6.34E-05	0.03358
GO:0000776~kinetochore	16	8.36E-05	0.04407
GO:0046930~pore complex	22	8.14E-05	0.04295
GO:0005643~nuclear pore	21	9.18E-05	0.04826
Molecular function			
GO:0000166~nucleotide binding	341	5.41E-18	5.94E-15
GO:0032553~ribonucleotide binding	274	2.95E-17	3.24E-14
GO:0032555~purine ribonucleotide binding	274	2.95E-17	3.24E-14
GO:0017076~purine nucleotide binding	282	6.42E-15	7.07E-12
GO:0003677~DNA binding	244	1.74E-14	1.91E-11
GO:0008270~zinc ion binding	287	4.96E-14	5.44E-11
GO:0005524~ATP binding	221	2.35E-13	2.58E-10
GO:0032559~adenyl ribonucleotide binding	221	3.08E-13	3.38E-10
GO:0001883~purine nucleoside binding	231	9.20E-12	1.01E-08
GO:0001882~nucleoside binding	231	2.33E-11	2.56E-08
GO:0030554~adenyl nucleotide binding	228	2.76E-11	3.03E-08
GO:0004386~helicase activity	51	1.07E-10	1.17E-07
GO:0019899~enzyme binding	34	1.14E-08	1.25E-05
GO:0003729~mRNA binding	68	2.38E-08	2.61E-05
GO:0046914~transition metal ion binding	323	7.25E-07	7.96E-04
GO:0008026~ATP-dependent helicase activity	34	1.59E-06	0.00174
GO:0070035~purine NTP-dependent helicase activity	34	1.59E-06	0.00174
GO:0015631~tubulin binding	30	5.58E-06	0.00611
GO:0008094~DNA-dependent ATPase activity	20	5.41E-06	0.00592
GO:0003678~DNA helicase activity	21	8.99E-06	0.00982
GO:0016251~general RNA polymerase II transcription factor activity	35	1.64E-05	0.01783
GO:0008017~microtubule binding	27	3.39E-05	0.03655
GO:0046872~metal ion binding	385	4.03E-05	0.04332
KEGG pathway			
dme04120:Ubiquitin mediated proteolysis	42	4.07E-06	4.11E-04
dme03040:Spliceosome	44	3.35E-05	0.00338192
dme03030:DNA replication	19	7.19E-05	0.00723181
dme04144:Endocytosis	33	1.77E-04	0.01771768
dme04914:Progesterone-mediated oocyte maturation	20	4.39E-04	0.04337785

Table B2. Oocyte DAVID analysis, transcripts ≥3-fold higher in control than *wisp*

Term	Count	*P*-value	Bonferroni
Biological process			
GO:0007049~cell cycle	172	1.23E-22	2.84E-19
GO:0051276~chromosome organization	117	8.61E-21	9.89E-18
GO:0022402~cell cycle process	150	2.59E-20	1.98E-17
GO:0022403~cell cycle phase	131	7.43E-18	4.27E-15
GO:0000279~M phase	124	3.16E-17	1.45E-14
GO:0000087~M phase of mitotic cell cycle	67	4.98E-16	1.70E-13
GO:0007067~mitosis	66	5.61E-16	1.82E-13
GO:0000280~nuclear division	66	2.47E-15	7.02E-13
GO:0048285~organelle fission	68	3.70E-15	9.35E-13
GO:0006259~DNA metabolic process	84	5.28E-15	1.22E-12
GO:0000278~mitotic cell cycle	119	5.44E-15	1.14E-12
GO:0010605~negative regulation of macromolecule metabolic process	83	7.87E-12	1.51E-09
GO:0007059~chromosome segregation	53	9.97E-11	1.76E-08
GO:0051726~regulation of cell cycle	62	5.82E-10	9.55E-08
GO:0006260~DNA replication	43	1.38E-09	2.12E-07
GO:0051301~cell division	71	1.45E-09	2.08E-07
GO:0048610~reproductive cellular process	117	7.84E-09	1.06E-06
GO:0006325~chromatin organization	62	1.40E-08	1.79E-06
GO:0006974~response to DNA damage stimulus	44	2.39E-08	2.89E-06
GO:0065004~protein-DNA complex assembly	24	2.71E-08	3.12E-06
GO:0019953~sexual reproduction	147	2.85E-08	3.11E-06
GO:0051327~M phase of meiotic cell cycle	43	2.99E-08	3.13E-06
GO:0007126~meiosis	43	2.99E-08	3.13E-06
GO:0051321~meiotic cell cycle	44	4.15E-08	4.14E-06
GO:0000226~microtubule cytoskeleton organization	87	5.80E-08	5.56E-06
GO:0048477~oogenesis	118	7.58E-08	6.97E-06
GO:0010558~negative regulation of macromolecule biosynthetic process	56	9.57E-08	8.46E-06
GO:0031327~negative regulation of cellular biosynthetic process	56	9.57E-08	8.46E-06
GO:0009890~negative regulation of biosynthetic process	56	9.57E-08	8.46E-06
GO:0010629~negative regulation of gene expression	61	1.33E-07	1.13E-05
GO:0000070~mitotic sister chromatid segregation	27	1.58E-07	1.30E-05
GO:0007276~gamete generation	142	1.61E-07	1.27E-05
GO:0007292~female gamete generation	118	1.92E-07	1.47E-05
GO:0007017~microtubule-based process	103	2.18E-07	1.62E-05
GO:0032504~multicellular organism reproduction	144	2.33E-07	1.67E-05
GO:0048609~reproductive process in a multicellular organism	144	2.33E-07	1.67E-05
GO:0007346~regulation of mitotic cell cycle	37	3.50E-07	2.44E-05
GO:0000819~sister chromatid segregation	27	3.51E-07	2.37E-05

GO:0006281~DNA repair	39	3.81E-07	2.50E-05
GO:0051172~negative regulation of nitrogen compound metabolic process	50	6.45E-07	4.12E-05
GO:0045934~negative regulation of nucleobase, nucleoside, nucleotide and nucleic acid metabolic process	50	6.45E-07	4.12E-05
GO:0006323~DNA packaging	30	8.54E-07	5.30E-05
GO:0007051~spindle organization	67	9.31E-07	5.63E-05
GO:0051253~negative regulation of RNA metabolic process	43	1.02E-06	5.99E-05
GO:0045449~regulation of transcription	154	1.21E-06	6.94E-05
GO:0045892~negative regulation of transcription, DNA-dependent	41	1.66E-06	9.30E-05
GO:0003006~reproductive developmental process	109	1.78E-06	9.72E-05
GO:0051252~regulation of RNA metabolic process	131	2.44E-06	1.30E-04
GO:0009798~axis specification	51	4.82E-06	2.52E-04
GO:0006261~DNA-dependent DNA replication	27	5.49E-06	2.80E-04
GO:0045132~meiotic chromosome segregation	23	6.09E-06	3.04E-04
GO:0007143~female meiosis	25	8.25E-06	4.03E-04
GO:0007281~germ cell development	60	9.37E-06	4.49E-04
GO:0007052~mitotic spindle organization	58	1.13E-05	5.30E-04
GO:0016481~negative regulation of transcription	43	1.19E-05	5.48E-04
GO:0003002~regionalization	86	1.62E-05	7.27E-04
GO:0031328~positive regulation of cellular biosynthetic process	44	1.92E-05	8.50E-04
GO:0009891~positive regulation of biosynthetic process	44	1.92E-05	8.50E-04
GO:0007010~cytoskeleton organization	116	2.03E-05	8.79E-04
GO:0009994~oocyte differentiation	39	2.21E-05	9.39E-04
GO:0006350~transcription	99	2.24E-05	9.36E-04
GO:0006333~chromatin assembly or disassembly	23	2.32E-05	9.53E-04
GO:0010564~regulation of cell cycle process	29	3.06E-05	0.00123
GO:0006403~RNA localization	36	3.15E-05	0.00125
GO:0016071~mRNA metabolic process	57	3.38E-05	0.00132
GO:0010604~positive regulation of macromolecule metabolic process	44	3.82E-05	0.00146
GO:0034621~cellular macromolecular complex subunit organization	57	4.45E-05	0.00167
GO:0008356~asymmetric cell division	25	4.75E-05	0.00176
GO:0032989~cellular component morphogenesis	111	5.38E-05	0.00196
GO:0007389~pattern specification process	90	5.42E-05	0.00195
GO:0033043~regulation of organelle organization	38	5.97E-05	0.00211
GO:0033554~cellular response to stress	53	6.59E-05	0.00229
GO:0034728~nucleosome organization	17	6.97E-05	0.00239
GO:0043933~macromolecular complex subunit organization	72	7.30E-05	0.00246
GO:0000904~cell morphogenesis involved in differentiation	71	9.07E-05	0.00302
GO:0006397~mRNA processing	49	9.71E-05	0.00318
GO:0006270~DNA replication initiation	12	1.02E-04	0.00329
GO:0006277~DNA amplification	12	1.02E-04	0.00329

GO:0016458~gene silencing	34	1.12E-04	0.00357
GO:0016568~chromatin modification	39	1.30E-04	0.00410
GO:0046822~regulation of nucleocytoplasmic transport	16	1.72E-04	0.00534
GO:0048666~neuron development	79	1.95E-04	0.00597
GO:0007293~germarium-derived egg chamber formation	23	2.12E-04	0.00638
GO:0031023~microtubule organizing center organization	20	2.59E-04	0.00769
GO:0034622~cellular macromolecular complex assembly	46	2.59E-04	0.00761
GO:0048812~neuron projection morphogenesis	66	2.64E-04	0.00764
GO:0006357~regulation of transcription from RNA polymerase II promoter	47	2.68E-04	0.00768
GO:0009948~anterior/posterior axis specification	36	2.72E-04	0.00769
GO:0006275~regulation of DNA replication	10	2.77E-04	0.00774
GO:0007098~centrosome cycle	17	2.80E-04	0.00773
GO:0007062~sister chromatid cohesion	11	2.95E-04	0.00804
GO:0010557~positive regulation of macromolecule biosynthetic process	38	3.13E-04	0.00843
GO:0031175~neuron projection development	66	3.24E-04	0.00863
GO:0048024~regulation of nuclear mRNA splicing, via spliceosome	23	3.40E-04	0.00893
GO:0050684~regulation of mRNA processing	23	3.40E-04	0.00893
GO:0032386~regulation of intracellular transport	16	3.43E-04	0.00893
GO:0048469~cell maturation	35	3.48E-04	0.00894
GO:0048667~cell morphogenesis involved in neuron differentiation	66	3.97E-04	0.01009
GO:0000122~negative regulation of transcription from RNA polymerase II promoter	18	4.10E-04	0.01030
GO:0048599~oocyte development	33	4.10E-04	0.01020
GO:0043484~regulation of RNA splicing	24	4.13E-04	0.01016
GO:0033157~regulation of intracellular protein transport	15	4.17E-04	0.01015
GO:0042306~regulation of protein import into nucleus	15	4.17E-04	0.01015
GO:0007127~meiosis I	15	4.17E-04	0.01015
GO:0030030~cell projection organization	77	4.22E-04	0.01015
GO:0006355~regulation of transcription, DNA-dependent	107	4.63E-04	0.01104
GO:0065003~macromolecular complex assembly	61	4.99E-04	0.01175
GO:0051173~positive regulation of nitrogen compound metabolic process	36	5.08E-04	0.01184
GO:0045935~positive regulation of nucleobase, nucleoside, nucleotide and nucleic acid metabolic process	36	5.08E-04	0.01184
GO:0030261~chromosome condensation	17	5.14E-04	0.01186
GO:0007088~regulation of mitosis	17	5.14E-04	0.01186
GO:0051783~regulation of nuclear division	17	5.14E-04	0.01186
GO:0048858~cell projection morphogenesis	68	5.75E-04	0.01314
GO:0009952~anterior/posterior pattern formation	39	5.90E-04	0.01335
GO:0030707~ovarian follicle cell development	49	5.93E-04	0.01326
GO:0000075~cell cycle checkpoint	13	5.95E-04	0.01318

GO:0000578~embryonic axis specification	34	6.08E-04	0.01334
GO:0021700~developmental maturation	36	6.82E-04	0.01483
GO:0007140~male meiosis	12	6.90E-04	0.01486
GO:0006334~nucleosome assembly	12	6.90E-04	0.01486
GO:0051297~centrosome organization	18	7.06E-04	0.01505
GO:0008298~intracellular mRNA localization	20	7.12E-04	0.01505
GO:0007308~oocyte construction	32	7.24E-04	0.01516
GO:0008595~determination of anterior/posterior axis, embryo	33	7.75E-04	0.01606
GO:0007351~tripartite regional subdivision	33	7.75E-04	0.01606
GO:0051052~regulation of DNA metabolic process	11	7.78E-04	0.01599
GO:0032990~cell part morphogenesis	69	8.21E-04	0.01672
GO:0007307~eggshell chorion gene amplification	10	8.38E-04	0.01690
GO:0030182~neuron differentiation	88	9.02E-04	0.01803
GO:0007350~blastoderm segmentation	46	9.12E-04	0.01807
GO:0008380~RNA splicing	34	0.00110	0.02158
GO:0051225~spindle assembly	16	0.00113	0.02206
GO:0035282~segmentation	48	0.00117	0.02246
GO:0009880~embryonic pattern specification	48	0.00117	0.02246
GO:0060341~regulation of cellular localization	24	0.00136	0.02599
GO:0070201~regulation of establishment of protein localization	15	0.00144	0.02713
GO:0051223~regulation of protein transport	15	0.00144	0.02713
GO:0009953~dorsal/ventral pattern formation	34	0.00146	0.02732
GO:0000375~RNA splicing, via transesterification reactions	29	0.00151	0.02803
GO:0000902~cell morphogenesis	94	0.00159	0.02923
GO:0007309~oocyte axis specification	30	0.00160	0.02931
GO:0031497~chromatin assembly	14	0.00181	0.03278
GO:0010628~positive regulation of gene expression	33	0.00185	0.03313
GO:0051248~negative regulation of protein metabolic process	16	0.00191	0.03403
GO:0006267~pre-replicative complex assembly	7	0.00231	0.04066
GO:0048134~germ-line cyst formation	9	0.00232	0.04060
GO:0000398~nuclear mRNA splicing, via spliceosome	28	0.00260	0.04502
GO:0000377~RNA splicing, via transesterification reactions with bulged adenosine as nucleophile	28	0.00260	0.04502
Cellular compartment			
GO:0005694~chromosome	111	9.68E-22	4.54E-19
GO:0044427~chromosomal part	91	2.21E-18	1.04E-15
GO:0005654~nucleoplasm	82	6.55E-10	3.07E-07
GO:0044451~nucleoplasm part	71	1.95E-08	9.13E-06
GO:0043228~non-membrane-bounded organelle	193	3.52E-08	1.65E-05
GO:0043232~intracellular non-membrane-bounded organelle	193	3.52E-08	1.65E-05
GO:0000785~chromatin	39	4.47E-08	2.10E-05
GO:0031981~nuclear lumen	93	1.34E-06	6.28E-04
GO:0000228~nuclear chromosome	29	1.42E-06	6.66E-04

GO:0032993~protein-DNA complex	19	8.77E-06	0.00410
GO:0044454~nuclear chromosome part	26	9.41E-06	0.00440
GO:0000775~chromosome, centromeric region	23	9.53E-06	0.00446
GO:0005700~polytene chromosome	31	3.49E-05	0.01625
Molecular function			
GO:0003677~DNA binding	196	3.71E-17	3.16E-14
GO:0008270~zinc ion binding	220	2.75E-11	2.35E-08
GO:0003682~chromatin binding	29	8.92E-08	7.61E-05
GO:0046914~transition metal ion binding	241	1.41E-06	0.00120
GO:0043169~cation binding	288	1.72E-05	0.01457
GO:0003702~RNA polymerase II transcription factor activity	57	1.80E-05	0.01529
GO:0046872~metal ion binding	283	1.87E-05	0.01581
GO:0043167~ion binding	288	2.10E-05	0.01778
KEGG pathway			
dme04120:Ubiquitin mediated proteolysis	36	1.57E-07	1.38E-05
dme04914:Progesterone-mediated oocyte maturation	17	1.16E-04	0.01015
dme03030:DNA replication	15	1.25E-04	0.01092

Table B3. Oocyte DAVID analysis, total RNA transcripts downregulated in *wisp*

Term	Count	P-value	Bonferroni
Biological process			
GO:0006260~DNA replication	18	1.00E-09	1.26E-06
GO:0006261~DNA-dependent DNA replication	14	3.93E-09	4.95E-06
GO:0006259~DNA metabolic process	24	4.93E-08	6.20E-05
GO:0006270~DNA replication initiation	8	6.69E-08	8.41E-05
GO:0007059~chromosome segregation	16	8.34E-07	0.00105
GO:0051276~chromosome organization	25	1.09E-06	0.00137
GO:0030261~chromosome condensation	8	1.48E-05	0.01839
GO:0007049~cell cycle	37	1.75E-05	0.02183
GO:0006267~pre-replicative complex assembly	5	1.99E-05	0.02469
GO:0034984~cellular response to DNA damage stimulus	12	2.31E-05	0.02859
Cellular compartment			
GO:0044451~nucleoplasm part	25	3.63E-07	9.43E-05
GO:0005654~nucleoplasm	26	6.16E-07	1.60E-04
GO:0032993~protein-DNA complex	10	2.43E-06	6.32E-04
GO:0005656~pre-replicative complex	6	3.44E-06	8.94E-04
GO:0031974~membrane-enclosed lumen	39	4.52E-06	0.00117
GO:0044427~chromosomal part	23	6.27E-06	0.00163
GO:0070013~intracellular organelle lumen	38	6.29E-06	0.00163
GO:0043233~organelle lumen	38	6.29E-06	0.00163
GO:0005694~chromosome	26	7.75E-06	0.00201
GO:0031981~nuclear lumen	29	2.38E-05	0.00618
Molecular function			
GO:0001882~nucleoside binding	57	1.96E-09	7.84E-07
GO:0030554~adenyl nucleotide binding	55	8.97E-09	3.59E-06
GO:0001883~purine nucleoside binding	55	1.11E-08	4.45E-06
GO:0005524~ATP binding	50	8.41E-08	3.36E-05
GO:0032559~adenyl ribonucleotide binding	50	9.14E-08	3.66E-05
GO:0003677~DNA binding	53	1.32E-07	5.28E-05
GO:0017076~purine nucleotide binding	58	4.93E-07	1.97E-04
GO:0000166~nucleotide binding	66	7.03E-07	2.81E-04
GO:0032555~purine ribonucleotide binding	53	3.59E-06	0.00143
GO:0032553~ribonucleotide binding	53	3.59E-06	0.00143
KEGG pathway			
dme03030:DNA replication	9	7.08E-05	0.00459

Table B4. Embryo DAVID analysis, transcripts ≥2-fold higher in control than *wisp*

Term	Count	*P* value	Bonferroni
Biological process			
GO:0008104~protein localization	226	8.11E-33	2.57E-29
GO:0051276~chromosome organization	167	4.89E-26	1.55E-22
GO:0045184~establishment of protein localization	161	3.84E-22	1.22E-18
GO:0015031~protein transport	156	4.42E-21	1.40E-17
GO:0046907~intracellular transport	164	3.55E-18	1.13E-14
GO:0007242~intracellular signaling cascade	156	1.89E-17	5.97E-14
GO:0007010~cytoskeleton organization	219	5.97E-17	3.52E-13
GO:0006259~DNA metabolic process	123	3.23E-16	1.06E-12
GO:0051301~cell division	116	4.33E-16	1.41E-12
GO:0016192~vesicle-mediated transport	189	7.46E-16	2.46E-12
GO:0006325~chromatin organization	99	6.82E-15	2.15E-11
GO:0007059~chromosome segregation	75	1.83E-14	5.81E-11
GO:0007264~small GTPase mediated signal transduction	71	3.03E-14	9.60E-11
GO:0043933~macromolecular complex subunit organization	142	5.50E-14	1.74E-10
GO:0051726~regulation of cell cycle	95	1.10E-13	3.48E-10
GO:0000902~cell morphogenesis	200	3.86E-13	1.22E-09
GO:0016568~chromatin modification	70	9.05E-13	2.87E-09
GO:0000278~mitotic cell cycle	168	9.11E-13	2.89E-09
GO:0007049~cell cycle	260	1.37E-12	4.34E-09
GO:0030182~neuron differentiation	186	1.67E-12	5.28E-09
GO:0032989~cellular component morphogenesis	225	1.93E-12	6.12E-09
GO:0051656~establishment of organelle localization	52	3.76E-12	1.19E-08
GO:0051640~organelle localization	55	6.23E-12	1.98E-08
GO:0016044~membrane organization	151	6.53E-12	2.07E-08
GO:0006260~DNA replication	61	1.17E-11	3.71E-08
GO:0048285~organelle fission	85	2.13E-11	6.75E-08
GO:0033554~cellular response to stress	94	3.18E-11	1.01E-07
GO:0044087~regulation of cellular component biogenesis	53	3.24E-11	1.03E-07
GO:0033043~regulation of organelle organization	66	3.30E-11	1.05E-07
GO:0048610~reproductive cellular process	214	3.96E-11	1.26E-07
GO:0048666~neuron development	159	4.15E-11	1.31E-07
GO:0000087~M phase of mitotic cell cycle	82	6.03E-11	1.91E-07
GO:0034621~cellular macromolecular complex subunit organization	104	6.58E-11	2.08E-07
GO:0007067~mitosis	81	7.33E-11	2.32E-07
GO:0006350~transcription	198	1.05E-10	3.33E-07
GO:0065003~macromolecular complex assembly	120	1.15E-10	3.65E-07
GO:0060284~regulation of cell development	74	1.77E-10	5.60E-07
GO:0000280~nuclear division	81	1.80E-10	5.70E-07
GO:0006396~RNA processing	144	2.06E-10	6.53E-07

GO:0006468~protein amino acid phosphorylation	124	2.51E-10	7.96E-07
GO:0051960~regulation of nervous system development	56	2.94E-10	9.33E-07
GO:0070727~cellular macromolecule localization	118	3.31E-10	1.05E-06
GO:0032940~secretion by cell	68	3.34E-10	1.06E-06
GO:0007163~establishment or maintenance of cell polarity	64	4.14E-10	1.31E-06
GO:0030029~actin filament-based process	78	7.78E-10	2.46E-06
GO:0048477~oogenesis	222	1.16E-09	3.67E-06
GO:0030036~actin cytoskeleton organization	77	1.45E-09	4.60E-06
GO:0022604~regulation of cell morphogenesis	67	1.73E-09	5.49E-06
GO:0006796~phosphate metabolic process	225	2.19E-09	6.94E-06
GO:0006793~phosphorus metabolic process	225	2.19E-09	6.94E-06
GO:0003001~generation of a signal involved in cell-cell signaling	60	2.40E-09	7.62E-06
GO:0040008~regulation of growth	60	2.40E-09	7.62E-06
GO:0006974~response to DNA damage stimulus	65	2.54E-09	8.04E-06
GO:0007292~female gamete generation	223	2.56E-09	8.12E-06
GO:0060429~epithelium development	112	2.84E-09	9.00E-06
GO:0046903~secretion	69	2.95E-09	9.36E-06
GO:0000904~cell morphogenesis involved in differentiation	137	3.18E-09	1.01E-05
GO:0031175~neuron projection development	131	3.56E-09	1.13E-05
GO:0048489~synaptic vesicle transport	54	4.09E-09	1.30E-05
GO:0007269~neurotransmitter secretion	59	4.79E-09	1.52E-05
GO:0003006~reproductive developmental process	208	5.12E-09	1.62E-05
GO:0006261~DNA-dependent DNA replication	39	5.15E-09	1.63E-05
GO:0048812~neuron projection morphogenesis	130	5.66E-09	1.79E-05
GO:0000226~microtubule cytoskeleton organization	134	7.40E-09	2.34E-05
GO:0045449~regulation of transcription	306	7.52E-09	2.38E-05
GO:0048667~cell morphogenesis involved in neuron differentiation	130	9.58E-09	3.03E-05
GO:0006897~endocytosis	119	9.62E-09	3.05E-05
GO:0010324~membrane invagination	119	9.62E-09	3.05E-05
GO:0006928~cell motion	136	1.08E-08	3.42E-05
GO:0034613~cellular protein localization	89	1.20E-08	3.79E-05
GO:0006281~DNA repair	58	1.54E-08	4.89E-05
GO:0022402~cell cycle process	220	1.57E-08	4.97E-05
GO:0007143~female meiosis	41	1.69E-08	5.35E-05
GO:0002009~morphogenesis of an epithelium	106	1.72E-08	5.46E-05
GO:0007346~regulation of mitotic cell cycle	56	2.25E-08	7.13E-05
GO:0012501~programmed cell death	78	2.73E-08	8.66E-05
GO:0044265~cellular macromolecule catabolic process	105	3.75E-08	1.19E-04
GO:0007243~protein kinase cascade	39	4.26E-08	1.35E-04
GO:0008219~cell death	81	4.31E-08	1.36E-04
GO:0016265~death	81	6.07E-08	1.92E-04
GO:0007017~microtubule-based process	169	6.23E-08	1.98E-04
GO:0016071~mRNA metabolic process	102	6.80E-08	2.15E-04

GO:0006886~intracellular protein transport	85	7.31E-08	2.32E-04
GO:0007276~gamete generation	273	7.93E-08	2.51E-04
GO:0032535~regulation of cellular component size	55	1.11E-07	3.52E-04
GO:0034622~cellular macromolecular complex assembly	81	1.18E-07	3.75E-04
GO:0019953~sexual reproduction	278	1.60E-07	5.05E-04
GO:0007391~dorsal closure	53	1.64E-07	5.19E-04
GO:0001505~regulation of neurotransmitter levels	59	1.84E-07	5.83E-04
GO:0008360~regulation of cell shape	54	2.11E-07	6.69E-04
GO:0007267~cell-cell signaling	97	3.17E-07	0.00100
GO:0048729~tissue morphogenesis	110	3.47E-07	0.00110
GO:0008283~cell proliferation	65	3.81E-07	0.00121
GO:0009968~negative regulation of signal transduction	55	4.09E-07	0.00129
GO:0016569~covalent chromatin modification	35	5.11E-07	0.00162
GO:0016570~histone modification	35	5.11E-07	0.00162
GO:0070271~protein complex biogenesis	80	5.14E-07	0.00163
GO:0006461~protein complex assembly	80	5.14E-07	0.00163
GO:0010648~negative regulation of cell communication	55	6.17E-07	0.00195
GO:0010605~negative regulation of macromolecule metabolic process	134	6.23E-07	0.00197
GO:0006357~regulation of transcription from RNA polymerase II promoter	89	6.64E-07	0.00210
GO:0010608~posttranscriptional regulation of gene expression	64	6.70E-07	0.00212
GO:0016333~morphogenesis of follicular epithelium	22	7.20E-07	0.00228
GO:0043067~regulation of programmed cell death	58	7.43E-07	0.00235
GO:0010604~positive regulation of macromolecule metabolic process	70	7.86E-07	0.00249
GO:0008356~asymmetric cell division	36	7.97E-07	0.00252
GO:0000819~sister chromatid segregation	31	8.96E-07	0.00283
GO:0019226~transmission of nerve impulse	90	9.47E-07	0.00300
GO:0007293~germarium-derived egg chamber formation	38	1.00E-06	0.00316
GO:0007444~imaginal disc development	166	1.02E-06	0.00322
GO:0048813~dendrite morphogenesis	60	1.05E-06	0.00332
GO:0016358~dendrite development	60	1.05E-06	0.00332
GO:0016477~cell migration	82	1.13E-06	0.00357
GO:0016331~morphogenesis of embryonic epithelium	61	1.23E-06	0.00389
GO:0007268~synaptic transmission	87	1.29E-06	0.00409
GO:0009886~post-embryonic morphogenesis	145	1.51E-06	0.00476
GO:0030030~cell projection organization	149	1.62E-06	0.00514
GO:0006836~neurotransmitter transport	63	1.65E-06	0.00522
GO:0007281~germ cell development	106	1.92E-06	0.00607
GO:0051674~localization of cell	89	1.96E-06	0.00618
GO:0000070~mitotic sister chromatid segregation	30	1.98E-06	0.00627
GO:0009057~macromolecule catabolic process	118	2.00E-06	0.00632

GO:0007167~enzyme linked receptor protein signaling pathway	70	2.06E-06	0.00649
GO:0000165~MAPKKK cascade	29	2.27E-06	0.00718
GO:0050767~regulation of neurogenesis	39	2.37E-06	0.00748
GO:0035220~wing disc development	119	2.56E-06	0.00808
GO:0017145~stem cell division	32	2.73E-06	0.00863
GO:0009994~oocyte differentiation	67	2.74E-06	0.00866
GO:0006403~RNA localization	62	2.84E-06	0.00895
GO:0006323~DNA packaging	38	2.85E-06	0.00900
GO:0043087~regulation of GTPase activity	27	2.92E-06	0.00922
GO:0010941~regulation of cell death	58	3.22E-06	0.01016
GO:0048870~cell motility	85	3.26E-06	0.01027
GO:0051129~negative regulation of cellular component organization	34	3.47E-06	0.01092
GO:0048858~cell projection morphogenesis	132	3.63E-06	0.01143
GO:0007098~centrosome cycle	25	3.63E-06	0.01144
GO:0030707~ovarian follicle cell development	91	3.70E-06	0.01165
GO:0060341~regulation of cellular localization	39	3.86E-06	0.01217
GO:0016321~female meiosis chromosome segregation	24	3.98E-06	0.01253
GO:0045664~regulation of neuron differentiation	33	4.12E-06	0.01297
GO:0045935~positive regulation of nucleobase, nucleoside, nucleotide and nucleic acid metabolic process	60	4.25E-06	0.01339
GO:0051173~positive regulation of nitrogen compound metabolic process	60	4.25E-06	0.01339
GO:0031047~gene silencing by RNA	29	4.34E-06	0.01366
GO:0007015~actin filament organization	45	4.56E-06	0.01436
GO:0051130~positive regulation of cellular component organization	20	4.78E-06	0.01503
GO:0006397~mRNA processing	87	4.80E-06	0.01509
GO:0021700~developmental maturation	65	5.60E-06	0.01758
GO:0032990~cell part morphogenesis	135	5.62E-06	0.01764
GO:0051236~establishment of RNA localization	37	5.65E-06	0.01774
GO:0006605~protein targeting	55	5.92E-06	0.01859
GO:0045132~meiotic chromosome segregation	34	5.93E-06	0.01862
GO:0051056~regulation of small GTPase mediated signal transduction	49	6.73E-06	0.02110
GO:0010564~regulation of cell cycle process	45	6.89E-06	0.02161
GO:0006644~phospholipid metabolic process	45	6.89E-06	0.02161
GO:0048707~instar larval or pupal morphogenesis	140	7.29E-06	0.02282
GO:0042981~regulation of apoptosis	50	7.98E-06	0.02498
GO:0019637~organophosphate metabolic process	50	7.98E-06	0.02498
GO:0006915~apoptosis	42	8.31E-06	0.02599
GO:0032318~regulation of Ras GTPase activity	24	8.39E-06	0.02625
GO:0016310~phosphorylation	166	9.06E-06	0.02832
GO:0051225~spindle assembly	23	9.33E-06	0.02913

GO:0010629~negative regulation of gene expression	108	9.63E-06	0.03005
GO:0007051~spindle organization	97	1.00E-05	0.03126
GO:0000910~cytokinesis	43	1.03E-05	0.03214
GO:0050807~regulation of synapse organization	21	1.10E-05	0.03441
GO:0050657~nucleic acid transport	36	1.11E-05	0.03443
GO:0050658~RNA transport	36	1.11E-05	0.03443
GO:0051963~regulation of synaptogenesis	18	1.21E-05	0.03758
GO:0002165~instar larval or pupal development	163	1.23E-05	0.03819
GO:0022403~cell cycle phase	189	1.24E-05	0.03858
GO:0050803~regulation of synapse structure and activity	26	1.27E-05	0.03946
GO:0035194~posttranscriptional gene silencing by RNA	26	1.27E-05	0.03946
GO:0016441~posttranscriptional gene silencing	26	1.27E-05	0.03946
GO:0007409~axonogenesis	87	1.27E-05	0.03948
GO:0007552~metamorphosis	144	1.28E-05	0.03988
GO:0045995~regulation of embryonic development	32	1.44E-05	0.04451
GO:0007298~border follicle cell migration	37	1.45E-05	0.04477
GO:0032880~regulation of protein localization	25	1.47E-05	0.04541
GO:0006730~one-carbon metabolic process	41	1.54E-05	0.04768
Cellular compartment			
GO:0005694~chromosome	163	4.46E-17	2.77E-14
GO:0005654~nucleoplasm	145	5.42E-16	3.45E-13
GO:0031974~membrane-enclosed lumen	258	5.20E-14	3.23E-11
GO:0044427~chromosomal part	131	7.34E-14	4.56E-11
GO:0070013~intracellular organelle lumen	250	2.91E-13	1.81E-10
GO:0043233~organelle lumen	250	2.91E-13	1.81E-10
GO:0044451~nucleoplasm part	127	1.12E-12	6.93E-10
GO:0031981~nuclear lumen	184	2.19E-12	1.36E-09
GO:0043232~intracellular non-membrane-bounded organelle	378	4.76E-11	2.96E-08
GO:0043228~non-membrane-bounded organelle	378	4.76E-11	2.96E-08
GO:0005938~cell cortex	49	3.27E-09	2.03E-06
GO:0012505~endomembrane system	107	2.17E-08	1.35E-05
GO:0005700~polytene chromosome	53	2.90E-07	1.80E-04
GO:0005813~centrosome	35	3.15E-07	1.95E-04
GO:0005819~spindle	42	5.11E-07	3.17E-04
GO:0000785~chromatin	60	1.78E-06	0.00110
GO:0005856~cytoskeleton	150	1.87E-06	0.00116
GO:0005815~microtubule organizing center	37	3.00E-06	0.00186
GO:0005635~nuclear envelope	47	1.07E-05	0.00665
GO:0000775~chromosome, centromeric region	31	2.02E-05	0.01247
GO:0044454~nuclear chromosome part	39	2.63E-05	0.01618
GO:0005768~endosome	22	2.72E-05	0.01675
GO:0000228~nuclear chromosome	42	3.71E-05	0.02281
GO:0044430~cytoskeletal part	121	4.61E-05	0.02823

Molecular function			
GO:0032555~purine ribonucleotide binding	434	1.22E-26	1.77E-23
GO:0032553~ribonucleotide binding	434	1.22E-26	1.77E-23
GO:0000166~nucleotide binding	538	2.19E-26	3.18E-23
GO:0017076~purine nucleotide binding	455	1.95E-25	2.82E-22
GO:0032559~adenyl ribonucleotide binding	356	1.51E-22	2.20E-19
GO:0005524~ATP binding	354	3.87E-22	5.61E-19
GO:0001883~purine nucleoside binding	379	8.67E-22	1.26E-18
GO:0001882~nucleoside binding	381	1.36E-21	1.97E-18
GO:0030554~adenyl nucleotide binding	375	3.95E-21	5.73E-18
GO:0003677~DNA binding	351	1.64E-12	2.38E-09
GO:0004386~helicase activity	70	4.33E-12	6.29E-09
GO:0008270~zinc ion binding	417	9.76E-12	1.42E-08
GO:0070035~purine NTP-dependent helicase activity	51	2.10E-09	3.05E-06
GO:0008026~ATP-dependent helicase activity	51	2.10E-09	3.05E-06
GO:0019899~enzyme binding	45	3.17E-09	4.61E-06
GO:0003729~mRNA binding	96	1.05E-08	1.52E-05
GO:0008092~cytoskeletal protein binding	108	2.05E-08	2.98E-05
GO:0004672~protein kinase activity	132	5.15E-08	7.48E-05
GO:0060589~nucleoside-triphosphatase regulator activity	77	7.77E-08	1.13E-04
GO:0004674~protein serine/threonine kinase activity	100	1.04E-07	1.51E-04
GO:0030695~GTPase regulator activity	75	1.56E-07	2.27E-04
GO:0003779~actin binding	65	7.88E-07	0.00114
GO:0005096~GTPase activator activity	44	9.03E-07	0.00131
GO:0005083~small GTPase regulator activity	59	9.40E-07	0.00136
GO:0008134~transcription factor binding	50	2.53E-06	0.00366
GO:0015631~tubulin binding	40	7.15E-06	0.01032
GO:0003682~chromatin binding	38	9.51E-06	0.01370
GO:0004004~ATP-dependent RNA helicase activity	27	1.12E-05	0.01613
GO:0008186~RNA-dependent ATPase activity	27	1.12E-05	0.01613
GO:0030528~transcription regulator activity	264	1.38E-05	0.01988
GO:0008047~enzyme activator activity	49	1.53E-05	0.02194
GO:0008017~microtubule binding	37	1.79E-05	0.02565
GO:0042802~identical protein binding	70	2.49E-05	0.03552
GO:0016879~ligase activity, forming carbon-nitrogen bonds	68	2.59E-05	0.03686
GO:0016779~nucleotidyltransferase activity	48	2.63E-05	0.03748
GO:0004518~nuclease activity	50	2.75E-05	0.03908
GO:0035091~phosphoinositide binding	18	3.17E-05	0.04499
KEGG pathway			
dme04144:Endocytosis	51	1.10E-06	1.21E-04
dme04330:Notch signaling pathway	18	9.98E-05	1.09E-02
dme04120:Ubiquitin mediated proteolysis	53	2.78E-04	3.01E-02

Table B5. Embryo DAVID analysis, transcripts ≥3-fold higher in control than *wisp*

Term	Count	*P* value	Bonferroni
Biological process			
GO:0048610~reproductive cellular process	224	4.32E-10	1.36E-06
GO:0003006~reproductive developmental process	220	2.30E-09	7.23E-06
GO:0019953~sexual reproduction	291	1.87E-08	5.88E-05
GO:0051276~chromosome organization	177	1.97E-08	6.21E-05
GO:0048477~oogenesis	230	3.37E-08	1.06E-04
GO:0007276~gamete generation	284	3.99E-08	1.26E-04
GO:0007292~female gamete generation	231	5.20E-08	1.63E-04
GO:0045449~regulation of transcription	306	5.29E-08	1.66E-04
GO:0010605~negative regulation of macromolecule metabolic process	141	5.67E-08	1.78E-04
GO:0006396~RNA processing	161	7.44E-08	2.34E-04
GO:0006350~transcription	206	1.84E-07	5.77E-04
GO:0007444~imaginal disc development	170	2.05E-07	6.45E-04
GO:0060429~epithelium development	117	2.32E-07	7.28E-04
GO:0032504~multicellular organism reproduction	286	2.36E-07	7.42E-04
GO:0048609~reproductive process in a multicellular organism	286	2.36E-07	7.42E-04
GO:0010629~negative regulation of gene expression	112	3.18E-07	1.00E-03
GO:0032989~cellular component morphogenesis	224	3.80E-07	0.00119
GO:0006468~protein amino acid phosphorylation	131	6.36E-07	0.00200
GO:0048598~embryonic morphogenesis	97	7.91E-07	0.00248
GO:0030707~ovarian follicle cell development	97	7.91E-07	0.00248
GO:0007423~sensory organ development	139	1.10E-06	0.00344
GO:0048729~tissue morphogenesis	113	1.58E-06	0.00494
GO:0002009~morphogenesis of an epithelium	109	1.73E-06	0.00542
GO:0001700~embryonic development via the syncytial blastoderm	94	1.75E-06	0.00548
GO:0016071~mRNA metabolic process	116	1.81E-06	0.00568
GO:0051301~cell division	122	2.31E-06	0.00724
GO:0006928~cell motion	138	2.89E-06	0.00905
GO:0035282~segmentation	95	3.60E-06	0.01124
GO:0009880~embryonic pattern specification	95	3.60E-06	0.01124
GO:0035220~wing disc development	119	4.62E-06	0.01442
GO:0048569~post-embryonic organ development	118	5.80E-06	0.01808
GO:0000902~cell morphogenesis	197	6.19E-06	0.01927
GO:0007389~pattern specification process	178	7.23E-06	0.02247
GO:0010648~negative regulation of cell communication	60	7.47E-06	0.02322
GO:0009968~negative regulation of signal transduction	60	7.47E-06	0.02322
GO:0006397~mRNA processing	99	8.21E-06	0.02549
GO:0045934~negative regulation of nucleobase, nucleoside, nucleotide and nucleic acid metabolic process	88	8.22E-06	0.02552
GO:0051172~negative regulation of nitrogen compound metabolic	88	8.22E-06	0.02552

process			
GO:0009792~embryonic development ending in birth or egg hatching	95	9.03E-06	0.02798
GO:0007560~imaginal disc morphogenesis	116	9.12E-06	0.02827
GO:0048563~post-embryonic organ morphogenesis	116	9.12E-06	0.02827
GO:0048749~compound eye development	105	1.06E-05	0.03282
GO:0001709~cell fate determination	63	1.12E-05	0.03466
GO:0016481~negative regulation of transcription	79	1.18E-05	0.03643
GO:0001654~eye development	108	1.18E-05	0.03653
GO:0010558~negative regulation of macromolecule biosynthetic process	97	1.33E-05	0.04089
GO:0009890~negative regulation of biosynthetic process	97	1.33E-05	0.04089
GO:0031327~negative regulation of cellular biosynthetic process	97	1.33E-05	0.04089
GO:0007472~wing disc morphogenesis	93	1.47E-05	0.04515
GO:0003002~regionalization	165	1.49E-05	0.04566
GO:0051253~negative regulation of RNA metabolic process	74	1.58E-05	0.04860
Cellular compartment			
GO:0005694~chromosome	181	1.36E-14	8.29E-12
GO:0044427~chromosomal part	142	2.14E-10	1.31E-07
GO:0031981~nuclear lumen	199	6.04E-09	3.69E-06
GO:0005654~nucleoplasm	151	7.67E-07	4.69E-04
GO:0031974~membrane-enclosed lumen	274	8.10E-07	4.96E-04
GO:0070013~intracellular organelle lumen	265	4.06E-06	0.00248
GO:0043233~organelle lumen	265	4.06E-06	0.00248
GO:0005886~plasma membrane	231	1.60E-05	0.00975
GO:0005700~polytene chromosome	57	2.50E-05	0.01519
GO:0044451~nucleoplasm part	129	5.00E-05	0.03011
Molecular function			
GO:0003677~DNA binding	368	3.97E-16	6.34E-13
GO:0008270~zinc ion binding	463	7.16E-14	1.02E-10
GO:0046872~metal ion binding	637	1.46E-09	2.09E-06
GO:0043169~cation binding	646	6.87E-09	9.81E-06
GO:0043167~ion binding	646	9.79E-09	1.40E-05
GO:0004672~protein kinase activity	139	2.41E-08	3.43E-05
GO:0030528~transcription regulator activity	261	1.12E-07	1.59E-04
GO:0004674~protein serine/threonine kinase activity	107	1.90E-07	2.72E-04
GO:0046914~transition metal ion binding	520	2.92E-07	4.16E-04
KEGG pathway			
dme00564:Glycerophospholipid metabolism	31	5.79E-05	0.00618
dme03040:Spliceosome	62	5.92E-05	0.00631
dme04120:Ubiquitin mediated proteolysis	54	1.85E-04	0.01963
dme04144:Endocytosis	48	2.95E-04	0.03106

Table B6. Embryo poly(A) downregulated minus embryo total RNA downregulated

Term	Count	*P*-value	Bonferroni
Biological process			
GO:0008104~protein localization	260	1.16E-35	3.86E-32
GO:0051276~chromosome organization	190	2.49E-27	8.29E-24
GO:0045184~establishment of protein localization	182	3.72E-22	1.24E-18
GO:0015031~protein transport	178	7.27E-22	2.42E-18
GO:0007010~cytoskeleton organization	264	4.65E-21	1.55E-17
GO:0046907~intracellular transport	193	6.65E-21	2.22E-17
GO:0016192~vesicle-mediated transport	228	3.45E-20	1.15E-16
GO:0000278~mitotic cell cycle	210	4.76E-19	1.59E-15
GO:0006259~DNA metabolic process	141	2.89E-17	9.61E-14
GO:0051301~cell division	132	1.09E-16	3.70E-13
GO:0007059~chromosome segregation	86	4.49E-16	1.48E-12
GO:0006325~chromatin organization	113	1.08E-15	3.70E-12
GO:0007049~cell cycle	314	2.58E-15	8.51E-12
GO:0048285~organelle fission	103	6.17E-15	2.07E-11
GO:0016044~membrane organization	181	2.19E-14	7.29E-11
GO:0006396~RNA processing	176	1.07E-13	3.57E-10
GO:0051726~regulation of cell cycle	107	1.40E-13	4.66E-10
GO:0000280~nuclear division	98	1.45E-13	4.82E-10
GO:0016568~chromatin modification	79	2.91E-13	9.69E-10
GO:0033554~cellular response to stress	111	3.97E-13	1.32E-09
GO:0006350~transcription	239	4.96E-13	1.65E-09
GO:0007067~mitosis	96	4.99E-13	1.66E-09
GO:0000087~M phase of mitotic cell cycle	97	4.99E-13	1.66E-09
GO:0043933~macromolecular complex subunit organization	160	5.63E-13	1.87E-09
GO:0070727~cellular macromolecule localization	142	1.39E-12	4.63E-09
GO:0007242~intracellular signaling cascade	165	3.88E-12	1.29E-08
GO:0000226~microtubule cytoskeleton organization	165	5.63E-12	1.87E-08
GO:0000902~cell morphogenesis	228	6.33E-12	2.11E-08
GO:0006260~DNA replication	68	1.21E-11	4.02E-08
GO:0034613~cellular protein localization	109	1.63E-11	5.43E-08
GO:0051640~organelle localization	60	2.77E-11	9.21E-08
GO:0010324~membrane invagination	145	2.91E-11	9.69E-08
GO:0006897~endocytosis	145	2.91E-11	9.69E-08
GO:0022402~cell cycle process	270	3.22E-11	1.07E-07
GO:0033043~regulation of organelle organization	74	3.31E-11	1.10E-07
GO:0022604~regulation of cell morphogenesis	79	3.61E-11	1.20E-07
GO:0051656~establishment of organelle localization	56	3.85E-11	1.28E-07
GO:0032989~cellular component morphogenesis	257	5.30E-11	1.76E-07
GO:0030182~neuron differentiation	210	8.37E-11	2.79E-07

GO:0006468~protein amino acid phosphorylation	144	9.85E-11	3.28E-07
GO:0006974~response to DNA damage stimulus	76	1.24E-10	4.12E-07
GO:0044265~cellular macromolecule catabolic process	128	1.63E-10	5.42E-07
GO:0010604~positive regulation of macromolecule metabolic process	89	1.75E-10	5.84E-07
GO:0016071~mRNA metabolic process	125	2.04E-10	6.80E-07
GO:0006281~DNA repair	69	2.14E-10	7.13E-07
GO:0006886~intracellular protein transport	104	2.32E-10	7.74E-07
GO:0007017~microtubule-based process	207	2.60E-10	8.67E-07
GO:0007163~establishment or maintenance of cell polarity	72	4.21E-10	1.40E-06
GO:0030029~actin filament-based process	89	4.98E-10	1.66E-06
GO:0044087~regulation of cellular component biogenesis	57	4.98E-10	1.66E-06
GO:0065003~macromolecular complex assembly	136	5.78E-10	1.92E-06
GO:0048610~reproductive cellular process	245	7.44E-10	2.48E-06
GO:0048666~neuron development	180	7.83E-10	2.61E-06
GO:0030036~actin cytoskeleton organization	88	8.63E-10	2.87E-06
GO:0060284~regulation of cell development	82	1.10E-09	3.65E-06
GO:0007264~small GTPase mediated signal transduction	71	1.41E-09	4.71E-06
GO:0032940~secretion by cell	75	2.33E-09	7.76E-06
GO:0051960~regulation of nervous system development	61	2.49E-09	8.29E-06
GO:0008360~regulation of cell shape	65	2.63E-09	8.75E-06
GO:0010557~positive regulation of macromolecule biosynthetic process	80	3.35E-09	1.12E-05
GO:0008283~cell proliferation	79	3.48E-09	1.16E-05
GO:0045935~positive regulation of nucleobase, nucleoside, nucleotide and nucleic acid metabolic process	76	3.88E-09	1.29E-05
GO:0051173~positive regulation of nitrogen compound metabolic process	76	3.88E-09	1.29E-05
GO:0040008~regulation of growth	67	4.78E-09	1.59E-05
GO:0045449~regulation of transcription	362	8.62E-09	2.87E-05
GO:0007143~female meiosis	46	9.34E-09	3.11E-05
GO:0007051~spindle organization	123	1.03E-08	3.44E-05
GO:0034621~cellular macromolecular complex subunit organization	113	1.16E-08	3.86E-05
GO:0048477~oogenesis	256	1.26E-08	4.18E-05
GO:0000819~sister chromatid segregation	37	1.39E-08	4.62E-05
GO:0003001~generation of a signal involved in cell-cell signaling	66	1.53E-08	5.10E-05
GO:0010608~posttranscriptional regulation of gene expression	77	1.73E-08	5.75E-05
GO:0007292~female gamete generation	258	1.96E-08	6.54E-05
GO:0007052~mitotic spindle organization	108	2.52E-08	8.40E-05
GO:0003006~reproductive developmental process	241	2.65E-08	8.82E-05
GO:0007269~neurotransmitter secretion	65	2.74E-08	9.11E-05
GO:0007346~regulation of mitotic cell cycle	63	2.86E-08	9.54E-05
GO:0046903~secretion	76	2.95E-08	9.83E-05

GO:0000070~mitotic sister chromatid segregation	36	2.99E-08	9.96E-05
GO:0051254~positive regulation of RNA metabolic process	59	3.02E-08	1.01E-04
GO:0048489~synaptic vesicle transport	59	3.02E-08	1.01E-04
GO:0006261~DNA-dependent DNA replication	42	3.10E-08	1.03E-04
GO:0031328~positive regulation of cellular biosynthetic process	89	3.28E-08	1.09E-04
GO:0012501~programmed cell death	89	3.28E-08	1.09E-04
GO:0009891~positive regulation of biosynthetic process	89	3.28E-08	1.09E-04
GO:0010628~positive regulation of gene expression	72	3.58E-08	1.19E-04
GO:0009057~macromolecule catabolic process	144	3.93E-08	1.31E-04
GO:0031175~neuron projection development	148	4.87E-08	1.62E-04
GO:0006796~phosphate metabolic process	258	5.46E-08	1.82E-04
GO:0006793~phosphorus metabolic process	258	5.46E-08	1.82E-04
GO:0006397~mRNA processing	107	5.68E-08	1.89E-04
GO:0045941~positive regulation of transcription	71	6.16E-08	2.05E-04
GO:0060429~epithelium development	125	6.45E-08	2.15E-04
GO:0048812~neuron projection morphogenesis	147	7.11E-08	2.37E-04
GO:0046486~glycerolipid metabolic process	43	7.51E-08	2.50E-04
GO:0008219~cell death	92	8.95E-08	2.98E-04
GO:0032774~RNA biosynthetic process	80	9.23E-08	3.07E-04
GO:0045893~positive regulation of transcription, DNA-dependent	57	9.99E-08	3.33E-04
GO:0030261~chromosome condensation	26	1.25E-07	4.15E-04
GO:0016265~death	92	1.32E-07	4.39E-04
GO:0006366~transcription from RNA polymerase II promoter	62	1.51E-07	5.02E-04
GO:0000904~cell morphogenesis involved in differentiation	153	1.61E-07	5.37E-04
GO:0006351~transcription, DNA-dependent	78	1.63E-07	5.41E-04
GO:0022403~cell cycle phase	233	1.92E-07	6.40E-04
GO:0048667~cell morphogenesis involved in neuron differentiation	146	2.36E-07	7.86E-04
GO:0006461~protein complex assembly	93	2.59E-07	8.62E-04
GO:0070271~protein complex biogenesis	93	2.59E-07	8.62E-04
GO:0006928~cell motion	153	2.73E-07	9.08E-04
GO:0006357~regulation of transcription from RNA polymerase II promoter	104	2.95E-07	9.82E-04
GO:0007243~protein kinase cascade	42	3.06E-07	0.0010201
GO:0019953~sexual reproduction	328	3.17E-07	0.0010555
GO:0007276~gamete generation	320	3.28E-07	0.0010913
GO:0006644~phospholipid metabolic process	54	3.30E-07	0.0010971
GO:0043632~modification-dependent macromolecule catabolic process	94	3.43E-07	0.0011423
GO:0032535~regulation of cellular component size	61	4.35E-07	0.0014489
GO:0019941~modification-dependent protein catabolic process	93	5.33E-07	0.0017739
GO:0001505~regulation of neurotransmitter levels	66	5.39E-07	0.0017944
GO:0006323~DNA packaging	44	6.38E-07	0.0021241
GO:0050767~regulation of neurogenesis	45	6.45E-07	0.0021478

GO:0009968~negative regulation of signal transduction	62	6.74E-07	0.0022429
GO:0007267~cell-cell signaling	111	7.89E-07	0.002626
GO:0002009~morphogenesis of an epithelium	117	8.34E-07	0.0027758
GO:0034660~ncRNA metabolic process	76	9.84E-07	0.0032717
GO:0007268~synaptic transmission	101	1.03E-06	0.0034254
GO:0051329~interphase of mitotic cell cycle	22	1.05E-06	0.003481
GO:0051325~interphase	22	1.05E-06	0.003481
GO:0006650~glycerophospholipid metabolic process	38	1.05E-06	0.0034871
GO:0010648~negative regulation of cell communication	62	1.08E-06	0.0035875
GO:0019226~transmission of nerve impulse	104	1.08E-06	0.0036064
GO:0043067~regulation of programmed cell death	65	2.17E-06	0.007207
GO:0006605~protein targeting	64	2.32E-06	0.0077101
GO:0016197~endosome transport	21	2.47E-06	0.008195
GO:0050803~regulation of synapse structure and activity	30	2.60E-06	0.0086159
GO:0051603~proteolysis involved in cellular protein catabolic process	97	2.77E-06	0.0091862
GO:0044257~cellular protein catabolic process	97	2.77E-06	0.0091862
GO:0051252~regulation of RNA metabolic process	300	2.77E-06	0.0091924
GO:0000910~cytokinesis	50	3.21E-06	0.0106329
GO:0019637~organophosphate metabolic process	58	3.42E-06	0.0113221
GO:0007391~dorsal closure	57	3.63E-06	0.0120227
GO:0030163~protein catabolic process	104	3.65E-06	0.0120809
GO:0051493~regulation of cytoskeleton organization	35	3.76E-06	0.01246
GO:0002165~instar larval or pupal development	195	3.85E-06	0.012743
GO:0032268~regulation of cellular protein metabolic process	73	3.96E-06	0.0130961
GO:0008356~asymmetric cell division	39	4.09E-06	0.0135277
GO:0048488~synaptic vesicle endocytosis	27	4.11E-06	0.0136079
GO:0007281~germ cell development	122	4.78E-06	0.0157932
GO:0022613~ribonucleoprotein complex biogenesis	56	6.07E-06	0.0200038
GO:0034622~cellular macromolecular complex assembly	88	6.17E-06	0.0203413
GO:0000279~M phase	218	6.94E-06	0.0228405
GO:0030030~cell projection organization	172	7.39E-06	0.0243003
GO:0009791~post-embryonic development	200	7.73E-06	0.0254133
GO:0010564~regulation of cell cycle process	51	8.17E-06	0.0268461
GO:0008105~asymmetric protein localization	26	8.62E-06	0.0282897
GO:0010941~regulation of cell death	65	1.09E-05	0.0356807
GO:0030707~ovarian follicle cell development	104	1.13E-05	0.0369022
GO:0060341~regulation of cellular localization	43	1.19E-05	0.0390012
GO:0007298~border follicle cell migration	42	1.24E-05	0.0403818
GO:0043484~regulation of RNA splicing	42	1.24E-05	0.0403818
GO:0032990~cell part morphogenesis	157	1.24E-05	0.0404863
GO:0048729~tissue morphogenesis	122	1.30E-05	0.04242
GO:0032970~regulation of actin filament-based process	23	1.32E-05	0.0430347

GO:0032956~regulation of actin cytoskeleton organization	23	1.32E-05	0.0430347
GO:0048585~negative regulation of response to stimulus	19	1.34E-05	0.0437617
GO:0030384~phosphoinositide metabolic process	32	1.34E-05	0.0437991
GO:0006338~chromatin remodeling	32	1.34E-05	0.0437991
GO:0008654~phospholipid biosynthetic process	33	1.38E-05	0.044825
GO:0007015~actin filament organization	50	1.38E-05	0.0448669
GO:0009994~oocyte differentiation	75	1.39E-05	0.045229
GO:0051129~negative regulation of cellular component organization	37	1.39E-05	0.0452828
GO:0045664~regulation of neuron differentiation	36	1.40E-05	0.0456419
Cellular Compartment			
GO:0031974~membrane-enclosed lumen	319	9.42E-19	6.13E-16
GO:0005694~chromosome	191	2.82E-18	1.84E-15
GO:0043233~organelle lumen	310	4.93E-18	3.21E-15
GO:0070013~intracellular organelle lumen	310	4.93E-18	3.21E-15
GO:0005654~nucleoplasm	170	1.39E-17	9.03E-15
GO:0031981~nuclear lumen	223	8.23E-15	5.35E-12
GO:0043232~intracellular non-membrane-bounded organelle	467	6.49E-14	4.23E-11
GO:0043228~non-membrane-bounded organelle	467	6.49E-14	4.23E-11
GO:0044427~chromosomal part	151	8.92E-14	5.81E-11
GO:0044451~nucleoplasm part	149	1.49E-13	9.71E-11
GO:0012505~endomembrane system	137	4.38E-13	2.85E-10
GO:0005938~cell cortex	56	9.46E-10	6.16E-07
GO:0005813~centrosome	41	1.99E-08	1.29E-05
GO:0005819~spindle	50	2.08E-08	1.36E-05
GO:0005856~cytoskeleton	185	4.64E-08	3.02E-05
GO:0005794~Golgi apparatus	96	3.29E-07	2.14E-04
GO:0005815~microtubule organizing center	43	7.94E-07	5.17E-04
GO:0005635~nuclear envelope	56	1.61E-06	0.0010466
GO:0005700~polytene chromosome	59	1.67E-06	0.0010888
GO:0000228~nuclear chromosome	51	2.49E-06	0.0016183
GO:0044454~nuclear chromosome part	46	6.69E-06	0.0043448
GO:0005789~endoplasmic reticulum membrane	49	7.23E-06	0.0046934
GO:0042175~nuclear envelope-endoplasmic reticulum network	50	7.35E-06	0.0047719
GO:0005768~endosome	25	1.26E-05	0.0081665
GO:0005681~spliceosome	46	2.02E-05	0.013064
GO:0044430~cytoskeletal part	145	3.26E-05	0.0209702
GO:0016327~apicolateral plasma membrane	32	3.76E-05	0.0241983
GO:0000785~chromatin	65	7.30E-05	0.0464249
Molecular function			
GO:0000166~nucleotide binding	645	1.11E-30	1.77E-27
GO:0032553~ribonucleotide binding	511	1.65E-28	2.64E-25
GO:0032555~purine ribonucleotide binding	511	1.65E-28	2.64E-25

GO:0017076~purine nucleotide binding	535	1.35E-26	2.15E-23
GO:0032559~adenyl ribonucleotide binding	421	6.87E-25	1.10E-21
GO:0005524~ATP binding	419	1.60E-24	2.56E-21
GO:0001883~purine nucleoside binding	446	4.96E-23	7.92E-20
GO:0001882~nucleoside binding	448	1.16E-22	1.85E-19
GO:0030554~adenyl nucleotide binding	442	1.74E-22	2.77E-19
GO:0008270~zinc ion binding	508	1.41E-14	2.25E-11
GO:0003677~DNA binding	416	6.46E-13	1.03E-09
GO:0004386~helicase activity	78	7.33E-12	1.17E-08
GO:0003729~mRNA binding	118	8.09E-12	1.29E-08
GO:0019899~enzyme binding	53	2.28E-11	3.64E-08
GO:0008026~ATP-dependent helicase activity	58	4.85E-10	7.73E-07
GO:0070035~purine NTP-dependent helicase activity	58	4.85E-10	7.73E-07
GO:0008092~cytoskeletal protein binding	128	1.62E-09	2.59E-06
GO:0016779~nucleotidyltransferase activity	62	1.45E-08	2.31E-05
GO:0008134~transcription factor binding	61	2.59E-08	4.14E-05
GO:0004674~protein serine/threonine kinase activity	116	8.25E-08	1.32E-04
GO:0003779~actin binding	76	1.87E-07	2.99E-04
GO:0015631~tubulin binding	48	2.69E-07	4.29E-04
GO:0004672~protein kinase activity	151	3.13E-07	4.99E-04
GO:0008017~microtubule binding	44	1.49E-06	0.0023681
GO:0060589~nucleoside-triphosphatase regulator activity	83	6.49E-06	0.0103107
GO:0046914~transition metal ion binding	593	8.39E-06	0.0133079
GO:0003682~chromatin binding	43	9.26E-06	0.0146667
GO:0030695~GTPase regulator activity	81	1.02E-05	0.0161191
GO:0043566~structure-specific DNA binding	25	1.12E-05	0.0177629
GO:0004004~ATP-dependent RNA helicase activity	30	1.26E-05	0.0198994
GO:0008186~RNA-dependent ATPase activity	30	1.26E-05	0.0198994
GO:0003712~transcription cofactor activity	42	1.60E-05	0.0252827
GO:0005083~small GTPase regulator activity	64	2.03E-05	0.0318264
GO:0003924~GTPase activity	74	2.86E-05	0.044638
GO:0042802~identical protein binding	81	2.86E-05	0.0446407
KEGG pathway			
dme03040:Spliceosome	71	1.05E-04	0.0116223
dme04320:Dorso-ventral axis formation	22	2.41E-04	0.0263651
dme04144:Endocytosis	53	2.83E-04	0.0309255
dme03018:RNA degradation	35	3.05E-04	0.033305
dme04120:Ubiquitin mediated proteolysis	62	3.34E-04	0.0363751
dme00970:Aminoacyl-tRNA biosynthesis	27	0.006009	0.4877783

Table B7. Oocyte poly(A) downregulated minus oocyte total downregulated

Term	Count	*P*-value	Bonferroni
Biological process			
GO:0007049~cell cycle	212	5.61E-16	1.50E-12
GO:0022402~cell cycle process	181	3.87E-13	5.23E-10
GO:0022403~cell cycle phase	159	4.55E-12	4.09E-09
GO:0007067~mitosis	76	5.49E-12	3.70E-09
GO:0000279~M phase	150	1.30E-11	7.01E-09
GO:0000087~M phase of mitotic cell cycle	76	1.34E-11	6.00E-09
GO:0000280~nuclear division	76	3.15E-11	1.21E-08
GO:0048285~organelle fission	78	1.12E-10	3.79E-08
GO:0051276~chromosome organization	129	3.84E-10	1.15E-07
GO:0000278~mitotic cell cycle	145	4.57E-10	1.23E-07
GO:0006259~DNA metabolic process	95	1.33E-08	3.25E-06
GO:0006974~response to DNA damage stimulus	54	3.62E-07	8.13E-05
GO:0019953~sexual reproduction	199	5.42E-07	1.12E-04
GO:0007010~cytoskeleton organization	168	9.72E-07	1.87E-04
GO:0007276~gamete generation	194	1.35E-06	2.43E-04
GO:0000226~microtubule cytoskeleton organization	113	1.98E-06	3.34E-04
GO:0048477~oogenesis	157	2.07E-06	3.28E-04
GO:0032504~multicellular organism reproduction	197	2.12E-06	3.17E-04
GO:0048609~reproductive process in a multicellular organism	197	2.12E-06	3.17E-04
GO:0048610~reproductive cellular process	151	2.25E-06	3.20E-04
GO:0007292~female gamete generation	158	3.63E-06	4.89E-04
GO:0016071~mRNA metabolic process	79	5.27E-06	6.76E-04
GO:0043933~macromolecular complex subunit organization	103	5.55E-06	6.80E-04
GO:0051726~regulation of cell cycle	71	5.96E-06	6.99E-04
GO:0033554~cellular response to stress	74	6.82E-06	7.66E-04
GO:0007059~chromosome segregation	58	7.18E-06	7.75E-04
GO:0006397~mRNA processing	68	1.32E-05	1.37E-03
GO:0006281~DNA repair	47	1.38E-05	1.38E-03
GO:0051321~meiotic cell cycle	51	2.08E-05	2.00E-03
GO:0003006~reproductive developmental process	146	2.34E-05	2.18E-03
GO:0007017~microtubule-based process	134	2.92E-05	2.62E-03
GO:0008380~RNA splicing	49	5.25E-05	4.55E-03
GO:0006350~transcription	137	7.94E-05	6.67E-03
GO:0006325~chromatin organization	72	8.02E-05	6.53E-03
GO:0007126~meiosis	48	8.26E-05	6.53E-03
GO:0051327~M phase of meiotic cell cycle	48	8.26E-05	6.53E-03
GO:0051301~cell division	80	8.66E-05	6.65E-03
GO:0010605~negative regulation of macromolecule metabolic process	90	8.72E-05	6.51E-03

GO:0065003~macromolecular complex assembly	87	8.77E-05	6.37E-03
GO:0033043~regulation of organelle organization	50	9.37E-05	6.63E-03
GO:0009057~macromolecule catabolic process	106	1.04E-04	7.15E-03
GO:0006260~DNA replication	45	1.13E-04	7.57E-03
GO:0044265~cellular macromolecule catabolic process	94	1.17E-04	7.70E-03
GO:0000375~RNA splicing, via transesterification reactions	41	1.41E-04	9.00E-03
GO:0007051~spindle organization	83	1.72E-04	1.07E-02
GO:0046907~intracellular transport	114	2.09E-04	1.28E-02
GO:0000819~sister chromatid segregation	29	2.14E-04	1.27E-02
GO:0000398~nuclear mRNA splicing, via spliceosome	40	2.24E-04	1.31E-02
GO:0000377~RNA splicing, via transesterification reactions with bulged adenosine as nucleophile	40	2.24E-04	1.31E-02
GO:0051028~mRNA transport	17	2.49E-04	1.42E-02
GO:0008104~protein localization	145	2.73E-04	1.52E-02
GO:0007281~germ cell development	76	3.38E-04	1.84E-02
GO:0034621~cellular macromolecular complex subunit organization	74	3.39E-04	1.81E-02
GO:0032989~cellular component morphogenesis	152	3.52E-04	1.84E-02
GO:0000070~mitotic sister chromatid segregation	28	3.66E-04	1.88E-02
GO:0006323~DNA packaging	33	3.68E-04	1.86E-02
GO:0007346~regulation of mitotic cell cycle	41	4.04E-04	2.00E-02
GO:0006468~protein amino acid phosphorylation	88	4.16E-04	2.02E-02
GO:0009891~positive regulation of biosynthetic process	55	4.27E-04	2.03E-02
GO:0031328~positive regulation of cellular biosynthetic process	55	4.27E-04	2.03E-02
GO:0035220~wing disc development	84	4.35E-04	2.04E-02
GO:0010564~regulation of cell cycle process	35	4.46E-04	2.05E-02
GO:0010629~negative regulation of gene expression	71	4.75E-04	2.15E-02
GO:0045449~regulation of transcription	205	5.20E-04	2.31E-02
GO:0030182~neuron differentiation	126	5.46E-04	2.39E-02
GO:0000902~cell morphogenesis	136	6.60E-04	2.83E-02
GO:0045184~establishment of protein localization	106	6.79E-04	2.87E-02
GO:0007143~female meiosis	28	7.09E-04	2.94E-02
GO:0009968~negative regulation of signal transduction	43	7.13E-04	2.92E-02
GO:0010648~negative regulation of cell communication	43	7.13E-04	2.92E-02
GO:0003002~regionalization	111	7.75E-04	3.12E-02
GO:0018130~heterocycle biosynthetic process	25	9.10E-04	3.60E-02
GO:0007389~pattern specification process	119	1.01E-03	3.94E-02
GO:0007242~intracellular signaling cascade	105	1.12E-03	4.30E-02
GO:0015031~protein transport	103	1.17E-03	4.43E-02
GO:0051252~regulation of RNA metabolic process	171	1.18E-03	4.38E-02
GO:0010941~regulation of cell death	46	1.19E-03	4.36E-02
GO:0043067~regulation of programmed cell death	46	1.19E-03	4.36E-02
GO:0031175~neuron projection development	89	1.22E-03	4.43E-02

GO:0006396~RNA processing	97	1.34E-03	4.76E-02
GO:0030030~cell projection organization	105	1.42E-03	4.97E-02
GO:0006928~cell motion	94	1.43E-03	4.94E-02
GO:0030163~protein catabolic process	80	1.43E-03	4.90E-02
GO:0000904~cell morphogenesis involved in differentiation	93	1.46E-03	4.91E-02
Cellular compartment			
GO:0005694~chromosome	130	1.12E-14	6.08E-12
GO:0044427~chromosomal part	102	1.59E-10	8.61E-08
GO:0005654~nucleoplasm	105	4.46E-08	2.42E-05
GO:0044451~nucleoplasm part	92	2.68E-07	1.45E-04
GO:0005700~polytene chromosome	43	2.12E-06	1.15E-03
GO:0031981~nuclear lumen	124	4.01E-05	2.15E-02
Molecular function			
GO:0003677~DNA binding	240	5.36E-08	6.18E-05
GO:0008270~zinc ion binding	291	1.15E-06	1.33E-03
GO:0003729~mRNA binding	75	4.49E-06	5.16E-03
GO:0000166~nucleotide binding	370	8.91E-06	1.02E-02
GO:0019899~enzyme binding	38	2.44E-05	2.77E-02
GO:0016251~general RNA polymerase II transcription factor activity	36	3.70E-05	4.18E-02
GO:0004672~protein kinase activity	95	3.89E-05	4.39E-02
KEGG pathway			
dme04120:Ubiquitin mediated proteolysis	50	9.32E-09	9.32E-07
dme03040:Spliceosome	52	7.18E-08	7.18E-06
dme04914:Progesterone-mediated oocyte maturation	23	5.21E-05	5.20E-03
dme03030:DNA replication	19	2.94E-04	2.89E-02
dme04144:Endocytosis	37	3.01E-04	2.97E-02

Table B8. Embryo poly(A) downregulated minus Embryo total downregulated

Term	Count	*P*-value	Bonferroni
Biological process			
GO:0008104~protein localization	260	1.16E-35	3.86E-32
GO:0051276~chromosome organization	190	2.49E-27	8.29E-24
GO:0045184~establishment of protein localization	182	3.72E-22	1.24E-18
GO:0015031~protein transport	178	7.27E-22	2.42E-18
GO:0007010~cytoskeleton organization	264	4.65E-21	1.55E-17
GO:0046907~intracellular transport	193	6.65E-21	2.22E-17
GO:0016192~vesicle-mediated transport	228	3.45E-20	1.15E-16
GO:0000278~mitotic cell cycle	210	4.76E-19	1.59E-15
GO:0006259~DNA metabolic process	141	2.89E-17	9.61E-14
GO:0051301~cell division	132	1.09E-16	3.70E-13

GO:0007059~chromosome segregation	86	4.49E-16	1.48E-12
GO:0006325~chromatin organization	113	1.08E-15	3.70E-12
GO:0007049~cell cycle	314	2.58E-15	8.51E-12
GO:0048285~organelle fission	103	6.17E-15	2.07E-11
GO:0016044~membrane organization	181	2.19E-14	7.29E-11
GO:0006396~RNA processing	176	1.07E-13	3.57E-10
GO:0051726~regulation of cell cycle	107	1.40E-13	4.66E-10
GO:0000280~nuclear division	98	1.45E-13	4.82E-10
GO:0016568~chromatin modification	79	2.91E-13	9.69E-10
GO:0033554~cellular response to stress	111	3.97E-13	1.32E-09
GO:0006350~transcription	239	4.96E-13	1.65E-09
GO:0007067~mitosis	96	4.99E-13	1.66E-09
GO:0000087~M phase of mitotic cell cycle	97	4.99E-13	1.66E-09
GO:0043933~macromolecular complex subunit organization	160	5.63E-13	1.87E-09
GO:0070727~cellular macromolecule localization	142	1.39E-12	4.63E-09
GO:0007242~intracellular signaling cascade	165	3.88E-12	1.29E-08
GO:0000226~microtubule cytoskeleton organization	165	5.63E-12	1.87E-08
GO:0000902~cell morphogenesis	228	6.33E-12	2.11E-08
GO:0006260~DNA replication	68	1.21E-11	4.02E-08
GO:0034613~cellular protein localization	109	1.63E-11	5.43E-08
GO:0051640~organelle localization	60	2.77E-11	9.21E-08
GO:0010324~membrane invagination	145	2.91E-11	9.69E-08
GO:0006897~endocytosis	145	2.91E-11	9.69E-08
GO:0022402~cell cycle process	270	3.22E-11	1.07E-07
GO:0033043~regulation of organelle organization	74	3.31E-11	1.10E-07
GO:0022604~regulation of cell morphogenesis	79	3.61E-11	1.20E-07
GO:0051656~establishment of organelle localization	56	3.85E-11	1.28E-07
GO:0032989~cellular component morphogenesis	257	5.30E-11	1.76E-07
GO:0030182~neuron differentiation	210	8.37E-11	2.79E-07
GO:0006468~protein amino acid phosphorylation	144	9.85E-11	3.28E-07
GO:0006974~response to DNA damage stimulus	76	1.24E-10	4.12E-07
GO:0044265~cellular macromolecule catabolic process	128	1.63E-10	5.42E-07
GO:0010604~positive regulation of macromolecule metabolic process	89	1.75E-10	5.84E-07
GO:0016071~mRNA metabolic process	125	2.04E-10	6.80E-07
GO:0006281~DNA repair	69	2.14E-10	7.13E-07
GO:0006886~intracellular protein transport	104	2.32E-10	7.74E-07
GO:0007017~microtubule-based process	207	2.60E-10	8.67E-07
GO:0007163~establishment or maintenance of cell polarity	72	4.21E-10	1.40E-06
GO:0030029~actin filament-based process	89	4.98E-10	1.66E-06
GO:0044087~regulation of cellular component biogenesis	57	4.98E-10	1.66E-06
GO:0065003~macromolecular complex assembly	136	5.78E-10	1.92E-06
GO:0048610~reproductive cellular process	245	7.44E-10	2.48E-06

GO:0048666~neuron development	180	7.83E-10	2.61E-06
GO:0030036~actin cytoskeleton organization	88	8.63E-10	2.87E-06
GO:0060284~regulation of cell development	82	1.10E-09	3.65E-06
GO:0007264~small GTPase mediated signal transduction	71	1.41E-09	4.71E-06
GO:0032940~secretion by cell	75	2.33E-09	7.76E-06
GO:0051960~regulation of nervous system development	61	2.49E-09	8.29E-06
GO:0008360~regulation of cell shape	65	2.63E-09	8.75E-06
GO:0010557~positive regulation of macromolecule biosynthetic process	80	3.35E-09	1.12E-05
GO:0008283~cell proliferation	79	3.48E-09	1.16E-05
GO:0045935~positive regulation of nucleobase, nucleoside, nucleotide and nucleic acid metabolic process	76	3.88E-09	1.29E-05
GO:0051173~positive regulation of nitrogen compound metabolic process	76	3.88E-09	1.29E-05
GO:0040008~regulation of growth	67	4.78E-09	1.59E-05
GO:0045449~regulation of transcription	362	8.62E-09	2.87E-05
GO:0007143~female meiosis	46	9.34E-09	3.11E-05
GO:0007051~spindle organization	123	1.03E-08	3.44E-05
GO:0034621~cellular macromolecular complex subunit organization	113	1.16E-08	3.86E-05
GO:0048477~oogenesis	256	1.26E-08	4.18E-05
GO:0000819~sister chromatid segregation	37	1.39E-08	4.62E-05
GO:0003001~generation of a signal involved in cell-cell signaling	66	1.53E-08	5.10E-05
GO:0010608~posttranscriptional regulation of gene expression	77	1.73E-08	5.75E-05
GO:0007292~female gamete generation	258	1.96E-08	6.54E-05
GO:0007052~mitotic spindle organization	108	2.52E-08	8.40E-05
GO:0003006~reproductive developmental process	241	2.65E-08	8.82E-05
GO:0007269~neurotransmitter secretion	65	2.74E-08	9.11E-05
GO:0007346~regulation of mitotic cell cycle	63	2.86E-08	9.54E-05
GO:0046903~secretion	76	2.95E-08	9.83E-05
GO:0000070~mitotic sister chromatid segregation	36	2.99E-08	9.96E-05
GO:0051254~positive regulation of RNA metabolic process	59	3.02E-08	1.01E-04
GO:0048489~synaptic vesicle transport	59	3.02E-08	1.01E-04
GO:0006261~DNA-dependent DNA replication	42	3.10E-08	1.03E-04
GO:0031328~positive regulation of cellular biosynthetic process	89	3.28E-08	1.09E-04
GO:0012501~programmed cell death	89	3.28E-08	1.09E-04
GO:0009891~positive regulation of biosynthetic process	89	3.28E-08	1.09E-04
GO:0010628~positive regulation of gene expression	72	3.58E-08	1.19E-04
GO:0009057~macromolecule catabolic process	144	3.93E-08	1.31E-04
GO:0031175~neuron projection development	148	4.87E-08	1.62E-04
GO:0006796~phosphate metabolic process	258	5.46E-08	1.82E-04
GO:0006793~phosphorus metabolic process	258	5.46E-08	1.82E-04
GO:0006397~mRNA processing	107	5.68E-08	1.89E-04
GO:0045941~positive regulation of transcription	71	6.16E-08	2.05E-04

GO:0060429~epithelium development	125	6.45E-08	2.15E-04
GO:0048812~neuron projection morphogenesis	147	7.11E-08	2.37E-04
GO:0046486~glycerolipid metabolic process	43	7.51E-08	2.50E-04
GO:0008219~cell death	92	8.95E-08	2.98E-04
GO:0032774~RNA biosynthetic process	80	9.23E-08	3.07E-04
GO:0045893~positive regulation of transcription, DNA-dependent	57	9.99E-08	3.33E-04
GO:0030261~chromosome condensation	26	1.25E-07	4.15E-04
GO:0016265~death	92	1.32E-07	4.39E-04
GO:0006366~transcription from RNA polymerase II promoter	62	1.51E-07	5.02E-04
GO:0000904~cell morphogenesis involved in differentiation	153	1.61E-07	5.37E-04
GO:0006351~transcription, DNA-dependent	78	1.63E-07	5.41E-04
GO:0022403~cell cycle phase	233	1.92E-07	6.40E-04
GO:0048667~cell morphogenesis involved in neuron differentiation	146	2.36E-07	7.86E-04
GO:0006461~protein complex assembly	93	2.59E-07	8.62E-04
GO:0070271~protein complex biogenesis	93	2.59E-07	8.62E-04
GO:0006928~cell motion	153	2.73E-07	9.08E-04
GO:0006357~regulation of transcription from RNA polymerase II promoter	104	2.95E-07	9.82E-04
GO:0007243~protein kinase cascade	42	3.06E-07	0.0010201
GO:0019953~sexual reproduction	328	3.17E-07	0.0010555
GO:0007276~gamete generation	320	3.28E-07	0.0010913
GO:0006644~phospholipid metabolic process	54	3.30E-07	0.0010971
GO:0043632~modification-dependent macromolecule catabolic process	94	3.43E-07	0.0011423
GO:0032535~regulation of cellular component size	61	4.35E-07	0.0014489
GO:0019941~modification-dependent protein catabolic process	93	5.33E-07	0.0017739
GO:0001505~regulation of neurotransmitter levels	66	5.39E-07	0.0017944
GO:0006323~DNA packaging	44	6.38E-07	0.0021241
GO:0050767~regulation of neurogenesis	45	6.45E-07	0.0021478
GO:0009968~negative regulation of signal transduction	62	6.74E-07	0.0022429
GO:0007267~cell-cell signaling	111	7.89E-07	0.002626
GO:0002009~morphogenesis of an epithelium	117	8.34E-07	0.0027758
GO:0034660~ncRNA metabolic process	76	9.84E-07	0.0032717
GO:0007268~synaptic transmission	101	1.03E-06	0.0034254
GO:0051329~interphase of mitotic cell cycle	22	1.05E-06	0.003481
GO:0051325~interphase	22	1.05E-06	0.003481
GO:0006650~glycerophospholipid metabolic process	38	1.05E-06	0.0034871
GO:0010648~negative regulation of cell communication	62	1.08E-06	0.0035875
GO:0019226~transmission of nerve impulse	104	1.08E-06	0.0036064
GO:0043067~regulation of programmed cell death	65	2.17E-06	0.007207
GO:0006605~protein targeting	64	2.32E-06	0.0077101
GO:0016197~endosome transport	21	2.47E-06	0.008195
GO:0050803~regulation of synapse structure and activity	30	2.60E-06	0.0086159

GO:0051603~proteolysis involved in cellular protein catabolic process	97	2.77E-06	0.0091862
GO:0044257~cellular protein catabolic process	97	2.77E-06	0.0091862
GO:0051252~regulation of RNA metabolic process	300	2.77E-06	0.0091924
GO:0000910~cytokinesis	50	3.21E-06	0.0106329
GO:0019637~organophosphate metabolic process	58	3.42E-06	0.0113221
GO:0007391~dorsal closure	57	3.63E-06	0.0120227
GO:0030163~protein catabolic process	104	3.65E-06	0.0120809
GO:0051493~regulation of cytoskeleton organization	35	3.76E-06	0.01246
GO:0002165~instar larval or pupal development	195	3.85E-06	0.012743
GO:0032268~regulation of cellular protein metabolic process	73	3.96E-06	0.0130961
GO:0008356~asymmetric cell division	39	4.09E-06	0.0135277
GO:0048488~synaptic vesicle endocytosis	27	4.11E-06	0.0136079
GO:0007281~germ cell development	122	4.78E-06	0.0157932
GO:0022613~ribonucleoprotein complex biogenesis	56	6.07E-06	0.0200038
GO:0034622~cellular macromolecular complex assembly	88	6.17E-06	0.0203413
GO:0000279~M phase	218	6.94E-06	0.0228405
GO:0030030~cell projection organization	172	7.39E-06	0.0243003
GO:0009791~post-embryonic development	200	7.73E-06	0.0254133
GO:0010564~regulation of cell cycle process	51	8.17E-06	0.0268461
GO:0008105~asymmetric protein localization	26	8.62E-06	0.0282897
GO:0010941~regulation of cell death	65	1.09E-05	0.0356807
GO:0030707~ovarian follicle cell development	104	1.13E-05	0.0369022
GO:0060341~regulation of cellular localization	43	1.19E-05	0.0390012
GO:0007298~border follicle cell migration	42	1.24E-05	0.0403818
GO:0043484~regulation of RNA splicing	42	1.24E-05	0.0403818
GO:0032990~cell part morphogenesis	157	1.24E-05	0.0404863
GO:0048729~tissue morphogenesis	122	1.30E-05	0.04242
GO:0032970~regulation of actin filament-based process	23	1.32E-05	0.0430347
GO:0032956~regulation of actin cytoskeleton organization	23	1.32E-05	0.0430347
GO:0048585~negative regulation of response to stimulus	19	1.34E-05	0.0437617
GO:0030384~phosphoinositide metabolic process	32	1.34E-05	0.0437991
GO:0006338~chromatin remodeling	32	1.34E-05	0.0437991
GO:0008654~phospholipid biosynthetic process	33	1.38E-05	0.044825
GO:0007015~actin filament organization	50	1.38E-05	0.0448669
GO:0009994~oocyte differentiation	75	1.39E-05	0.045229
GO:0051129~negative regulation of cellular component organization	37	1.39E-05	0.0452828
GO:0045664~regulation of neuron differentiation	36	1.40E-05	0.0456419
Cellular Compartment			
GO:0031974~membrane-enclosed lumen	319	9.42E-19	6.13E-16
GO:0005694~chromosome	191	2.82E-18	1.84E-15
GO:0043233~organelle lumen	310	4.93E-18	3.21E-15

GO:0070013~intracellular organelle lumen	310	4.93E-18	3.21E-15
GO:0005654~nucleoplasm	170	1.39E-17	9.03E-15
GO:0031981~nuclear lumen	223	8.23E-15	5.35E-12
GO:0043232~intracellular non-membrane-bounded organelle	467	6.49E-14	4.23E-11
GO:0043228~non-membrane-bounded organelle	467	6.49E-14	4.23E-11
GO:0044427~chromosomal part	151	8.92E-14	5.81E-11
GO:0044451~nucleoplasm part	149	1.49E-13	9.71E-11
GO:0012505~endomembrane system	137	4.38E-13	2.85E-10
GO:0005938~cell cortex	56	9.46E-10	6.16E-07
GO:0005813~centrosome	41	1.99E-08	1.29E-05
GO:0005819~spindle	50	2.08E-08	1.36E-05
GO:0005856~cytoskeleton	185	4.64E-08	3.02E-05
GO:0005794~Golgi apparatus	96	3.29E-07	2.14E-04
GO:0005815~microtubule organizing center	43	7.94E-07	5.17E-04
GO:0005635~nuclear envelope	56	1.61E-06	0.0010466
GO:0005700~polytene chromosome	59	1.67E-06	0.0010888
GO:0000228~nuclear chromosome	51	2.49E-06	0.0016183
GO:0044454~nuclear chromosome part	46	6.69E-06	0.0043448
GO:0005789~endoplasmic reticulum membrane	49	7.23E-06	0.0046934
GO:0042175~nuclear envelope-endoplasmic reticulum network	50	7.35E-06	0.0047719
GO:0005768~endosome	25	1.26E-05	0.0081665
GO:0005681~spliceosome	46	2.02E-05	0.013064
GO:0044430~cytoskeletal part	145	3.26E-05	0.0209702
GO:0016327~apicolateral plasma membrane	32	3.76E-05	0.0241983
GO:0000785~chromatin	65	7.30E-05	0.0464249
Molecular function			
GO:0000166~nucleotide binding	645	1.11E-30	1.77E-27
GO:0032553~ribonucleotide binding	511	1.65E-28	2.64E-25
GO:0032555~purine ribonucleotide binding	511	1.65E-28	2.64E-25
GO:0017076~purine nucleotide binding	535	1.35E-26	2.15E-23
GO:0032559~adenyl ribonucleotide binding	421	6.87E-25	1.10E-21
GO:0005524~ATP binding	419	1.60E-24	2.56E-21
GO:0001883~purine nucleoside binding	446	4.96E-23	7.92E-20
GO:0001882~nucleoside binding	448	1.16E-22	1.85E-19
GO:0030554~adenyl nucleotide binding	442	1.74E-22	2.77E-19
GO:0008270~zinc ion binding	508	1.41E-14	2.25E-11
GO:0003677~DNA binding	416	6.46E-13	1.03E-09
GO:0004386~helicase activity	78	7.33E-12	1.17E-08
GO:0003729~mRNA binding	118	8.09E-12	1.29E-08
GO:0019899~enzyme binding	53	2.28E-11	3.64E-08
GO:0008026~ATP-dependent helicase activity	58	4.85E-10	7.73E-07
GO:0070035~purine NTP-dependent helicase activity	58	4.85E-10	7.73E-07
GO:0008092~cytoskeletal protein binding	128	1.62E-09	2.59E-06

GO:0016779~nucleotidyltransferase activity	62	1.45E-08	2.31E-05
GO:0008134~transcription factor binding	61	2.59E-08	4.14E-05
GO:0004674~protein serine/threonine kinase activity	116	8.25E-08	1.32E-04
GO:0003779~actin binding	76	1.87E-07	2.99E-04
GO:0015631~tubulin binding	48	2.69E-07	4.29E-04
GO:0004672~protein kinase activity	151	3.13E-07	4.99E-04
GO:0008017~microtubule binding	44	1.49E-06	0.0023681
GO:0060589~nucleoside-triphosphatase regulator activity	83	6.49E-06	0.0103107
GO:0046914~transition metal ion binding	593	8.39E-06	0.0133079
GO:0003682~chromatin binding	43	9.26E-06	0.0146667
GO:0030695~GTPase regulator activity	81	1.02E-05	0.0161191
GO:0043566~structure-specific DNA binding	25	1.12E-05	0.0177629
GO:0004004~ATP-dependent RNA helicase activity	30	1.26E-05	0.0198994
GO:0008186~RNA-dependent ATPase activity	30	1.26E-05	0.0198994
GO:0003712~transcription cofactor activity	42	1.60E-05	0.0252827
GO:0005083~small GTPase regulator activity	64	2.03E-05	0.0318264
GO:0003924~GTPase activity	74	2.86E-05	0.044638
GO:0042802~identical protein binding	81	2.86E-05	0.0446407
KEGG pathway			
dme03040:Spliceosome	71	1.05E-04	0.0116223
dme04320:Dorso-ventral axis formation	22	2.41E-04	0.0263651
dme04144:Endocytosis	53	2.83E-04	0.0309255
dme03018:RNA degradation	35	3.05E-04	0.033305
dme04120:Ubiquitin mediated proteolysis	62	3.34E-04	0.0363751
dme00970:Aminoacyl-tRNA biosynthesis	27	0.006009	0.4877783

REFERENCES

Anderson, M. A., Jodoin, J. N., Lee, E., Hales, K. G., Hays, T. S. and Lee, L. A. (2009). asunder Is a Critical Regulator of Dynein-Dynactin Localization during Drosophila Spermatogenesis. *Molecular Biology of the Cell* **20**, 2709-2721.
Andruss, B. F., Bolduc, C. and Beckingham, K. (2004). Movement of calmodulin between cells in the ovary and embryo of drosophila. *Genesis* **38**, 93-103.
Ashburner, M. (1989). Drosophila. A laboratory handbook.
Avila, F. W. and Wolfner, M. F. (2009). Acp36DE is required for uterine conformational changes in mated Drosophila females. *Proceedings of the National Academy of Sciences of the United States of America* **106**, 15796-15800.
Bard, J., Zhelkovsky, A. M., Helmling, S., Earnest, T. N., Moore, C. L. and Bohm, A. (2000). Structure of yeast poly(A) polymerase alone and in complex with 3 '-dATP. *Science* **289**, 1346-1349.
Barkoff, A. F., Dickson, K. S., Gray, N. K. and Wickens, M. (2000). Translational control of cyclin B1 mRNA during meiotic maturation: coordinated repression and cytoplasmic polyadenylation. *Developmental biology* **220**, 97-109.
Barnard, D. C., Ryan, K., Manley, J. L. and Richter, J. D. (2004). Symplekin and xGLD-2 are required for CPEB-mediated cytoplasmic polyadenylation. *Cell* **119**, 641-51.
Barreau, C., Benson, E., Gudmannsdottir, E., Newton, F. and White-Cooper, H. (2008). Post-meiotic transcription in Drosophila testes. *Development* **135**, 1897-1902.
Bashirullah, A., Halsell, S. R., Cooperstock, R. L., Kloc, M., Karaiskakis, A., Fisher, W. W., Fu, W., Hamilton, J. K., Etkin, L. D. and Lipshitz, H. D. (1999). Joint action of two RNA degradation pathways controls the timing of maternal transcript elimination at the midblastula transition in Drosophila melanogaster. *EMBO J* **18**, 2610-20.
Belloc, E., Pique, M. and Mendez, R. (2008). Sequential waves of polyadenylation and deadenylation define a translation circuit that drives meiotic progression. *Biochem Soc Trans* **36**, 665-70.
Benoit, B., Mitou, G., Chartier, A., Temme, C., Zaessinger, S., Wahle, E., Busseau, I. and Simonelig, M. (2005). An essential cytoplasmic function for the nuclear poly(A) binding protein, PABP2, in poly(A) tail length control and early development in Drosophila. *Dev Cell* **9**, 511-22.
Benoit, P., Papin, C., Kwak, J. E., Wickens, M. and Simonelig, M. (2008). PAP- and GLD-2-type poly(A) polymerases are required sequentially in cytoplasmic polyadenylation and oogenesis in Drosophila. *Development* **135**, 1969-79.
Bernhardt, M. L., Kim, A. M., O'Halloran, T. V. and Woodruff, T. K. (2011). Zinc requirement during meiosis I-meiosis II transition in mouse oocytes is independent of the MOS-MAPK pathway. *Biol Reprod* **84**, 526-36.
Betran, E., Thornton, K. and Long, M. (2002). Retroposed new genes out of the X in Drosophila. *Genome Research* **12**, 1854-1859.
Boswell, R. E. and Mahowald, A. P. (1985). tudor, a gene required for assembly of the germ plasm in Drosophila melanogaster. *Cell* **43**, 97-104.
Braun, R. E. (1998). Post-transcriptional control of gene expression during spermatogenesis. *Seminars in cell & developmental biology* **9**, 483-489.

Brent, A. E., MacQueen, A. and Hazelrigg, T. (2000). The Drosophila wispy gene is required for RNA localization and other microtubule-based events of meiosis and early embryogenesis. *Genetics* **154**, 1649-62.
Castagnetti, S. and Ephrussi, A. (2003). Orb and a long poly(A) tail are required for efficient oskar translation at the posterior pole of the Drosophila oocyte. *Development* **130**, 835-43.
Chang, J. S., Tan, L. and Schedl, P. (1999). The Drosophila CPEB homolog, orb, is required for oskar protein expression in oocytes. *Dev Biol* **215**, 91-106.
Chen, D. H. and McKearin, D. M. (2003). A discrete transcriptional silencer in the bam gene determines asymmetric division of the Drosophila germline stem cell. *Development* **130**, 1159-1170.
Chintapalli, V. R., Wang, J. and Dow, J. A. (2007). Using FlyAtlas to identify better Drosophila melanogaster models of human disease. *Nat Genet* **39**, 715-20.
Choi, T., Fukasawa, K., Zhou, R., Tessarollo, L., Borror, K., Resau, J. and Vande Woude, G. F. (1996). The Mos/mitogen-activated protein kinase (MAPK) pathway regulates the size and degradation of the first polar body in maturing mouse oocytes. *Proc Natl Acad Sci U S A* **93**, 7032-5.
Clark, A. G. Eisen, M. B. Smith, D. R. Bergman, C. M. Oliver, B. Markow, T. A. Kaufman, T. C. Kellis, M. Gelbart, W. Iyer, V. N. et al. (2007). Evolution of genes and genomes on the Drosophila phylogeny. *Nature* **450**, 203-218.
Cui, J., Sackton, K. L., Horner, V. L., Kumar, K. E. and Wolfner, M. F. (2008). Wispy, the Drosophila homolog of GLD-2, is required during oogenesis and egg activation. *Genetics* **178**, 2017-29.
De Nadai, C., Huitorel, P., Chiri, S. and Ciapa, B. (1998). Effect of wortmannin, an inhibitor of phosphatidylinositol 3-kinase, on the first mitotic divisions of the fertilized sea urchin egg. *J Cell Sci* **111 (Pt 17)**, 2507-18.
Deng, M. Q., Huang, X. Y., Tang, T. S. and Sun, F. Z. (1998). Spontaneous and fertilization-induced Ca2+ oscillations in mouse immature germinal vesicle-stage oocytes. *Biol Reprod* **58**, 807-13.
Dennis, G., Jr., Sherman, B. T., Hosack, D. A., Yang, J., Gao, W., Lane, H. C. and Lempicki, R. A. (2003). DAVID: Database for Annotation, Visualization, and Integrated Discovery. *Genome Biol* **4**, P3.
Dickson, K. S., Bilger, A., Ballantyne, S. and Wickens, M. P. (1999). The cleavage and polyadenylation specificity factor in *Xenopus laevis* oocytes is a cytoplasmic factor involved in regulated polyadenylation. *Mol Cell Biol* **19**, 5707-17.
Dietzl, G., Chen, D., Schnorrer, F., Su, K. C., Barinova, Y., Fellner, M., Gasser, B., Kinsey, K., Oppel, S., Scheiblauer, S. et al. (2007). A genome-wide transgenic RNAi library for conditional gene inactivation in Drosophila. *Nature* **448**, 151-U1.
Doane, W. W. (1960). Completion of meiosis in uninseminated eggs of *Drosophila melanogaster*. *Science* **132**, 677-8.
Ducibella, T., Schultz, R. M. and Ozil, J.-P. (2006). Role of calcium signals in early development. *Seminars in cell & developmental biology* **17**, 324-32.
Duffy, J. B. (2002). GAL4 system in Drosophila: a fly geneticist's Swiss army knife. *Genesis* **34**, 1-15.
Endow, S. A. and Komma, D. J. (1997). Spindle dynamics during meiosis in Drosophila oocytes. *J Cell Biol* **137**, 1321-36.

Fabian, L., Wei, H. C., Rollins, J., Noguchi, T., Blankenship, J. T., Bellamkonda, K., Polevoy, G., Gervais, L., Guichet, A., Fuller, M. T. et al. (2010). Phosphatidylinositol 4,5-bisphosphate Directs Spermatid Cell Polarity and Exocyst Localization in Drosophila. *Molecular Biology of the Cell* **21**, 1546-1555.
Fabrizio, J. J., Hime, G., Lemmon, S. K. and Bazinet, C. (1998). Genetic dissection of sperm individualization in Drosophila melanogaster. *Development* **125**, 1833-1843.
Fuentes, J. J., Genesca, L., Kingsbury, T. J., Cunningham, K. W., Perez-Riba, M., Estivill, X. and de la Luna, S. (2000). DSCR1, overexpressed in Down syndrome, is an inhibitor of calcineurin-mediated signaling pathways. *Hum Mol Genet* **9**, 1681-90.
Fuller, M. T. (1993). Spermatogenesis. In *The development of Drosophila melanogaster*, vol. 1, pp. 71-147.
Fuller, M. T. (1998). Genetic control of cell proliferation and differentiation in Drosophila spermatogenesis. *Seminars in cell & developmental biology* **9**, 433-444.
Galili, G., Kawata, E. E., Smith, L. D. and Larkins, B. A. (1988). Role of the 3'-poly(A) sequence in translational regulation of messenger RNAs in Xenopus laevis oocytes. *Journal of Biological Chemistry* **263**, 5764-5770.
Ghosh-Roy, A., Desai, B. S. and Ray, K. (2005). Dynein light chain 1 regulates dynamin-mediated F-actin assembly during sperm individualization in Drosophila. *Molecular Biology of the Cell* **16**, 3107-3116.
Ghosh-Roy, A., Kulkarni, M., Kumar, V., Shirolikar, S. and Ray, K. (2004). Cytoplasmic dynein-dynactin complex is required for spermatid growth but not axoneme assembly in Drosophila. *Molecular Biology of the Cell* **15**, 2470-2483.
Giusti, A. F., Carroll, D. J., Abassi, Y. A. and Foltz, K. R. (1999). Evidence that a starfish egg Src family tyrosine kinase associates with PLC-gamma1 SH2 domains at fertilization. *Dev Biol* **208**, 189-99.
Gong, Z., Son, W., Chung, Y. D., Kim, J., Shin, D. W., McClung, C. A., Lee, Y., Lee, H. W., Chang, D. J., Kaang, B. K. et al. (2004). Two interdependent TRPV channel subunits, inactive and Nanchung, mediate hearing in Drosophila. *J Neurosci* **24**, 9059-66.
Gorlach, J., Fox, D. S., Cutler, N. S., Cox, G. M., Perfect, J. R. and Heitman, J. (2000). Identification and characterization of a highly conserved calcineurin binding protein, CBP1/calcipressin, in Cryptococcus neoformans. *EMBO J* **19**, 3618-29.
Griffith, L. C., Verselis, L. M., Aitken, K. M., Kyriacou, C. P., Danho, W. and Greenspan, R. J. (1993). Inhibition of calcium/calmodulin-dependent protein kinase in Drosophila disrupts behavioral plasticity. *Neuron* **10**, 501-9.
Hake, L. E. and Richter, J. D. (1994). CPEB is a specificity factor that mediates cytoplasmic polyadenylation during Xenopus oocyte maturation. *Cell* **79**, 617-27.
Hansen, D. V., Tung, J. J. and Jackson, P. K. (2006). CaMKII and polo-like kinase 1 sequentially phosphorylate the cytostatic factor Emi2/XErp1 to trigger its destruction and meiotic exit. *Proc Natl Acad Sci U S A* **103**, 608-13.
Hardie, R. C. (2007). TRP channels and lipids: from Drosophila to mammalian physiology. *J Physiol* **578**, 9-24.
Harteneck, C., Frenzel, H. and Kraft, R. (2007). N-(p-amylcinnamoyl)anthranilic acid (ACA): a phospholipase A(2) inhibitor and TRP channel blocker. *Cardiovasc Drug Rev* **25**, 61-75.
Heifetz, Y., Yu, J. and Wolfner, M. F. (2001). Ovulation triggers activation of Drosophila oocytes. *Dev Biol* **234**, 416-24.

Hense, W., Baines, J. F. and Parsch, J. (2007). X chromosome inactivation during Drosophila spermatogenesis. *PLoS Biology* **5**.
Horner, V. L., Czank, A., Jang, J. K., Singh, N., Williams, B. C., Puro, J., Kubli, E., Hanes, S. D., McKim, K. S., Wolfner, M. F. et al. (2006). The Drosophila calcipressin *sarah* is required for several aspects of egg activation. *Current biology : CB* **16**, 1441-6.
Horner, V. L. and Wolfner, M. F. (2008a). Mechanical stimulation by osmotic and hydrostatic pressure activates Drosophila oocytes in vitro in a calcium-dependent manner. *Dev Biol* **316**, 100-9.
Horner, V. L. and Wolfner, M. F. (2008b). Transitioning from egg to embryo: triggers and mechanisms of egg activation. *Dev Dyn* **237**, 527-44.
Hurst, D., Rylett, C. M., Isaac, R. E. and Shirras, A. D. (2003). The Drosophila angiotensin-converting enzyme homologue Ance is required for spermiogenesis. *Developmental biology* **254**, 238-247.
Ivanovska, I., Lee, E., Kwan, K. M., Fenger, D. D. and Orr-Weaver, T. L. (2004). The Drosophila MOS ortholog is not essential for meiosis. *Curr Biol* **14**, 75-80.
Jan, C. H., Friedman, R. C., Ruby, J. G. and Bartel, D. P. (2011). Formation, regulation and evolution of Caenorhabditis elegans 3'UTRs. *Nature* **469**, 97-101.
Juge, F., Zaessinger, S., Temme, C., Wahle, E. and Simonelig, M. (2002). Control of poly(A) polymerase level is essential to cytoplasmic polyadenylation and early development in Drosophila. *EMBO J* **21**, 6603-13.
Kadyk, L. C. and Kimble, J. (1998). Genetic regulation of entry into meiosis in *Caenorhabditis elegans*. *Development* **125**, 1803-13.
Kashiwabara, S., Noguchi, J., Zhuang, T., Ohmura, K., Honda, A., Sugiura, S., Miyamoto, K., Takahashi, S., Inoue, K., Ogura, A. et al. (2002). Regulation of spermatogenesis by testis-specific, cytoplasmic poly(A) polymerase TPAP. *Science (New York, N Y)* **298**, 1999-2002.
Kashiwabara, S., Zhuang, T., Yamagata, K., Noguchi, J., Fukamizu, A. and Baba, T. (2000). Identification of a novel isoform of poly(A) polymerase, TPAP, specifically present in the cytoplasm of spermatogenic cells. *Dev Biol* **228**, 106-15.
Keene, J. D., Komisarow, J. M. and Friedersdorf, M. B. (2006). RIP-Chip: the isolation and identification of mRNAs, microRNAs and protein components of ribonucleoprotein complexes from cell extracts. *Nat Protoc* **1**, 302-7.
Kim, A. M., Bernhardt, M. L., Kong, B. Y., Ahn, R. W., Vogt, S., Woodruff, T. K. and O'Halloran, T. V. (2011). Zinc sparks are triggered by fertilization and facilitate cell cycle resumption in mammalian eggs. *ACS Chem Biol* **6**, 716-23.
Kim, J., Chung, Y. D., Park, D. Y., Choi, S., Shin, D. W., Soh, H., Lee, H. W., Son, W., Yim, J., Park, C. S. et al. (2003). A TRPV family ion channel required for hearing in Drosophila. *Nature* **424**, 81-4.
Kim, J. H. and Richter, J. D. (2006). Opposing polymerase-deadenylase activities regulate cytoplasmic polyadenylation. *Mol Cell* **24**, 173-83.
Kim, J. H. and Richter, J. D. (2007). RINGO/cdk1 and CPEB mediate poly(A) tail stabilization and translational regulation by ePAB. *Genes Dev* **21**, 2571-9.
Kim, K. W., Nykamp, K., Suh, N., Bachorik, J. L., Wang, L. and Kimble, J. (2009). Antagonism between GLD-2 binding partners controls gamete sex. *Dev Cell* **16**, 723-33.
Kim, K. W., Wilson, T. L. and Kimble, J. (2010). GLD-2/RNP-8 cytoplasmic poly(A) polymerase is a broad-spectrum regulator of the oogenesis program. *Proceedings of the National Academy of Sciences of the United States of America* **107**, 17445-50.

King, P. E. and Rafai, J. (1970). A possible mechanism for initiating the parthenogenetic development of eggs in a parasitoid Hymenopteran, Nasonia vitripennis. *The Entomologist* **106**, 118-120.
Kingsbury, T. J. and Cunningham, K. W. (2000). A conserved family of calcineurin regulators. *Genes Dev* **14**, 1595-604.
Kleene, K. C., Distel, R. J. and Hecht, N. B. (1984). Translational regulation and deadenylation of a protamine messenger RNa during spermiogenesis in the mouse. *Developmental biology* **105**, 71-79.
Krauchunas, A. R., Horner, V. L. and Wolfner, M. F. (2012). Protein phosphorylation changes reveal new candidates in the regulation of egg activation and early embryogenesis in D. melanogaster. *Developmental biology*.
Krauchunas, A. R. and Wolfner, M. F. (2013). Molecular changes during egg activation. *Curr Top Dev Biol* **102**, 267-92.
Kwak, J. E., Drier, E., Barbee, S. A., Ramaswami, M., Yin, J. C. and Wickens, M. (2008). GLD2 poly(A) polymerase is required for long-term memory. *Proc Natl Acad Sci U S A* **105**, 14644-9.
Kwak, J. E., Wang, L., Ballantyne, S., Kimble, J. and Wickens, M. (2004). Mammalian GLD-2 homologs are poly(A) polymerases. *Proc Natl Acad Sci U S A* **101**, 4407-12.
Kwak, J. E. and Wickens, M. (2007). A family of poly(U) polymerases. *RNA* **13**, 860-7.
Lee, S. J., Madden, P. J. and Shen, S. S. (1998). U73122 blocked the cGMP-induced calcium release in sea urchin eggs. *Exp Cell Res* **242**, 328-40.
Lewis, J. D., Song, Y., de Jong, M. E., Bagha, S. M. and Ausio, J. (2003). A walk though vertebrate and invertebrate protamines. *Chromosoma* **111**, 473-482.
Lin, H. F. and Wolfner, M. F. (1991). The Drosophila maternal-effect gene fs(1)Ya encodes a cell cycle-dependent nuclear envelope component required for embryonic mitosis. *Cell* **64**, 49-62.
Mahowald, A. P., Goralski, T. J. and Caulton, J. H. (1983). In vitro activation of Drosophila eggs. *Dev Biol* **98**, 437-45.
Malcuit, C., Kurokawa, M. and Fissore, R. A. (2006). Calcium oscillations and mammalian egg activation. *J Cell Physiol* **206**, 565-73.
Manier, M. K., Belote, J. M., Berben, K. S., Novikov, D., Stuart, W. T. and Pitnick, S. (2010). Resolving Mechanisms of Competitive Fertilization Success in Drosophila melanogaster. *Science* **328**, 354-357.
Marinotti, O., Nguyen, Q. K., Calvo, E., James, A. A. and Ribeiro, J. M. C. (2005). Microarray analysis of genes showing variable expression following a blood meal in Anopheles gambiae. *Insect Molecular Biology* **14**, 365-373.
Markoulaki, S., Matson, S., Abbott, A. L. and Ducibella, T. (2003). Oscillatory CaMKII activity in mouse egg activation. *Dev Biol* **258**, 464-74.
Markow, T. A., Beall, S. and Matzkin, L. M. (2009). Egg size, embryonic development time and ovoviviparity in Drosophila species. *J Evol Biol* **22**, 430-4.
Martin, G., Keller, W. and Doublie, S. (2000). Crystal structure of mammalian poly(A) polymerase in complex with an analog of ATP. *EMBO Journal* **19**, 4193-4203.
McQuilton, P., St Pierre, S. E. and Thurmond, J. (2012). FlyBase 101--the basics of navigating FlyBase. *Nucleic Acids Res* **40**, D706-14.
Meisel, R. P., Han, M. V. and Hahn, M. W. (2009). A complex suite of forces drives gene traffic from Drosophila X chromosomes. *Genome Biol Evol* **1**, 176-88.

Mendez, R., Murthy, K. G., Ryan, K., Manley, J. L. and Richter, J. D. (2000). Phosphorylation of CPEB by Eg2 mediates the recruitment of CPSF into an active cytoplasmic polyadenylation complex. *Mol Cell* **6**, 1253-9.
Mendez, R. and Richter, J. D. (2001). Translational control by CPEB: A means to the end. *Nature reviews Molecular cell biology* **2**, 521-529.
Miao, Y. L., Stein, P., Jefferson, W. N., Padilla-Banks, E. and Williams, C. J. (2012). Calcium influx-mediated signaling is required for complete mouse egg activation. *Proc Natl Acad Sci U S A* **109**, 4169-74.
Miyawaki, A., Llopis, J., Heim, R., McCaffery, J. M., Adams, J. A., Ikura, M. and Tsien, R. Y. (1997). Fluorescent indicators for Ca2+ based on green fluorescent proteins and calmodulin. *Nature* **388**, 882-7.
Miyazaki, S. and Ito, M. (2006). Calcium signals for egg activation in mammals. *J Pharmacol Sci* **100**, 545-52.
Mochida, S. and Hunt, T. (2007). Calcineurin is required to release Xenopus egg extracts from meiotic M phase. *Nature* **449**, 336-40.
Montell, C. (2005). Drosophila TRP channels. *Pflugers Arch* **451**, 19-28.
Nakanishi, T., Kubota, H., Ishibashi, N., Kumagai, S., Watanabe, H., Yamashita, M., Kashiwabara, S., Miyado, K. and Baba, T. (2006). Possible role of mouse poly(A) polymerase mGLD-2 during oocyte maturation. *Dev Biol* **289**, 115-26.
Nishiyama, T., Yoshizaki, N., Kishimoto, T. and Ohsumi, K. (2007). Transient activation of calcineurin is essential to initiate embryonic development in Xenopus laevis. *Nature* **449**, 341-5.
Noguchi, T. and Miller, K. G. (2003). A role for actin dynamics in individualization during spermatogenesis in Drosophila melanogaster. *Development* **130**, 1805-1816.
Novoa, I., Gallego, J., Ferreira, P. G. and Mendez, R. (2010). Mitotic cell-cycle progression is regulated by CPEB1 and CPEB4-dependent translational control. *Nat Cell Biol* **12**, 447-56.
Olivieri, G. and Olivieri, A. (1965). Autoradiographic study of nucleic acid synthesis during spermatogenesis in Drosophila melanogaster. *Mutat Res* **2**, 366-80.
Page, A. W. and Orr-Weaver, T. L. (1997). Activation of the meiotic divisions in Drosophila oocytes. *Dev Biol* **183**, 195-207.
Parry, H., McDougall, A. and Whitaker, M. (2005). Microdomains bounded by endoplasmic reticulum segregate cell cycle calcium transients in syncytial Drosophila embryos. *J Cell Biol* **171**, 47-59.
Pesin, J. A. and Orr-Weaver, T. L. (2007). Developmental role and regulation of cortex, a meiosis-specific anaphase-promoting complex/cyclosome activator. *PLoS Genet* **3**, e202.
Peters, J.-M. (2006). The anaphase promoting complex/cyclosome: a machine designed to destroy. *Nat Rev Mol Cell Biol.* **116**, 221-234.
Philip, P. J. M., Sudaka, I. and Melygoubert, B. (1992). Fluorescent staining of the actin cytoskeleton in human lymphocytes, monocytes, and polymorphonuclear cells using a DNase1/anti-DNase1 immunoglobulin fluorescein conjugated system. *Histochemistry* **97**, 83-86.
Pique, M., Lopez, J. M., Foissac, S., Guigo, R. and Mendez, R. (2008). A combinatorial code for CPE-mediated translational control. *Cell* **132**, 434-448.
Pleiss, J. A., Whitworth, G. B., Bergkessel, M. and Guthrie, C. (2007). Rapid, transcript-specific changes in splicing in response to environmental stress. *Mol Cell* **27**, 928-37.
Preiss, T., Muckenthaler, M. and Hentze, M. W. (1998). Poly(A)-tail-promoted translation in yeast: Implications for translational control. *RNA* **4**, 1321-1331.

Raja, S. J. and Renkawitz-Pohl, R. (2006). Replacement by Drosophila melanogaster protamines and Mst77F of histones during chromatin condensation in late spermatids and role of sesame in the removal of these proteins from the male pronucleus (vol 25, pg 6165, 2005). *Molecular and Cellular Biology* **26**, 3682-3682.
Rathke, C., Baarends, W. M., Jayaramaiah-Raja, S., Bartkuhn, M., Renkawitz, R. and Renkawitz-Pohl, R. (2007). Transition from a nucleosome-based to a protamine-based chromatin configuration during spermiogenesis in Drosophila. *Journal of Cell Science* **120**, 1689-1700.
Raz, T. and Shalgi, R. (1998). Early events in mammalian egg activation. *Hum Reprod* **13 Suppl 4**, 133-45.
Regen, D. M. (1996). Tensions and stresses of ellipsoidal chambers. *Ann Biomed Eng* **24**, 400-17.
Rice, A., Parrington, J., Jones, K. T. and Swann, K. (2000). Mammalian sperm contain a Ca(2+)-sensitive phospholipase C activity that can generate InsP(3) from PIP(2) associated with intracellular organelles. *Dev Biol* **228**, 125-35.
Richter, J. D. (2007). CPEB: a life in translation. *Trends Biochem Sci* **32**, 279-85.
Rorth, P. (1998). Gal4 in the Drosophila female germline. *Mech Dev* **78**, 113-8.
Rouhana, L., Wang, L., Buter, N., Kwak, J. E., Schiltz, C. A., Gonzalez, T., Kelley, A. E., Landry, C. F. and Wickens, M. (2005). Vertebrate GLD2 poly(A) polymerases in the germline and the brain. *RNA* **11**, 1117-30.
Roux, M. M., Townley, I. K., Raisch, M., Reade, A., Bradham, C., Humphreys, G., Gunaratne, H. J., Killian, C. E., Moy, G., Su, Y. H. et al. (2006). A functional genomic and proteomic perspective of sea urchin calcium signaling and egg activation. *Dev Biol* **300**, 416-33.
Sackton, K. L., Buehner, N. A. and Wolfner, M. F. (2007). Modulation of MAPK activities during egg activation in Drosophila. *Fly* **1**, 222-227.
Sackton, K. L., Lopez, J. M., Berman, C. L. and Wolfner, M. F. (2009). YA is needed for proper nuclear organization to transition between meiosis and mitosis in Drosophila. *BMC Dev Biol* **9**, 43.
Salles, F. J., Lieberfarb, M. E., Wreden, C., Gergen, J. P. and Strickland, S. (1994). Coordinate initiation of Drosophila development by regulated polyadenylation of maternal messenger RNAs. *Science (New York, N Y)* **266**, 1996-9.
Salles, F. J. and Strickland, S. (1999). Analysis of poly(A) tail lengths by PCR: the PAT assay. *Methods Mol Biol* **118**, 441-8.
Santel, A., Winhauer, T., Blumer, N. and RenkawitzPohl, R. (1997). The Drosophila don juan (dj) gene encodes a novel sperm specific protein component characterized by an unusual domain of a repetitive amino acid motif. *Mechanisms of Development* **64**, 19-30.
Sartain, C. V., Cui, J., Meisel, R. P. and Wolfner, M. F. (2011). The poly(A) polymerase GLD2 is required for spermatogenesis in Drosophila melanogaster. *Development* **138**, 1619-29.
Sartain, C. V. and Wolfner, M. F. (2013). Calcium and egg activation in Drosophila. *Cell Calcium* **53**, 10-5.
Sato, K., Tokmakov, A. A., Iwasaki, T. and Fukami, Y. (2000). Tyrosine kinase-dependent activation of phospholipase Cgamma is required for calcium transient in Xenopus egg fertilization. *Dev Biol* **224**, 453-69.
Saunders, C. M., Larman, M. G., Parrington, J., Cox, L. J., Royse, J., Blayney, L. M., Swann, K. and Lai, F. A. (2002). PLC zeta: a sperm-specific trigger of Ca(2+) oscillations in eggs and embryo development. *Development* **129**, 3533-44.

Schafer, M., Kuhn, R., Bosse, F. and Schafer, U. (1990). A conserved element in the lader mediates postmeiotic translation as well as cytoplasmic polyadenylation of a Drosophila spermatocyte messenger RNA. *EMBO Journal* **9**, 4519-4525.
Smyth, G. K. and Speed, T. (2003). Normalization of cDNA microarray data. *Methods* **31**, 265-73.
Snabes, M. C., Boyd, A. E., Pardue, R. L. and Bryan, J. (1981). A DNase1 binding immunoprecipitation assay for actin. *Journal of Biological Chemistry* **256**, 6291-6295.
Sousa-Neves, R. and Schinaman, J. M. A novel genetic tool for clonal analysis of fourth chromosome mutations. *Fly (Austin)* **6**, 49-56.
Spradling, A. C. (1993). Developmental Genetics of Oogenesis. In *The Development of Drosophila melanogaster*, vol. 1, pp. 1-69. Cold Spring Harbor: Cold Spring Harbor Laboratory Press.
Stebbins-Boaz, B., Hake, L. E. and Richter, J. D. (1996). CPEB controls the cytoplasmic polyadenylation of cyclin, Cdk2 and c-mos mRNAs and is necessary for oocyte maturation in Xenopus. *The EMBO journal* **15**, 2582-92.
Stricker, S. A. (1999). Comparative biology of calcium signaling during fertilization and egg activation in animals. *Dev Biol* **211**, 157-76.
Swan, A. and Schupbach, T. (2007). The Cdc20 (Fzy)/Cdh1-related protein, Cort, cooperates with Fzy in cyclin destruction and anaphase progression in meiosis I and II in Drosophila. *Development* **134**, 891-9.
Swann, K., Saunders, C. M., Rogers, N. T. and Lai, F. A. (2006). PLCzeta(zeta): a sperm protein that triggers Ca2+ oscillations and egg activation in mammals. *Seminars in cell & developmental biology* **17**, 264-73.
Tadros, W., Goldman, A. L., Babak, T., Menzies, F., Vardy, L., Orr-Weaver, T., Hughes, T. R., Westwood, J. T., Smibert, C. A. and Lipshitz, H. D. (2007). SMAUG is a major regulator of maternal mRNA destabilization in Drosophila and its translation is activated by the PAN GU kinase. *Dev Cell* **12**, 143-55.
Tadros, W., Houston, S. A., Bashirullah, A., Cooperstock, R. L., Semotok, J. L., Reed, B. H. and Lipshitz, H. D. (2003). Regulation of maternal transcript destabilization during egg activation in Drosophila. *Genetics* **164**, 989-1001.
Tadros, W. and Lipshitz, H. D. (2005). Setting the stage for development: mRNA translation and stability during oocyte maturation and egg activation in Drosophila. *Dev Dyn* **232**, 593-608.
Tadros, W. and Lipshitz, H. D. (2009). The maternal-to-zygotic transition: a play in two acts. *Development* **136**, 3033-42.
Takeo, S., Hawley, R. S. and Aigaki, T. (2010). Calcineurin and its regulation by Sra/RCAN is required for completion of meiosis in Drosophila. *Dev Biol* **344**, 957-67.
Takeo, S., Swanson, S. K., Nandanan, K., Nakai, Y., Aigaki, T., Washburn, M. P., Florens, L. and Hawley, R. S. (2012). Shaggy/glycogen synthase kinase 3beta and phosphorylation of Sarah/regulator of calcineurin are essential for completion of Drosophila female meiosis. *Proc Natl Acad Sci U S A* **109**, 6382-9.
Takeo, S., Tsuda, M., Akahori, S., Matsuo, T. and Aigaki, T. (2006). The calcineurin regulator sra plays an essential role in female meiosis in Drosophila. *Curr Biol* **16**, 1435-40.
Tamura, K., Subramanian, S. and Kumar, S. (2004). Temporal patterns of fruit fly (Drosophila) evolution revealed by mutation clocks. *Molecular Biology and Evolution* **21**, 36-44.
Tates, A. D. (1971). Cytodifferentiation during spermatogenesis in *Drosophila melanogaster*: an electron microscope study. In *Ph.D. Dissertation*. Leiden: Rijksuniversiteit.

Texada, M. J., Simonette, R. A., Johnson, C. B., Deery, W. J. and Beckingham, K. M. (2008). yuri gagarin is required for actin, tubulin and basal body functions in Drosophila spermatogenesis. *Journal of Cell Science* **121**, 1926-1936.
Tian, L., Hires, S. A., Mao, T., Huber, D., Chiappe, M. E., Chalasani, S. H., Petreanu, L., Akerboom, J., McKinney, S. A., Schreiter, E. R. et al. (2009). Imaging neural activity in worms, flies and mice with improved GCaMP calcium indicators. *Nat Methods* **6**, 875-81.
Tokuyasu, K. T. (1974). Dynamics of spermiogenesis in Drosophila melanogaster 4: Nuclear transformation. *Journal of Ultrastructure Research* **48**, 284-303.
Tokuyasu, K. T., Hardy, R. W. and Peacock, W. J. (1972). Dynamics of spermiogenesis in Drosophila melanogaster 1: Individualization process. *Zeitschrift Fur Zellforschung Und Mikroskopische Anatomie* **124**, 479-&.
Townley, I. K., Roux, M. M. and Foltz, K. R. (2006). Signal transduction at fertilization: the Ca2+ release pathway in echinoderms and other invertebrate deuterostomes. *Semin Cell Dev Biol* **17**, 293-302.
Turner, J. M. A. (2007). Meiotic sex chromosome inactivation. *Development* **134**, 1823-1831.
Tusher, V. G., Tibshirani, R. and Chu, G. (2001). Significance analysis of microarrays applied to the ionizing radiation response. *Proc Natl Acad Sci U S A* **98**, 5116-21.
VanBerkum, M. F. and Goodman, C. S. (1995). Targeted disruption of Ca(2+)-calmodulin signaling in Drosophila growth cones leads to stalls in axon extension and errors in axon guidance. *Neuron* **14**, 43-56.
Vardy, L. and Orr-Weaver, T. L. (2007a). Regulating translation of maternal messages: multiple repression mechanisms. *Trends Cell Biol* **17**, 547-54.
Vardy, L. and Orr-Weaver, T. L. (2007b). The Drosophila PNG kinase complex regulates the translation of cyclin B. *Dev Cell* **12**, 157-66.
Vardy, L., Pesin, J. A. and Orr-Weaver, T. L. (2009). Regulation of Cyclin A protein in meiosis and early embryogenesis. *Proc Natl Acad Sci U S A* **106**, 1838-43.
Vibranovski, M. D., Chalopin, D. S., Lopes, H. F., Long, M. Y. and Karr, T. L. (2010). Direct Evidence for Postmeiotic Transcription During Drosophila melanogaster Spermatogenesis. *Genetics* **186**, 431-U678.
Vibranovski, M. D., Lopes, H. F., Karr, T. L. and Long, M. (2009). Stage-specific expression profiling of Drosophila spermatogenesis suggests that meiotic sex chromosome inactivation drives genomic relocation of testis-expressed genes. *PLoS Genet* **5**, e1000731.
Walker, R. G., Willingham, A. T. and Zuker, C. S. (2000). A Drosophila mechanosensory transduction channel. *Science* **287**, 2229-34.
Wang, L., Eckmann, C. R., Kadyk, L. C., Wickens, M. and Kimble, J. (2002). A regulatory cytoplasmic poly(A) polymerase in *Caenorhabditis elegans*. *Nature* **419**, 312-6.
Weil, T. T., Parton, R., Davis, I. and Gavis, E. R. (2008). Changes in bicoid mRNA anchoring highlight conserved mechanisms during the oocyte-to-embryo transition. *Curr Biol* **18**, 1055-61.
Went, D. F. and Krause, G. (1974). Egg activation in Pimpla turionellae (Hym.). *Naturwissenschaften* **61**, 407-8.
Whitaker, M. Genetically encoded probes for measurement of intracellular calcium. *Methods Cell Biol* **99**, 153-82.
Whitaker, M. (2006). Calcium at fertilization and in early development. *Physiol Rev* **86**, 25-88.
Whitaker, M. (2008). Calcium signalling in early embryos. *Philos Trans R Soc Lond B Biol Sci* **363**, 1401-18.

Williams, B. C., Dernburg, A. F., Puro, J., Nokkala, S. and Goldberg, M. L. (1997). The Drosophila kinesin-like protein KLP3A is required for proper behavior of male and female pronuclei at fertilization. *Development* **124**, 2365-76.
Wreden, C., Verrotti, A. C., Schisa, J. A., Lieberfarb, M. E. and Strickland, S. (1997). Nanos and pumilio establish embryonic polarity in Drosophila by promoting posterior deadenylation of hunchback mRNA. *Development* **124**, 3015-23.
Wu, J. Q. and Kornbluth, S. (2008). Across the meiotic divide - CSF activity in the post-Emi2/XErp1 era. *J Cell Sci* **121**, 3509-14.
Xu, Z., Kopf, G. S. and Schultz, R. M. (1994). Involvement of inositol 1,4,5-trisphosphate-mediated Ca2+ release in early and late events of mouse egg activation. *Development* **120**, 1851-9.
Zhang, Y., Sturgill, D., Parisi, M., Kumar, S. and Oliver, B. (2007). Constraint and turnover in sex-biased gene expression in the genus Drosophila. *Nature* **450**, 233-U2.